AD_____

Award Number: DAMD17-98-1-8538

TITLE: A Novel Approach to the Elucidation of the Mechanism of Development of Androgen-Independent Growth of Prostate Cancer

PRINCIPAL INVESTIGATOR: James L. Mohler, M.D.

CONTRACTING ORGANIZATION: University of North Carolina at Chapel Hill
Chapel Hille, North Carolina 27599-1350

REPORT DATE: January 2001

TYPE OF REPORT: Final

PREPARED FOR: U.S. Army Medical Research and Materiel Command
Fort Detrick, Maryland 21702-5012

NOTICE

USING GOVERNMENT DRAWINGS, SPECIFICATIONS, OR OTHER DATA INCLUDED IN THIS DOCUMENT FOR ANY PURPOSE OTHER THAN GOVERNMENT PROCUREMENT DOES NOT IN ANY WAY OBLIGATE THE U.S. GOVERNMENT. THE FACT THAT THE GOVERNMENT FORMULATED OR SUPPLIED THE DRAWINGS, SPECIFICATIONS, OR OTHER DATA DOES NOT LICENSE THE HOLDER OR ANY OTHER PERSON OR CORPORATION; OR CONVEY ANY RIGHTS OR PERMISSION TO MANUFACTURE, USE, OR SELL ANY PATENTED INVENTION THAT MAY RELATE TO THEM.

LIMITED RIGHTS LEGEND

Award Number: DAMD17-98-1-8538
Organization: University of North Carolina at Chapel Hill
Location of Limited Rights Data (Pages):

Those portions of the technical data contained in this report marked as limited rights data shall not, without the written permission of the above contractor, be (a) released or disclosed outside the government, (b) used by the Government for manufacture or, in the case of computer software documentation, for preparing the same or similar computer software, or (c) used by a party other than the Government, except that the Government may release or disclose technical data to persons outside the Government, or permit the use of technical data by such persons, if (i) such release, disclosure, or use is necessary for emergency repair or overhaul or (ii) is a release or disclosure of technical data (other than detailed manufacturing or process data) to, or use of such data by, a foreign government that is in the interest of the Government and is required for evaluational or informational purposes, provided in either case that such release, disclosure or use is made subject to a prohibition that the person to whom the data is released or disclosed may not further use, release or disclose such data, and the contractor or subcontractor or subcontractor asserting the restriction is notified of such release, disclosure or use. This legend, together with the indications of the portions of this data which are subject to such limitations, shall be included on any reproduction hereof which includes any part of the portions subject to such limitations.

THIS TECHNICAL REPORT HAS BEEN REVIEWED AND IS APPROVED FOR PUBLICATION.

N Narasimha Murthy
7/05/2001

REPORT DOCUMENTATION PAGE

Form Approved
OMB No. 074-0188

1. AGENCY USE ONLY (Leave blank)	2. REPORT DATE	3. REPORT TYPE AND DATES COVERED
	January 2001	Final (1 Jul 98 - 31 Dec 01)

4. TITLE AND SUBTITLE
A Novel Approach to the Elucidation of the Mechanism of Development of Androgen-Independent Growth of Prostate Cancer

5. FUNDING NUMBERS
DAMD17-98-1-8538

6. AUTHOR(S)
James L. Mohler, M.D.

7. PERFORMING ORGANIZATION NAME(S) AND ADDRESS(ES)
University of North Carolina at Chapel Hill
Chapel Hill, North Carolina 27599-1350

E-Mail: jmohler@med.unc.edu

8. PERFORMING ORGANIZATION REPORT NUMBER

9. SPONSORING / MONITORING AGENCY NAME(S) AND ADDRESS(ES)
U.S. Army Medical Research and Materiel Command
Fort Detrick, Maryland 21702-5012

10. SPONSORING / MONITORING AGENCY REPORT NUMBER

11. SUPPLEMENTARY NOTES
This report contains colored photos

12a. DISTRIBUTION / AVAILABILITY STATEMENT
Distribution authorized to U.S. Government agencies only (proprietary information, Jan 01). Other requests for this document shall be referred to U.S. Army Medical Research and Materiel Command, 504 Scott Street, Fort Detrick, Maryland 21702-5012.

12b. DISTRIBUTION CODE

13. ABSTRACT ***(Maximum 200 Words)***

The human prostate cancer (CaP) xenograft, CWR22 regresses after castration and recurs several months after removal of androgen (recurrent CWR22). Two subtracted cDNA library pools constructed from 20-day castrate CWR22 (non-proliferating tumor in androgen absence) and recurrent CWR22 (proliferating tumor in androgen absence) were compared to identify genes whose gain of function (gene expression elevated in recurrent CWR22 vs. 20-day castrate CWR22) or loss of suppression (gene expression elevated in 20-day castrate CWR22 vs. recurrent CWR22) were associated with onset of cellular proliferation. Of 1057 clones examined, 11 candidate genes were identified, all of which were upregulated in recurrent CWR22. Northern analysis confirmed differential expression of 9 genes. Western analysis revealed an association between tomoregulin, elongation factor alpha and thioredoxin reductase and the onset of androgen-independent growth. Immunohistochemistry revealed expression of tomoregulin in small foci of proliferating cells first recognized on day 90 after castration. Candidate genes will be characterized in a large number of prostatectomy specimens of androgen-dependent and independent CaP and then in an invaluable set of serial biopsies obtained before and after castration of men with advanced CaP. One of these genes may represent an appropriate target to prevent, delay or treat androgen-independent growth of CaP.

14. SUBJECT TERMS
Prostate Cancer

15. NUMBER OF PAGES
69

16. PRICE CODE

17. SECURITY CLASSIFICATION OF REPORT	18. SECURITY CLASSIFICATION OF THIS PAGE	19. SECURITY CLASSIFICATION OF ABSTRACT	20. LIMITATION OF ABSTRACT
Unclassified	Unclassified	Unclassified	Unlimited

Table of Contents

Introduction

Background: Prostate cancer (CaP) undergoes apoptosis and regression following androgen deprivation but recurs despite the absence of testicular androgens. Many investigators are comparing androgen-dependent (early) CaP to androgen-independent (late) CaP in clinical specimens or cell lines using molecular approaches. These experiments may uncover many genes whose expression is altered, only a few of which are critical for the development of androgen-independent growth. We are studying a human CaP xenograft, CWR22, that retains the biological characteristics exhibited by most human CaPs, including regression following castration and recurrence several months after the removal of androgen (recurrent CWR22).[1-3] The recurrent xenograft provides an opportunity to investigate the mechanism(s) responsible for the recovery of proliferative capacity. Preliminary studies have identified transcripts using differential expression analysis that are down regulated in androgen-withdrawn CWR22 but up-regulated in recurrent CWR22 despite the continued absence of androgen. We are using an approach developed for identification of androgen-regulated genes to identify genes that may be uniquely associated with cellular proliferation in the absence of androgen.

Scope of Research: Additional gene products uniquely associated with cellular proliferation were sought by comparison of CWR22 tumors that exist in androgen absence but differ in proliferative capacity. cDNA libraries from 20 day castrate mice bearing CWR22 tumors (proliferation undetectable) and recurrent CWR22 (proliferative rate similar to androgen-dependent CWR22) were studied using cDNA library subtraction to evaluate the possibilities that proliferation is triggered by either gain of function (gene expression elevated in recurrent CWR22 relative to 20 day castrate CWR22) or loss of suppression (gene expression elevated in 20 day castrate CWR22 relative to recurrent CWR22).

Purpose: Genes that are directly associated with the onset of cellular proliferation in androgen absence may be targeted using gene therapy approaches to prevent the development of androgen-independence or kill androgen-independent cells.

Body

Aim 1) Identify genes that are differentially expressed in the absence of androgen in dormant versus proliferating tumors in the CWR22 model.

CWR22 tumors were obtained from mice 20d after castration (n=4), 20d castrate mice treated with 48h testosterone propionate (TP) (n=4) and mice 5 months after castration (recurrent CWR22) (n=6). Total RNA was isolated and poly (A) RNA was purified using the Oligotex mRNA Midi Spin-Column Protocol (Qiagen). Three subtractive hybridizations were performed: a subtraction to identify genes overexpressed in recurrent CWR22 compared to 20d castrates, a subtraction to identify genes suppressed in recurrent CWR22 compared to 20d castrates and a control subtraction, using the PCR-Select cDNA Subtraction Kit (Clontech). PCR products from the subtracted cDNA libraries were ligated into the pGEM-T Easy Vector System 11, a TA cloning system (Promega Corp) and transformed into JM109 high efficiency competent cells (Promega). Transformed cells were plated on LB/AMP/XGAL/IPTG plates. Plasmids

containing inserts were identified using blue/white screening. DNA was prepared from white colonies.

Multiple duplicate slot blot membranes were prepared. 1ug of poly (A) mRNA from the 20d castrate CWR22 and recurrent CWR22 was radiolabeled as first strand cDNA by random priming with ^{32}P-dCTP, heat denatured, mixed with hybridization solution at 10 cpm/μl, and hybridized to duplicate membranes at 68°C overnight. After hybridization and washing, membranes were exposed to X-ray film with an intensifying screen at -80° C for 1h. Autoradiographs of duplicate blots hybridized to recurrent CWR22 and 20d castrate CWR22 probes were then analyzed to identify genes differentially hybridized to the two probes. A total of 1057 clones were examined by doing two screenings of both libraries. The inserts were sequenced and BLAST searched. For details regarding collection of research specimens, identification of differentially expressed genes using subtractive hybridization, estimation of subtraction efficiency, cloning and slot blot analysis, see first annual report.

Eleven candidate genes were identified:

1) a human chromosome 3 gene that encodes arginine-rich protein that has been found to be mutated in many CaP tumors;[6]
2) thioredoxin-binding protein 2 (TBP2) also known as vitamin D-upregulated 1 (VDUP1) gene;[7]
3) translation elongation factor 1 alpha (EF-1α) which has a truncated homologue in prostate cancer known as prostate tumor inducing gene-1 (PTI-1);[8]
4) Mxi1, a transcriptional regulator from the Myc family, that has been shown to be expressed in prostate tumors;[9]
5) carcinoembryonic antigen (CEA) that has been shown to be elevated in the plasma of approximately one-half of androgen-independent prostate cancer patients;[10]
6) a human alpha 1 gene sequence with homology to sperm antigen-36;
7) a novel EGF-like molecule known as tomoregulin;[11]
8) MHC class III gene;
9) tRNA synthetase;
10) an unknown gene on human chromosome 22; and
11) ribosomal protein S10.

Northern blot analysis using intact CWR22, 20 day castrate CWR22, 20 day castrate CWR22 + TP 48h and recurrent CWR22 mRNA was used to 1) confirm differential expression between 20 day castrate CWR22 and recurrent CWR22 and 2) distinguish androgen regulation and proliferation association. DNAs from the 11 candidate genes were amplified with T7/SP6 primers (Promega) using thermal cycling conditions 95°C for 8 min, 94°C for 1 min, 46°C for 1 min and 72°C for 1 min 30 sec for 30 cycles followed by a 10 minute extension at 72°C. PCR products were purified using microspin filter tubes (Whatman, Markson, WA). 10 μg of total RNA from intact CWR22, 20 day castrate CWR22, 20 day castrate CWR22 + TP 48h and recurrent CWR22 were glyoxylated and fractionated through 1% agarose gels and transferred to Biotrans nylon neutral membrane (ICN Biomedicals, Inc, Aurora, OH). 12.5 ng purified insert DNA was labeled with [^{32}p]-dCTP (Amersham Corp., Arlington Heights, IL) using the random prime labeling kit (Boerhringer Manheim, Indianapolis, IN). Membranes were hybridized in

aqueous solution (5x SCC, 5x Denhardt's solution, 1% SDS and 100ug/ml salmon sperm DNA) overnight at 68°C. After washing at 50°C for 1h in 0.1x SSC, 0.1% SDS, the membranes were exposed to X-ray film (Eastman Kodak Co., Rochester, NY) with an intensifying screen at –80°C.

Mxi1, EF1α, tomoregulin, human α1 gene sequence with homology to sperm antigen 36 and human ribosome S10 were proliferation-associated and not androgen-regulated whereas MCH class III, tRNA synthetase, thioredoxin-reductase were both proliferation-associated and androgen-regulated. RNAs increased 1 fold (MHC class III, tRNA synthetase, human α1 gene sequence with homology to sperm antigen 36), 2 fold (Mxi1) or many fold (tomoregulin) or decreased to 50% (EF1α, human ribosome S10) or 25% (thioredoxin-reductase) when recurrent CWR22 tumors were compared to 20 day castrate CWR22 tumors. MCH class III and tRNA synthetase RNAs increased two fold and thioredoxin-reductase RNA decreased when 20 day castrate CWR22 tumors were stimulated with 48h TP.

Key research accomplishments:

- CWR22 tumors from 20 day castrate mice, 20 day castrate mice + TP 48 h and 5 month castrate mice (recurrent) have been obtained and RNAs prepared.
- Constructed cDNA library from pooled poly A RNA from CWR22 tumors from 20 day castrate mice and recurrent CWR22 tumors. Northern blots from CWR22 tumor RNAs were generated.
- Compared cDNA libraries from 20 day castrate CWR22 (non-proliferating tumor in androgen absence) and recurrent CWR22 (proliferative tumor in androgen absence) tumors using subtractive hybridization.
- Identified 11 candidate genes that were differentially expressed in the absence of androgen in dormant (20 day castrate CWR22) versus proliferating (recurrent CWR22) tumors in the CRW22 model.
- Confirmed 8 candidate genes that were associated with proliferation of which 3 were androgen-regulated and 5 were not androgen-regulated using northern analysis of CWR22 20 day castrate, testosterone boosted and recurrent CWR22 mRNA and labeled cDNA as probes.

Aim 2) Relate the onset of expression of androgen-regulated genes identified in preliminary studies and proliferation-associated genes identified in Aim 1 to the onset of androgen-independent proliferation using the CWR22 model

The expression of previously identified androgen-regulated genes was characterized. The RNA expression of NKX3.1, PSA, hK2, α-enolase, α-tubulin were described previously.[14] Using Northern blotting, Western blotting and immunohistochemistry, IGFBP-5 was found androgen-regulated in CWR22 tumors and was more highly expressed in CaP as compared to BPH or PIN.[15] Using these same techniques, androgen regulation of cell cycle proteins CDK1 and CDK2, cyclins A, B1 and D1, and the cyclin-dependent kinase inhibitors p21 and p27 was demonstrated.[16] The same approach used to identify androgen-regulated transcripts was

employed for characterization of genes identified in Aim 1 and demonstration of their expression in association with proliferation in CWR22 tumors.

CWR22 tumors were harvested from mice castrated for 2, 6, 12, 14, 20, 30, 60, 80, 90, 98, 105, 115, 120, and 150 days and from 6, 12 and 20 day castrate mice treated with 48h testosterone propionate (TP). Serum prostate-specific antigen (PSA) levels have been determined for all mice at the time of sacrifice and tumor harvest. Tissues were frozen at –80 °C until use.

Image analysis of immunodetected Ki-67 proliferation antigen in paraffin sections of CWR22 tumors was performed to determine precisely the onset of cellular proliferation in CWR22 tumors after castration. Previously, the essential criteria of immunostaining were examined to establish a linear relationship between AR protein content and mean optical density (MOD) of the immunoperoxidase-substrate reaction product.[12] Our image analysis method was modified to automatically quantitate Ki-67 proliferation antigen in formalin-fixed, paraffin-embedded sections of CWR22 tumors to determine precisely the time of onset of proliferation in CWR22 tumors after castration. IHC of Ki-67 in paraffin sections of CWR22 tumors followed by quantitation of positive cells by automated video image analysis revealed that cellular proliferation is not detected by image analysis until 120d after castration when IHC revealed multiple foci of proliferating cells.[13] PSA increased 120d after castration (21.3 ± 4.1 vs. 11.1 ± 1.8 ng/ml at 90d, p=0.01) and these foci expressed increased levels of PSA when adjacent sections were stained for Ki-67 and PSA. The appearance of proliferating tumor cells that expressed androgen receptor and PSA 120 days after castration indicated that these foci likely were precursors of recurrent tumors.

Days after castration	No. of Tumors	% Ki-67 ± SE	PSA (ng/ml) ± SE
CWR22	12	73.5 ± 4.4	246.7 ± 55.3
1	2	56.9 ± 7.5	
2	4	26.1 ± 5.6	169.0 ± 53.7
4	2	9.4 ± 8.1	
6	6	0.8 ± 0.5	109.9 ± 76.3
12	6	0.3 ± 0.3	18.8 ± 10.8
32	4	0.1 ± 0.3	5.6 ± 4.1
64	2	0.4 ± 0.2	
90	4	0.8 ± 0.5	11.1 ± 1.8
120	4	3.3 ± 1.2	21.3 ± 4.1
CWR22	12	49.1 ± 7.4	261.5 ± 12.3

Of the 8 candidate genes from Aim 1, 2 were expected to be associated generally with growth (ribosomal protein S10, tRNA synthetase), 1 was conceptually unlikely (MHC class III gene), 1 has only partial sequence known (a human alpha 1 gene sequence with homology to sperm antigen-36) and antibody is not available for the Mxi1 gene product (personal communication from HP Koeffler) or thioredoxin-binding protein 2 / vitamin D-upregulated 1 gene (personal communication from M Matsui). Antibodies were obtained for 3 candidate gene products: tomoregulin from Choitsu Sakamoto, M.D., Ph.D., Nippon Medical School, Japan via collaboration and EF-1α and thioredoxin reductase-1 (the only member of the TBP2/VDUP1 family that was interesting due to a growing body of evidence that suggests oxidative stress may have a role in CaP carcinogenesis) from Upstate Biotechnology, Lake Placid, NY.

Lysates were prepared from frozen CWR22 tumors at the time points described. Tumor tissue (100mg) was pulverized in liquid nitrogen, allowed to thaw on ice, and mixed with 1.0 ml of

RIPA buffer with protease inhibitors (PBS, 1% NP40, 0.5% sodium deoxycholate, 0.1% SDS, 0.5mM phenylmethylsulfonyl fluoride, 10uM pepstatin, 4uM aprotinin, 80μM leupeptin, and 5 mM benzamidine). Tissue was homogenized on ice for 30s using a Biohomogenizer (Biospec Products, Inc., Bartlesville, OK), 2μl of 0.2M phenylmethylsulfonyl added and homogenates incubated 30 min on ice. Homogenates were centrifuged at 10,000xG for 20 min; supernatants were collected and centrifuged to prepare final lysates. Supernatant protein (100ug) from each sample was electrophoresed in 12% SDS-polyacrylamide gels, electroblotted to Immobilon-P membrane (Millipore Corp., Bedford, MA) and immunodetected.

Thioredoxin-reductase 1 protein levels in CWR22 tumors decreased on day 6 after castration and were increased 2-fold by 48 h TP treatment of a 6 day castrate mouse. Thioredoxin-reductase 1 was barely detectable on days 12, 32 and 64 after castration but it was expressed in recurrent CWR22 at levels similar to those in the androgen-dependent CWR22. Tomoregulin expression was highest in androgen-dependent and recurrent CWR22 tumors and was increased after TP treatment of 6 day castrate mice. EF-1α protein levels were reduced on day 12 after castration and remained low on day 32 after castration. EF1-alpha levels in recurrent CWR22 were similar to those in androgen-dependent CWR22.

IHC protocol have been attempted for routinely processed and frozen tissues for the 3 candidate gene products. For tomoregulin, IHC has been optimized using antigen retrieval with AR 10 antigen retrieval solution (Biogenex, San Ramon, CA) for 30 min in a vegetable steamer. Primary antibody was used at 1:800 dilution for 1h and detected with 1:200 biotinylated anti-mouse IgG (Vector Labs, Burlingame, CA). Tomoregulin expression was high in the androgen-dependent and recurrent CWR-22 and undetectable until day 120 after castration. Small foci of cells expressed tomoregulin that appeared similar to the foci recognized previously where androgen-independent cellular proliferation may begin.

The IHC protocol for thioredoxin reductase-1 has tried 95% EtOH, 4% paraformaldehyde and acetone fixation of frozen tissues and AR 10, glyca, citra and trypsin antigen retrieval for archived sections. Promising results have been obtained in standard sections using citra antigen retrieval. EF1α IHC has not been successful but many new antibodies have become available recently.

Key research accomplishments:

- CWR22 tumors have been obtained from mice castrated after intervals ranging from 2 weeks to 5 months. Tumors were collected approximately every 2 weeks. Serum PSA levels have been determined for all mice.
- The onsét of cellular proliferation in CWR22 tumors occurs in small foci of cells approximately 120 days after castration. These foci of Ki-67 expressing cells also demonstrate androgen receptor and PSA expression.
- Androgen-regulated genes previously identified[14] have been characterized for expression in CWR22 tumors. IGFBP-5 expression was determined in CWR22 and in CaP from patients.[15]
- Tomoregulin expression assessed by western blot and IHC was high in the androgen-dependent and recurrent CWR-22 and low until day 120 after castration when androgen-independent cellular proliferation begins.

Aim 3) Characterize the expression of genes associated with the onset of androgen-independent proliferation in the CWR22 model in serial prostate biopsies performed before and after castration in men with advanced prostate cancer

	Time from Castration	PSA ng/ml	T ng/dl	%Ki-67 ± SE
Responder	Prior	49	315	23.5 ± 16.5
	1 Month	7	<20	10.4 ± 12.6
	4 Months	2	<20	9.7 ± 4.9
Non responder	Prior	80	145	40.5 ± 12.3
	1 Month	22	31	55.0 ± 20.0
	4 Months	95	27	72.3 ± 15.2

Serum levels of PSA and testosterone (T) and tumor Ki-67 positivity (% Ki-67) of 2 men who underwent serial prostate biopsies prior to and after castration

Serial prostate biopsy specimens have been (14 men) or are currently being collected (5 men) from men with advanced CaP (all tissue acquisition is funded by NCI-PO1-CA77739). Specimens (both frozen and routine) have been collected from androgen-dependent CaP from 54 African Americans and 152 Caucasians treated by radical prostatectomy and from androgen-independent CaP from 10 African Americans and 15 Caucasians treated by transurethral resection. Two sets of serial biopsies obtained prior to castration and at intervals after castration in men with advanced CaP were examined using IHC and image analysis to determine comparability to our results using the CWR22 model (Table). A 58yo Caucasian with Gleason grade 3+5=8 metastatic (T2cNxM1b) CaP responded to castration symptomatically and serum PSA levels and cellular proliferation decreased. A 76yo African American with Gleason grade 5+5=10 locally advanced (T4N2Mx) CaP failed to respond to castration clinically or by PSA and cellular proliferation increased in spite of castration.

Work to be completed in Aim 3 depended on work completed in the previous two aims. We have collected all necessary tissues to complete Aim 3 but have not yet characterized fully candidate gene products for analysis in these tissues (although tomoregulin appears to warrant study).

Key Research Accomplishments:

Aim 1) Identify genes that are differentially expressed in the absence of androgen in dormant versus proliferating tumors in the CWR22 model.

- CWR22 tumors from 20 day castrate mice, 20 day castrate mice + TP 48 h and 5 month castrate mice (recurrent) have been obtained and RNAs prepared.
- Constructed cDNA library from pooled poly A RNA from CWR22 tumors from 20 day castrate mice and recurrent CWR22 tumors. Northern blots from CWR22 tumor RNAs were generated.
- Compared cDNA libraries from 20 day castrate CWR22 (non-proliferating tumor in androgen absence) and recurrent CWR22 (proliferative tumor in androgen absence) tumors using subtractive hybridization.

- Identified 11 candidate genes that were differentially expressed in the absence of androgen in dormant (20 day castrate CWR22) versus proliferating (recurrent CWR22) tumors in the CRW22 model.
- Confirmed 8 candidate genes that were associated with proliferation of which 3 were androgen-regulated and 5 were not androgen-regulated using northern analysis of CWR22 20 day castrate, testosterone boosted and recurrent CWR22 mRNA and labeled cDNA as probes.

Aim 2) Relate the onset of expression of androgen-regulated genes identified in preliminary studies and proliferation-associated genes identified in Aim 1 to the onset of androgen-independent proliferation using the CWR22 model.

- CWR22 tumors have been obtained from mice castrated after intervals ranging from 2 weeks to 5 months. Tumors were collected approximately every 2 weeks. Serum PSA levels have been determined for all mice.
- The onset of cellular proliferation in CWR22 tumors occurs in small foci of cells approximately 120 days after castration. These foci of Ki-67 expressing cells also demonstrate androgen receptor and PSA expression.
- Androgen-regulated genes previously identified[14] have been characterized for expression in CWR22 tumors. IGFBP-5 expression was determined in CWR22 and in CaP from patients.[15]
- Tomoregulin expression assessed by western blot and IHC was high in the androgen-dependent and recurrent CWR-22 and low until day 120 after castration when androgen-independent cellular proliferation begins.

Reportable Outcomes:

Manuscripts

Gregory CW, Hamil KG, Kim D, Hall SH, Pretlow TG, Mohler JL and French FS: Androgen receptor expression in androgen-independent prostate cancer is associated with increased expression of androgen-regulated genes. Cancer Res 58: 5718-5724, 1998.

Kim D, Gregory CW, Smith GJ and Mohler JL: Immunohistochemical quantitation of androgen receptor expression using color video image analysis. Cytometry 35:2-10, 1999.

Gregory CW, Kim D, Ye P, D'Ecole AJ, Pretlow TG, Mohler JL and French FS: Androgen receptor up-regulates insulin-like growth factor binding protein-5 (IGFBP-5) expression in a human prostate cancer xenograft. Endocrinology 140:2372-2381, !999.

Gregory CW, Johnson RT, Presnell SC, Mohler JL and French FS: Androgen receptor regulation of G1 cyclin and cyclin dependent kinase function in the CWR22 human prostate cancer xenograft. J Andrology (in press).

Kim D, Gregory CW, French FS, Maygarden SJ, Smith GJ and Mohler JL: Androgen receptor expression during the transition from androgen-dependent to androgen-independent growth in the CWR22 prostate cancer xenograft (submitted Amer J Pathol, Feb 2001).

Presentations

Gregory CW, Kim D, Smith GJ, French FS and Mohler JL: Evidence for androgen receptor-mediated growth of androgen-independent prostate cancer. Annual Meeting of the American Urological Associaion, Dallas, TX, May 3, 1999.

Moderator, Biology and Progression of Prostate Cancer. International Conference on Prostate Cancer Research: Bridging Basic Science to the Clinic, Iowa City, IA, June 24-27, 1999.

Controversies in Androgen Deprivation for Advanced Prostate Cancer. 69th Annual Meeting of the Carolina Urological Association, Charleston, SC, August 20-24, 1999.

Gregory CW, Johnson RT, Presnell SC, Wilson EM, French FS and Mohler JL: Androgen receptor function in androgen-independent prostate cancer. New Visions on Prostate Cancer from Young Investigators. 8th Prouts Neck Meeting on Prostate Cancer, Prouts Neck, ME, October 21-24, 1999.

The Androgen Receptor in Androgen-Independent Prostate Cancer. Society for Basic Urological Research Fall Symposium, Fort Myers, FL, November 11, 2000.

Kim D, Collins QF, Gregory CW, French FS and Mohler JL: Serial visualization of androgen receptor and proliferation-associated protein in CWR22 prostate cancer xenografts. Society for Basic Urological Research Fall Symposium, Fort Myers, FL, November 12, 2000.

Personnel Receiving Pay From Research Effort

James L. Mohler, M.D.
Christopher Gregory, Ph.D.
Tammy Morris

Conclusion

In summary, we have identified candidate genes differentially expressed in the absence of androgen in dormant (20 day castrate CWR22) versus proliferating (recurrent CWR22) tumors. Tomoregulin, a newly discovered EGF-like molecule, expression assessed by western blot and IHC was high in the androgen-dependent and recurrent CWR-22 and low until day 120 after castration when androgen-independent cellular proliferation begins. Tomoregulin as well as 2 other genes still under evaluation will be characterized in a large number of prostatectomy specimens of androgen-dependent and independent CaP and then in an invaluable set of serial biopsies of advanced human prostate cancer obtained before and after castration. Identification of critical genes associated with the onset of androgen-independent growth may yield candidates for manipulation using gene therapy that can be tested in the CWR22 model prior to investigation in human patients.

References:

1) Pretlow TG, Wolman SR, Micale MA, Pelley RJ, Kursh ED, Resnick MI, Bodner DR, Jacobberger JW, Delmoro CM, Giaconia JM, Pretlow TP: Xenografts of primary human prostatic carcinoma. J Natl Cancer Inst 85:394-398, 1993
2) Wainstein MA, He F, Robinson D, Kung H-J, Schwartz S, Giaconia JM, Edgehouse NL, Pretlow TP, Bodner DR, Kursh ED, Resnick MI, Amini SB, Pretlow TG: CWR22: Androgen-dependent xenograft model derived from a primary human prostatic carcinoma. Cancer Res 54:6049-6052, 1994
3) Nagabhushan M, Miller CM, Pretlow TP, Giaconia JM, Edgehouse NL, Schwartz S, Kung H-J, de Vere White RW, Gumerlock PH, Resnick MI, Amini SB, Pretlow TG: CWR22: the first human prostate cancer xenograft with strongly androgen-dependent and relapsed strains both in vivo and in soft agar. Cancer Res 56:3042-3046, 1996
4) Chirgwin JM, Przbyla AE, MacDonald RJ, and Rutter WJ: Isolation of biologically active ribonucleic acid from sources enriched in ribonuclease. American Chemical Society 78: 5294-5299, 1979.
5) Pederson T and Davis NG: Messenger RNA processing and nuclear structure: Isolation of nuclear ribonucleoprotein particles containing beta-globin messenger RNA precursors. J Cell Biol 87: 47-54, 1980.
6) Shridhar R, Shridar V, Rivard S, Siegfried JM, Pietraszkiewicz H, Ensley J, Pauley R, Grignon D, Sakr W, Miller OJ, Smith DI. Mutations in the arginine-rich protein gene, in lung, breast, and prostate cancers, and in squamous cell carcinoma of the head and neck. Cancer Res 56:5576-8, 1996.
7) Nishiyama A, Matsui M, Iwata S, Hirota K, Masutani H, Nakamura H, Takagi Y, Sono H, Gon Y, Yodoi J. Identification of thioredoxin-binding protein-2/vitamin D3 up-regulated protein 1 as a negative regulator of thioredoxin function and expression. J Biol Chem 274:21645-50, 1999.
8) Gopalkrishnan RV, Su ZZ, Goldstein NI, Fisher PB. Translational infidelity and human cancer: role of the PTI-1 oncogene. Int J Biochem Cell Biol 31:151-62, 1999.
9) Kawamata N, Park D, Wilczynski S, Yokota J, Koeffler HP. Point mutations of the Mxil gene are rare in prostate cancers. Prostate 29:191-3, 1996.
10) Feuer JA, Lush RM, Venzon D, Duray P, Tompkins A, Sartor O, Figg WD. Elevated carcinoembryonic antigen in patients with androgen-independent prostate cancer. J Invest Med 46:66-72, 1998.
11) Uchida T, Wada K, Akamatsu T, Yonezawa M, Hitoshi N, Mizoguchi A, Kasuga M, Sakamoto C. A novel epidermal growth factor-like molecule containing two follistatin modules stimulates tyrosine phosphorylation of erbB-4 in MKN28 gastric cancer cells. Biochem Biophys Res Comm 266:593-602, 1999.
12) Kim D, Gregory CW, Smith GJ and Mohler JL: Immunohistochemical quantitation of androgen receptor expression using color video image analysis. Cytometry 35:2-10, 1999.
13) Gregory CW, Kim D, French FS, Maygarden SJ, Smith GJ and Mohler JL: Androgen receptor expression during the transition from androgen-dependent to androgen-independent growth in the CWR22 prostate cancer xenograft (submitted Amer J Pathol, Feb 2001).
14) Gregory CW, Hamil KG, Kim D, Hall SH, Pretlow TG, Mohler JL and French FS: Androgen receptor expression in androgen-independent prostate cancer is associated with increased expression of androgen-regulated genes. Cancer Res 58: 5718-5724, 1998.

15) Gregory CW, Kim D, Ye P, D'Ecole AJ, Pretlow TG, Mohler JL and French FS: Androgen receptor up-regulates insulin-like growth factor binding protein-5 (IGFBP-5) expression in a human prostate cancer xenograft. Endocrinology 140:2372-2381, !999.
16) Gregory CW, Johnson RT, Presnell SC, Mohler JL and French FS: Androgen receptor regulation of G1 cyclin and cyclin dependent kinase function in the CWR22 human prostate cancer xenograft. J Andrology (in press)

Appendices

See attached pages

Cytometry 35:2-10 (1999)

Original Articles

Immunohistochemical Quantitation of Androgen Receptor Expression Using Color Video Image Analysis

Desok Kim,[1] Christopher W. Gregory,[2] Gary J. Smith,[3,4] and James L. Mohler[1,3,4]*

[1]Department of Surgery, Division of Urology, The Laboratories for Reproductive Biology, University of North Carolina, Chapel Hill, North Carolina

[2]Department of Pediatrics, University of North Carolina, Chapel Hill, North Carolina

[3]Department of Pathology, University of North Carolina, Chapel Hill, North Carolina

[4]UNC-Lineberger Comprehensive Cancer Center, University of North Carolina, Chapel Hill, North Carolina

Received 10 July 1998; Revision Received 31 August 1998; Accepted 4 September 1998

Background: The immunostaining features of the androgen receptor (AR) have been studied in prostate cancer (CaP) to predict the outcome of androgen deprivation therapies. We have developed an automatic video color image analysis system for quantitation of AR expression in large samples of prostatic nuclei.

Methods: Essential criteria of immunostaining have been examined to establish a linear relationship between AR protein content and mean optical density (MOD) of the immunoperoxidase-substrate reaction product. Titration of monoclonal AR antibody, F39.4.1, and concentration and reaction time of substrate were optimized using color video image analysis. The methodology was tested twice. First, CWR22 human CaP xenograft specimens, harvested from testosterone (T)-stimulated, castrated and T-resupplemented mice, were immunostained to demonstrate the dependence of AR expression on serum androgen levels. Second, AR expression was measured in archived clinical specimens.

Results: In CWR22 tumor-bearing mice castrated for 6 days, AR MOD decreased to 57% of T-stimulated, intact mice. After 72 hrs of T treatment, AR MOD returned to the level measured in T-stimulated, intact mice. Sixteen radical prostatectomy specimens and 16 transurethral resection of prostate (TURP) specimens were double-labeled with F39.4.1 and anti-cytokeratin MAb (13βE12) specific for basal epithelial cells. Benign epithelial cells exhibited lower AR MOD in prostatectomy compared to TURP specimens ($P < 0.01$). Differences in AR immunostaining intensity may have resulted from differences in tissue fixation of whole organ versus small tissue specimens.

Conclusions: AR immunostaining can be quantitated accurately using optimized immunohistochemical criteria and video image analysis. Cytometry 35:2-10, 1999.

Key terms: prostate cancer; immunohistochemistry; androgen receptor; video image analysis

Quantitation of the androgen receptor (AR) in the prostate has been performed traditionally using a biochemical radioligand binding method that compares the amount of AR in prostate tissue homogenates. The values obtained represent an average measurement of variation within different regions of the prostate or changes within populations of cells in response to androgen manipulation. Disadvantages of this method include the requirement for generous tissue samples, the production of radioactive waste products, and the inability to exclude nonmalignant cellular material from the assay process (1,2). Immunocytochemical analysis became possible when monoclonal and polyclonal antibodies specific for the AR were developed (3-6). Immunocytochemical analysis offers an advantage over biochemical methods because tissue architecture is preserved. Although designed originally for use on frozen material (7), avidin-biotin immunoperoxidase techniques can be modified for study of paraffin-embedded sections of routinely fixed and processed tissue, including archival

Contract grant sponsor: National Institutes of Health; Contract grant numbers: AG11343 (to J.L.M.), CA64865 (to D.K., J.L.M., and G.J.S.), P30-HD-18968 (DNA and tissue culture cores); Contract grant sponsor: American Foundation for Urologic Disease (to C.W.G.); Contract grant sponsor: Merck U.S. Human Health (to C.W.G.).

*Correspondence to: James L. Mohler, UNC-Lineberger Cancer Center, CB# 7295, University of North Carolina, Chapel Hill, NC 27599-7295.

E-mail: jmohler@med.unc.edu

material and diagnostic biopsy specimens. Furthermore, immunostaining intensity of a specific cell type can be measured using video image analysis.

Prostate cancer (CaP) is characterized by increased heterogeneity of AR immunostaining compared with benign prostate tissue (8). The variability of AR protein content per unit area increased with increasing Gleason grade and stage (9). Immunostaining features of AR expression in primary CaP have been correlated with response to androgen deprivation therapies. Biopsy specimens obtained before androgen deprivation treatment indicated that patients with CaP with a high percentage of AR-positive cells responded well to treatment (10) and that variation of nuclear AR immunostaining correlated inversely with the interval to tumor recurrence (11). Automated image analysis of transurethrally-resected prostate (TURP) specimens suggested that the mean optical density (MOD) of AR immunostaining predicts the outcome of patients treated with various therapies, including radical prostatectomy, radiation, and orchiectomy (12). Recently, the prognostic value of AR expression in patients undergoing hormone therapy was reestablished by image analysis based on a pattern-oriented approach that categorized two-dimensional histograms of MOD and relative total AR content per nucleus into four types (13). Considered together, these studies suggest that CaPs composed of cells homogeneously expressing relatively large amounts of AR protein respond favorably to androgen deprivation. Accurate and reproducible immunohistochemical analysis of AR expression is important for the assessment of the response to hormone therapy and may be important for the investigation of other aspects of the development and progression of CaP.

Accurate quantitation of antigens using immunohistochemistry and light microscopy depends on a linear relationship between the amount of antigen and the intensity of immunoperoxidase-3,3′-diaminobenzidine tetrahydrochloride (DAB) reaction products (14,15). Earlier studies of AR immunostaining of human CaP specimens have not described carefully optimization of immunohistochemical procedures so that one can be confident that variations in staining intensity reflect linearly the amount of antigen. The requirement for a shorter incubation time for cells with higher antigen content was first described by Benno et al.(14). They used quantitative immunohistochemistry and the peroxidase-antiperoxidase technique to detect tyrosine hydroxylase within the nucleus locus coeruleus of rat brain and found that the induction of tyrosine hydroxylase was associated with earlier saturation of chromogen reaction. In general, proper time of chromogen reaction must be determined for each experiment to avoid oversaturation that provides invalid quantitation of antigen content.

In this report, we describe methodology for quantitative immunohistochemistry and color video image analysis of AR expression. We then apply this methodology to show differences in AR immunostaining intensity with testosterone (T) levels in an androgen-dependent human CaP xenograft, CWR22, and in archived human prostate specimens.

MATERIALS AND METHODS

Preparation of Research Specimens

CWR22 propagated in nude mice (16) resembles the majority of human CaP in that it secretes prostate-specific antigen and undergoes apoptosis and regression after androgen deprivation but recurs after several months in the absence of testicular androgen (17–20). Nude mice were purchased from Harlan Sprague-Dawley, Inc. (Indianapolis, IN). CWR22 tumor cells obtained from the laboratory of Dr. Thomas Pretlow were transplanted as described previously (20). Sustained-release T pellets (12.5 mg; Innovative Research of America, Sarasota, FL) were placed subcutaneously into each animal 2 days before tumor injection. After tumor volume reached 1 cm^3 based on caliper measurements, animals were anesthetized with methoxyflurane and castrated, and testosterone pellets were removed. Six T-stimulated, intact mice bearing CWR22 tumors and three castrated animals with regressed CWR22 were exposed to methoxyflurane and killed by cervical dislocation. One animal with regressed CWR22 was injected with a bolus of T propionate (1.0 mg/ml) on day 6 after castration and killed 72 h later. Resected tumors were fixed immediately in 10% buffered formalin for 24–48 h, washed in phosphate-buffered saline for 24 h, and embedded in paraffin. A specimen (125 mm^3) of benign prostatic hyperplasia (BPH) obtained from a radical prostatectomy specimen was prepared by the same method for use as a positive control for AR immunostaining. Sixteen radical prostatectomy specimens from patients with clinically localized CaP and 16 TURP specimens of BPH were obtained from the pathology archives of the University of North Carolina Hospital at Chapel Hill, Chapel Hill, NC. Specimens were examined by a urologic pathologist, and all areas of BPH, prostatic intraepithelial neoplasia, and CaP were marked.

Optimization of Immunohistochemical Parameters

CWR22 xenograft specimens from T-stimulated, intact nude mice and the BPH specimen were used to optimize the variables resulting from the immunostaining procedure. Six-millimeter histological sections were cut from paraffin-embedded blocks. The avidin-biotin immunoperoxidase technique (7) was modified for the MicroProbe staining station (Fisher Scientific, Pittsburgh, PA) that uses capillary action (21). After deparaffinization and rehydration, tissue sections were heated to 100°C for 30 min in a vegetable steamer in the presence of antigen retrieval solution (Citra, pH 6.0; BioGenex, San Ramon, CA) and cooled for 5 min. Slides were preincubated with 2% normal horse serum for 5 min at 37°C and washed with automation buffer (Fisher Scientific). Three optimization procedures were performed as described previously (14) to achieve a linear relationship between the content of AR

protein and the MOD of the immunoperoxidase-substrate reaction product.

AR monoclonal antibody titration. Monoclonal antibody (MAb) F39.4.1 (BioGenex) specific for the N-terminal region of human AR (6) was used to detect AR. To optimize primary antibody concentration, slides were incubated in different dilutions of AR MAb (0.001–6.0 mg/ml in phosphate-buffered saline containing 0.1% bovine serum albumin, pH 7.4) for 120 min at 37°C. Slides were incubated in biotinylated anti-mouse immunoglobulin G (Vector Laboratories, Inc., Burlingame, CA) for 15 min at 37°C (1:200 in phosphate-buffered saline, pH 7.4) and in horseradish peroxidase-conjugated avidin-biotin complex (Vector Laboratories, Inc.) for 15 min at 37°C (1:100 in phosphate-buffered saline, pH 7.4). The immunoperoxidase complexes were visualized using 0.75 mg/ml DAB (Aldrich Chemical Co., Inc., Milwaukee, WI) in Tris buffer containing 0.003% hydrogen peroxide (pH 7.6) for 6 min at 37°C. Slides were dehydrated through graded alcohol solutions, cleaned with Hemo-De xylene substitute (Fisher Scientific), mounted with Permount (Fisher Scientific), and coverslipped.

Optimization of DAB concentration. To find the optimal concentration of DAB using a predetermined concentration of AR MAb, slides were processed and incubated in different concentrations of DAB (0.1–1.5 mg/ml in Tris buffer containing 0.003% hydrogen peroxide, pH 7.6) for 3 or 6 min at 37°C.

Optimization of DAB incubation time. To determine the optimal time of chromogen reaction using predetermined concentrations of AR MAb and DAB, slides were incubated for different times (3–15 minutes) at 37°C.

AR immunohistochemistry. Repeat staining of 12 BPH slides was performed to assess the reproducibility of immunostaining procedures. Histological sections of CWR22 tumor specimens were prepared from mice killed before castration, 6 days after castration, and after 72 h of T resupplementation. Sections were stained in two batches on the same day according to the appropriate parameters established by the procedures described above. Counterstaining was performed with hematoxylin (Gill's formula, 1:6 dilution; Fisher Scientific) for 12 s. A BPH slide was included in each batch as the external control to avoid variation of MOD caused during immunostaining and image acquisition. Nonimmune mouse immunoglobulin G (Vector Laboratories, Inc.) was used instead of AR MAb at the same protein concentration for the negative control slide prepared from the same tissue block as the specimen; negative control slides were nonreactive.

High-molecular-weight anticytokeratin immunohistochemistry. Archived radical prostatectomy specimens and TURP specimens were stained with high-molecular-weight anticytokeratin MAb 13bE12 (Enzo Diagnostics, Inc., Farmingdale, NY), which is specific for basal epithelial cells, to distinguish BPH glands from malignant and prostatic intraepithelial neoplasia glands. After elution by three changes of glycine buffer (pH 2.3) for 5 min at room temperature to remove unreacted antibodies, secondary staining was performed using 13bE12 at 1.7 mg/ml (1:50) for 30 min at 37°C. Subsequent amplification steps were performed at 37°C for 15 min each. The antibody reaction was visualized using 3-amino-9-ethylcarbazole (BioGenex). Counterstaining was performed, and slides were mounted with an aqueous mounting medium (Glycergel; Dako, Carpinteria, CA) and coverslips. Negative control slides consisted of four slides: two lacking the primary antibody in each labeling step and two lacking the secondary antibody in each labeling step; no slides showed cross-reaction between two labeling steps. One slide was prepared without the elution step: the cross-reaction was apparent in AR-positive tumor cells, and immunostaining intensity of the basal layer was decreased.

Video Microscopy and Digital Image Analysis

Image acquisition. The imaging hardware consisted of a Zeiss Axioskop microscope (Carl Zeiss, Inc., Thornwood, NY), a three-chip charge coupled device camera (C5810; Hamamatsu Photonics, Inc., Hamamatsu, Japan), a camera control board (Hamamatsu Photonics, Inc.), and a Pentium-based personal computer. Optical settings were calibrated using procedures described previously (22). Histological images were acquired from immunopositive areas, and intensity histograms were generated using Optimas 6.1 (Optimas Corp., Bothell, WA). Contrast and brightness were adjusted by manipulating gain and exposure time of the camera board and a rheostat setting at the microscope light source to generate maximum contrast while avoiding undersaturation or oversaturation of gray levels. A series of neutral filters was added to confirm the linearity of output in the final optical settings. Temporal variation of light output was frequently measured and found insignificant (<0.2%). Images were sampled randomly throughout histological sections, but areas that contained necrosis, preparation artifacts, or edges were avoided. Each field of view for AR-stained slides was digitized at total magnification 1200× using a 40× objective (numerical aperture, 1.3). A digitized image consisted of 512 × 480 pixels in 16.7 million color modes. Twenty images provided an adequate sample size because the average deviations from the MOD became stable (within ± 5%). Images were transported to a DEC 5000 workstation (Digital Equipment Corp., Maynard, MA) via on-campus Ethernet for further analysis.

Segmentation of nuclei in histological images. An immunostained histological section is shown in Figure 1A. The red, green, and blue planes of each color image were transformed into grayscale images. Each grayscale image was binarized automatically by applying an adaptive thresholding algorithm (23). The accuracy of segmentation depends on the window size selected; a window of 80 &multi; 80 pixels was selected that was four times larger than a typical nucleus. Nuclear masks were generated using the logical OR operation of three binary images, and their boundaries were smoothed by opening and closing with a 5 × 5 structuring element (24). Any remaining artifacts were eliminated by size and shape criteria (25). MOD values were calculated using Equation 1 (see below)

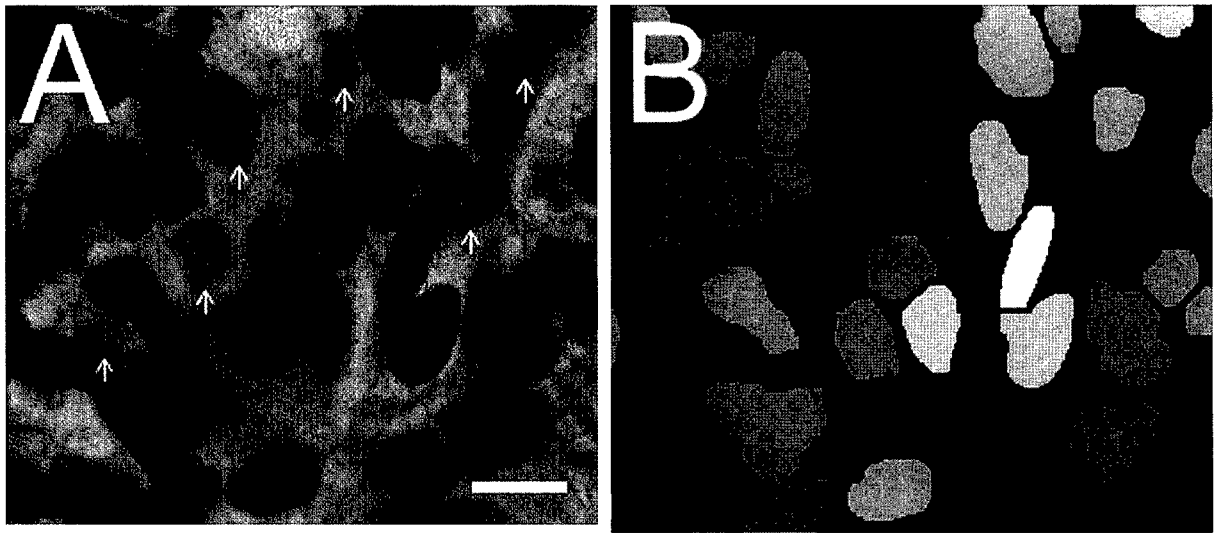

FIG. 1. Red, green, and blue parts of a color image of a sample field of view with AR immunostaining and hematoxylin counterstaining (**A**) were segmented using an adaptive thresholding algorithm and added to produce a set of binary masks for nuclear areas. Immunonegative nuclei (arrows) were removed using a linear discriminant analysis of their hue, saturation, and intensity values. MOD values were calculated and assigned to the nuclear mask as pixel intensity (**B**). Scale bar = 5 μm.

and were assigned to each nuclear mask as pixel intensity (Fig. 1B).

Classification of immunopositive nuclei. Each color image in the red, green, and blue color scheme was transformed to the hue, saturation, and intensity color scheme using an algorithm described by Gonzalez and Woods (26). From each segmented nuclear area, mean hue, saturation, and intensity values were calculated as classifying features of immunopositivity. A statistical pattern recognition technique was used because visual determination of immunopositive cells is highly subjective. Using a color image threshold tool in Optimas 6.1 (Optimas Corp.), 100 immunopositive nuclei were selected randomly from two CWR22 specimens: one from intact mice and one from castrated mice. One hundred immunonegative nuclei were obtained from negative controls. Mean hue, saturation, and intensity features of each nuclear image were measured to build a training set for classification. A set of unstandardized classification coefficients was obtained using a statistics software package, Statgraphics 4.0 (STSC, Inc., Rockville, MD). A test set was generated in a similar fashion and evaluated.

Feature extraction. MOD was calculated to represent the mean AR content of each nucleus classified as immunopositive:

$$\mathrm{MOD} = -\frac{1}{N}\sum_{i=1}^{N}\log\left(\frac{I_i}{I_o}\right) \qquad (1)$$

where N is the total number of pixels in a nuclear mask, I_i is the intensity level of the pixel i, and I_o is the intensity level of the background measured in each field of view. Background staining represented nonnuclear immunoperoxidase reaction. For each section stained for AR and counterstained with hematoxylin, an adjacent section was stained using the same procedure but without primary antibody. The amount of MOD contributed by hematoxylin in the AR-stained section was corrected for by subtracting the average MOD of nuclei in the adjacent section (see Appendix). This corrected MOD was used as a measure of relative concentration of AR in immunopositive cells.

Statistical analysis. Reproducibility of repeat staining was tested using analysis of variance. Differences in MOD of CWR22 specimens and human specimens were evaluated using Student's *t*-tests. Differences were considered significant if P values were <0.05.

RESULTS

Immunohistochemical Criteria for Quantitative Visualization of AR Protein Expression

Concentration of primary AR MAb. AR MAb was diluted from 6 to 0.001 μg/ml, and MOD was analyzed as a function of AR MAb concentration, whereas other variables were kept constant. For BPH and T-stimulated CWR22, the maximum of the linear portion of the curve occurred at 0.13 μg/ml (Fig. 2A). Higher concentrations of AR MAb increased background in CWR22 specimens, resulting in less contrast between nuclear AR staining and background and, hence, decreased MOD ($P < 0.001$).

Concentration of DAB. Different concentrations of DAB were used to define the saturation range of the DAB reaction while other variables were kept constant (3- or 6-min incubation at 37°C and 0.13 μg/ml AR MAb). MOD values increased starting near 0.3 mg/ml of DAB with 0.003 % H_2O_2 for the positive control BPH specimen. The concentration of 0.75 mg/ml used in the determination of the optimal concentration of AR MAb was well within the saturation range. After a 3-min incubation of DAB at 37°C, saturation was confirmed at 0.75 mg/ml (Fig. 2B).

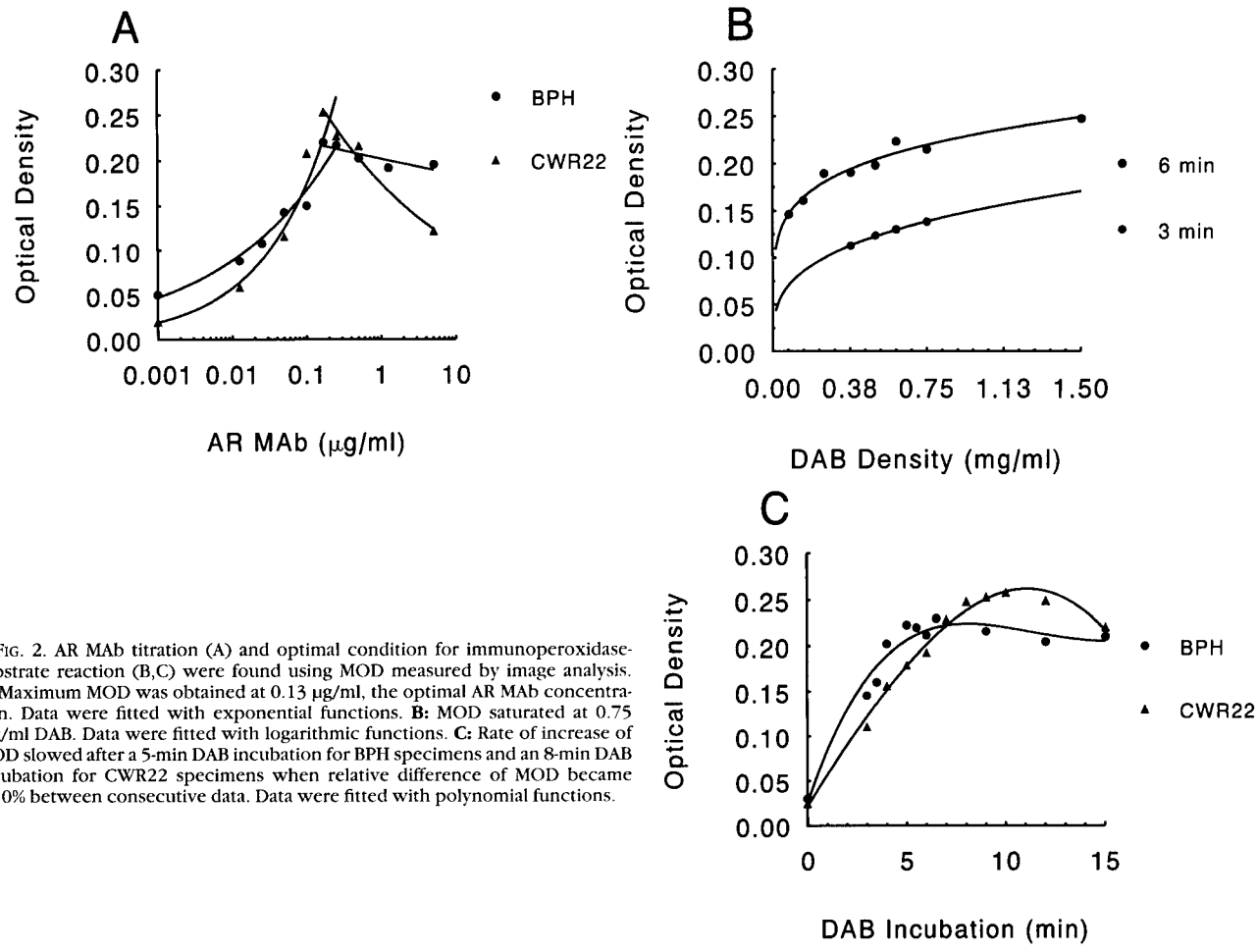

FIG. 2. AR MAb titration (A) and optimal condition for immunoperoxidase-substrate reaction (B,C) were found using MOD measured by image analysis. **A:** Maximum MOD was obtained at 0.13 μg/ml, the optimal AR MAb concentration. Data were fitted with exponential functions. **B:** MOD saturated at 0.75 mg/ml DAB. Data were fitted with logarithmic functions. **C:** Rate of increase of MOD slowed after a 5-min DAB incubation for BPH specimens and an 8-min DAB incubation for CWR22 specimens when relative difference of MOD became <10% between consecutive data. Data were fitted with polynomial functions.

Incubation time of DAB. MOD values were measured as a function of the incubation time for the DAB reaction to investigate the linearity range in BPH and CWR22 (Fig. 2C). MODs from different time points were fitted with polynomials, and relative differences of MOD between consecutive data were calculated. In BPH specimens, DAB color developed rapidly for 5 min (fast color-developing zone) and slowly between 5 and 8 min (slow color-developing zone). CWR22 required approximately 8 min to reach the slow color-developing zone, and saturated MOD values that occurred after 8 min were greater than those of BPH specimens. At 15 min, CWR22 specimens showed elevated background development that was reflected by a decrease of MOD compared with the MOD at 10 min ($P < 0.01$).

Classification of AR Immunopositivity

Segmented nuclear areas of visually confirmed AR-positive nuclei showed a widely variable combination of hue, saturation, and intensity components. A considerable number of AR-positive nuclei was distributed over a feature space where hue, saturation, and intensity components were continuously changing between two populations of AR-positive nuclei and AR-negative nuclei. A set of unstandardized coefficients was calculated using a linear discriminant analysis of the training set. For example, a discriminant function, D, was obtained for AR immunopositivity of CWR22 specimens:

$$D = -0.08168 \cdot H_i - 0.06180 \cdot S_i + 0.01191 \cdot I_i + 0.85885 \quad (2)$$

where H_i is the mean hue, S_i is the mean saturation, and I_i is the mean intensity of the ith nucleus. Minimum distance classification was used as a decision rule to evaluate the test set. The threshold to determine AR immunopositivity was set at −0.47, which was the mean of two centroid

Table 1
Classification Result: Linear Discrimination Analysis by Minimum Distance Classification

	Predicted	
	No. of AR-negative nuclei	No. of AR-positive nuclei
Actual		
No. of AR-negative nuclei (n = 189)	164 (87%)	32 (15%)
No. of AR-positive nuclei (n = 211)	25 (13%)	179 (85%)

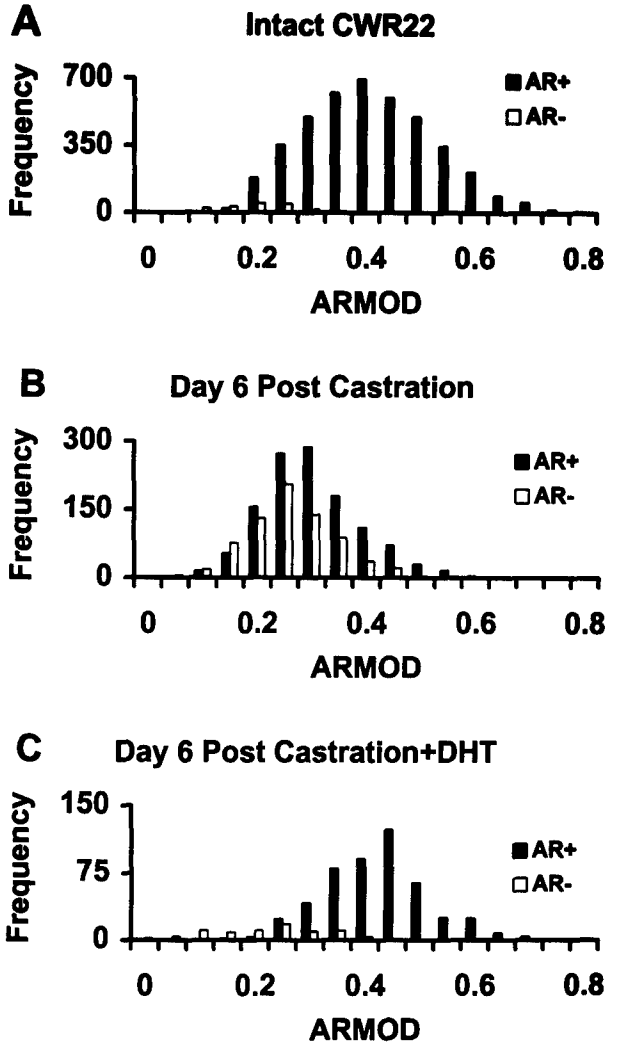

FIG. 3. The intensity of AR immunostaining in CWR22 specimens harvested from mice before and after castration and after castration and T resupplementation. Histological sections were stained with 0.13 μg/ml AR MAb for 120 min and counterstained with hematoxylin. AR was visualized by incubating for 8 min in 0.75 mg/ml DAB. AR expression of CWR22 tumors in mice castrated for 6 days decreased to 57% of T-stimulated, intact mice and was restored on T treatment. **A:** Intact CWR22. **B:** Day 6 after castration. **C:** Day 6 after castration + DHT.

locations; 4.05, representing AR-negative nuclei; and −4.99, representing AR-positive nuclei. Approximately 85% of AR-positive nuclei was classified correctly in the test set of 189 AR-negative nuclei and 211 AR-positive nuclei (Table 1).

Changes of AR Protein Expression of CWR22 Xenografts After Castration and During T Resupplementation

BPH controls showed high levels of AR protein expression as evidenced by uniform and intense immunostaining. The variation of mean MOD between BPH sections was <5.0%. The variation of mean MOD between two batches of BPH sections was not significant (analysis of variance, $P = 0.689$).

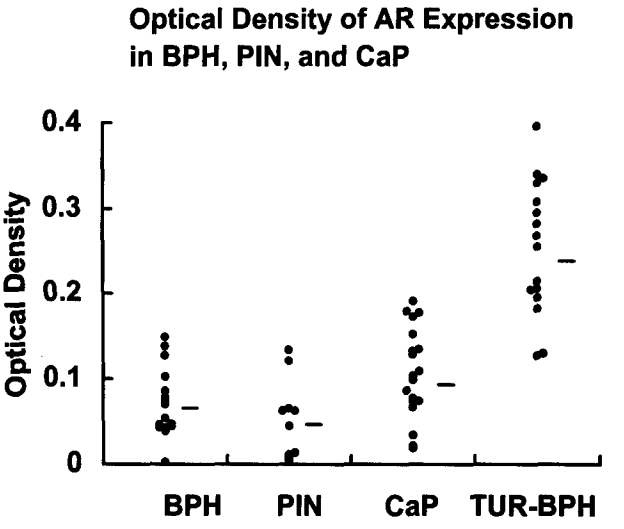

FIG. 4. The intensity of AR immunostaining in human prostatectomy specimens and TURP specimens. Histological sections were stained with 0.13 μg/ml AR MAb for 120 min, and AR was visualized by incubating 6 min in 0.75 mg/ml DAB. Sections were stained secondarily with 1.7 μg/ml anticytokeratin 13βE12 MAb for 30 min, and cytokeratin was visualized by incubating for 5 min with 3-amino-9-ethylcarbazole. Finally, sections were counterstained with hematoxylin.

The average MOD values of AR-positive nuclei were obtained by subtracting the intensity of hematoxylin-stained cells in negative control slides (MOD ± S.E., 0.12 ± 0.01). Most CWR22 nuclei in T-stimulated, intact nude mice showed nuclear localization of AR that stained intensely (MOD ± S.E., 0.26 ± 0.03). (Fig. 3). Serum T decreased to undetectable levels within 12 h after castration. In tumor-bearing mice castrated for 6 days, the average MOD values of AR-positive nuclei decreased to 57% of T-stimulated, intact mice (0.15 ± 0.06). After 72 h of T resupplementation, the average MOD values of AR-positive nuclei (0.27 ± 0.09) returned to the same level measured in T-stimulated, intact mice.

AR Immunostaining Intensity of Radical Prostatectomy and TURP Specimens

When double-labeled with AR MAb F39.4.1 and anticytokeratin MAb 13βE12, weak-to-intermediate intensity of AR immunostaining was observed in prostatectomy specimens. The basal layer was visualized in BPH and prostatic intraepithelial neoplasia glands, whereas no basal layers were observed in malignant glands. Epithelial cells of CaP glands showed higher average MOD values of AR-positive nuclei than BPH (0.11 ± 0.01 versus 0.07 ± 0.01; $P < 0.05$) (Fig. 4). Prostatic intraepithelial neoplasia, identified in 10 radical prostatectomy specimens, showed AR immunostaining similar to BPH (0.05 ± 0.02). BPH from TURP specimens (0.25 ± 0.02) showed significantly higher AR immunostaining intensity compared with BPH from radical prostatectomy specimens ($P < 0.01$).

DISCUSSION

In this study, optimal conditions for AR staining were achieved by avoiding nonspecific binding of AR MAb

Table 2
Summary of Immunohistochemical Studies of AR

Reference	Tissue samples	Features	Results
Sadi and Barrack, 1992 (11)	Frozen biopsy specimens from 17 patients with metastatic CaP	Variance of MOD measured using VIA	Patients with high variance of MOD showed shorter interval to recurrence Mean MOD values were not different among patients
Tilley et al., 1994 (12)	Frozen TURP specimens from 9 patients with clinically localized CaP, 5 patients with locally invasive CaP, and 16 patients with metastatic CaP	MOD of two AR antibodies and hematoxylin and percent AR positivity using VIA	Patients with progressive disease were separated retrospectively by discriminant factor analysis using all features
Takeda et al., 1995 (10)	Frozen prostate biopsy specimens from 62 patients with metastatic CaP	Manual counting of percent AR positivity	Patients with >48% AR positivity had better outcome
Ruizeveld de Winter et al., 1994 (8)	Frozen RRP specimens from 49 patients with localized CaP, frozen TURP specimens from 10 patients with metastatic CaP, and 20 patients with androgen-deprived CaP	Manual counting of percent AR positivity	No differences were found between 49 RRP and 10 TURP specimens from untreated patients with CaP No difference between 10 TURP untreated patients and 20 TURP androgen-deprived patients
Hobisch et al., 1995 (29)	Paraffin-embedded biopsy specimens of 22 distant metastases from 18 patients with CaP (17 androgen-deprived and 1 untreated)	Manual counting of percent AR positivity	All 22 biopsy specimens showed AR positivity 8 biopsy specimens showed >50% AR positivity 10 biopsy specimens showed 10%–50% AR positivity

RRP, radical prostatectomy; VIA, video image analysis.

while maximizing the signal/noise ratio (titration); oversaturation of chromogen reaction was avoided while maximizing the availability of chromogen to immunoperoxidase complexes. The extraction of immunostaining features was accomplished at the level of individual nuclei to provide more cell-specific information than previous studies that analyzed entire immunopositive areas (14). Western blot analysis indicated that CWR22 tumors harvested from T-stimulated intact mice had higher levels of AR content than CWR22 tumors obtained from castrated mice (27). Therefore, the minimum incubation time of DAB was determined using CWR22 tumors harvested from T-stimulated intact mice. Saturation of DAB reaction occurred after 5 min of incubation in BPH specimen versus 8 min in CWR22. The slow phase of color development after the initial fast phase was observed in both CWR22 and BPH sections. During this phase, color development of DAB may have continued among nuclei that express inherently less AR, e.g., basal epithelial nuclei in BPH (28).

AR expression has been described quantitatively by several groups using manual scoring or video image analysis of AR-positive cells (Table 2). The manual scoring used in several studies involved visual discrimination of immunopositive cells that is highly subjective because AR immunostaining is not all-or-none. Video image analysis is technically demanding; accurate segmentation of nuclei from histological images has proven difficult. Sadi and Barrack (11) avoided the necessity for segmentation by interactively placing a sampling window within nuclei. However, the mean and variance of AR immunostaining could have been affected by the nuclei selected for study, a selection made based on the very characteristic being studied. Tilley et al. (12) used an automated color video image analysis system that provided techniques such as automatic segmentation of nuclear images and discriminant analysis of color features. MOD was derived for each field as total integrated optical density divided by total area of positively stained nuclei within areas chosen visually to represent malignant tissue. In our study, color features were obtained from individual nuclei that should provide more accurate classification of immunopositivity, and MOD of each nucleus was defined to avoid field-to-field variability of immunostaining intensity and tissue thickness. CWR22 xenografts consist almost entirely of malignant epithelial cells, and hence, classification of benign versus malignant nuclei was not necessary.

Immunohistochemical quantitation techniques developed in this study were also applied to measure AR immunostaining intensity in clinical specimens. Lower AR immunostaining intensity of BPH epithelium in radical prostatectomy specimens compared with TURP specimens may have been primarily caused by fixation variability. BPH specimens prepared for positive controls were obtained from radical prostatectomy specimens and were fixed immediately in formalin. Control specimens showed more intense AR staining compared with archived sections of BPH obtained from radical prostatectomy specimens and the average MOD values of AR-positive nuclei were

similar to TURP specimens. TURP "chips" are collected and placed in formalin in the operating suite, whereas radical prostatectomy specimens are not placed in formalin until received in the Pathology Department 1-3 h after procurement. The method of tissue procurement as well as the time to fixation must be considered when comparing specimens among patients. When AR immunostaining was compared in CaP and BPH glands from the same prostatectomy specimens, CaP expressed higher levels of AR, a result consistent with an earlier report that CaP specimens had higher AR immunostaining and higher variance than BPH (9).

Further insights into the role of AR in the development and progression of BPH and CaP depend on accurate quantitation of AR expression. Automated video image analysis can be used to measure AR expression in research and clinical specimens of prostate tissue.

ACKNOWLEDGMENTS

The authors thank Dr. Madhabananda Sar for technical advice on AR immunohistochemistry; Patricia Magyar and Yeqing Chen for technical assistance with tissue processing and immunostaining; and Dr. Mary V. Iacocca who identified prostatic intraepithelial neoplasia in radical prostatectomy specimens.

APPENDIX

According to the Beer-Lambert law, light traveling through a medium that contains light-diffracting (absorbing) elements can be described as follows:

$$I = I_0 e^{-\xi\mu\tau} \quad (3)$$

where I is the amount of light coming out of the medium without diffraction, I_0 is the amount of light coming into the medium, ζ is a constant that relates the optical absorption to the content of element μ in the medium of thickness τ. Let $\delta = \zeta\mu\tau$ and solve for δ:

$$\delta = -\log_e(I/I_0) \quad (4)$$

The optical density can defined as $\delta = \delta(\mu$ &mgr), the probability a photon is absorbed per unit distance in a medium. If light goes through a medium that consists of two light-diffracting elements, Equation 3 becomes, when τ is constant,

$$I = I_0 e^{-(\xi_1\mu_1 + \xi_2\mu_2)\tau} \quad (5)$$

Similarly,

$$\xi_1\mu_1\tau + \xi_2\mu_2\tau = -\log_e(I/I_0) = \delta \quad (6)$$

Therefore, the optical density of the medium that consists of two light-diffracting elements is the sum of the optical densities defined for each element.

LITERATURE CITED

1. Charalambous D, Kitchen PR, Stillwell RG, Smart PJ, Rode J. A comparison between radioligand and immunohistochemical assay of hormone receptors in primary breast cancer. Aust N Z J Surg 1993;63:637-641.
2. Pertschuk LP, Schaeffer H, Feldman JG, Macchia RJ, Kim YD, Eisenberg K, Braithwaite LV, Axiotis CA, Prins G, Green GL. Immunostaining for prostate cancer androgen receptor in paraffin identifies a subset of men with a poor prognosis. Lab Invest 1995;73:302-305.
3. Chang C, Kokontis J. Identification of a new member of the steroid receptor super-family by cloning and sequence analysis. Biochem Biophys Res Commun 1988;55:971-977.
4. Husmann DA, Wilson CM, McPhaul MJ, Tilley WD, Wilson JD. Antipeptide antibodies to two distinct regions of the androgen receptor localize the receptor protein to the nuclei of target cells in the rat and human prostate. Endocrinology 1990;26:2359-2368.
5. Lubahn DB, Joseph DR, Sar M, Tan J, Higgs HN, Larson RE, French FS, Wilson EM. The human androgen receptor: Complementary deoxyribonucleic acid cloning, sequence analysis and gene expression in prostate. Mol Endocrinol 1988;2:1265-1275.
6. Zegers ND, Classen E, Neelen C, Mulder E, van Larr JH, Vorrhorst MM, Berrevoets CA, Brinkmann AO, van der Kwast ThH, de Winter JAR, Trapman J, Boersma WJA. Epitope prediction and confirmation for the human androgen receptor: Generation of monoclonal antibodies for multi-assay performance following the synthetic peptide strategy. Biochim Biophys Acta 1991;1073:23-32.
7. Sar M. Application of avidin-biotin complex technique to the localization of estradiol receptor in target tissues using monoclonal antibodies. In: Bullock GR, Petrusz P, editors. Techniques in Immunocytochemistry, Volume 3. New York: Academic Press; 1985, p. 43-54.
8. Ruizeveld de Winter JA, Trapman J, Vermey M, Mulder E, Zegers ND, van der Kwast TH. Androgen receptor expression in human tissues: An immunohistochemical study. J Histochem Cytochem 1991;39:927-936.
9. Magi-Galluzzi C, Xu X, Hlatky L, Hahnfeldt P, Kaplan I, Hsiao P, Chang C, Loda M. Heterogeneity of androgen receptor content in advanced prostate cancer. Mod Pathol 1997;10:839-845.
10. Takeda H, Akakura K, Masai M, Akimoto S, Yatani R, Shimazaki J. Androgen receptor content of prostate carcinoma cells estimated by immunohistochemistry is related to prognosis of patients with stage D2 prostate carcinoma. Cancer 1996;77:934-940.
11. Sadi MV, Barrack ER. Image analysis of androgen receptor immunostaining in metastatic prostate cancer. Heterogeneity as a predictor of response to hormonal therapy. Cancer 1993;71:2574-2580.
12. Tilley WD, Lim-Tio SS, Horsfall DJ, Aspinall JO, Marshall VR, Skinner JM. Detection of discrete androgen receptor epitopes in prostate cancer by immunostaining: Measurement by color video image analysis. Cancer Res 1994;54:4096-4102.
13. Prins GS, Sklarew RJ, Pertschuk LP. Image analysis of androgen receptor immunostaining in prostate cancer accurately predicts response to hormonal therapy. J Urol 1998;159:641-649.
14. Benno RH, Tucker LW, Joh TH, Reis DJ. Quantitative immunocytochemistry of tyrosine hydroxylase in rat brain. I. Development of a computer assisted method using the peroxidase-antiperoxidase technique. Brain Res 1982;246:225-236.
15. Nabors LB, Songu-Mize E, Mize RR. Quantitative immunocytochemistry using an image analyzer. II. Concentration standards for transmitter immunocytochemistry. J Neurosci Methods 1988;26:25-34.
16. Pretlow TG, Wolman SR, Micale MA, Pelley RJ, Kursh ED, Resnick MI, Bodner DR, Jacobberger JW, Delmoro CM, Giaconia JM. Xenografts of primary human prostatic carcinoma. J Natl Cancer Inst 1993;85:394-398.
17. Gregory CW, Sharief Y, Hamil KG, Hall SH, Pretlow TG, Mohler JL, French FS. Apoptosis in an androgen-dependent xenograft model derived from a primary human prostatic carcinoma [abstract]. Mol Biol Cell 1995;6:240.
18. Nagabhushan M, Miller CM, Pretlow TP, Giaconia JM, Edgehouse NL, Schwartz S, Kung HJ, de Vere White RW, Gumerlock PH, Resnick MI, Amini SB, Pretlow TG. CWR22: The first human prostate cancer xenograft with strongly androgen-dependent and relapsed strains both in vivo and in soft agar. Cancer Res 1996;56:3042-3046.
19. Tan J-A, Sharief Y, Hamil KG, Gregory CW, Zang D-Y, Sar M, Gumerlock PH, deVere White RW, Pretlow TG, Harris SE, Wilson EM, Mohler JL, French FS. Dehydroepiandrosterone activates mutant androgen receptors expressed in the androgen dependent human prostate cancer xenograft CWR22 and LNCaP cells. Mol Endocrinol 1997;11:450-459.

20. Wainstein MA, HE F, Robinson D, Kung H-J, Schwartz S, Giacona JM, Edgehouse NL, Pretlow TP, Bodner DR, Kursh ED, Resnick MI, Seftel A, Pretlow TG. CWR22: Androgen-dependent xenograft model derived from a primary human prostatic carcinoma. Cancer Res 1994;54: 6049-6052.
21. Brigati DJ, Budgeon LR, Unger ER, Koebler D, Cuomo C, Kennedy T, Perdomo JM. Immunocytochemistry is automated: Development of a robotic workstation based upon the capillary action principle. J Histotechnol 1988;11:165-183.
22. Mize RR, Holdefer RN, Nabors LB. Quantitative immunocytochemistry using an image analyzer. I. Hardware evaluation, image processing, and data analysis. J Neurosci Methods 1988;26:1-24.
23. Otsu N. A threshold selection method from gray-level histograms. IEEE Trans Systems Man Cybernetics 1979;9:62-66.
24. Serra J. Image analysis and mathematical morphology. Boston: Academic Press; 1982.
25. Kim D, Charlton JD, Coggins JM, Mohler JL. Semi-automated nuclear shape analysis of prostatic carcinoma and benign prostatic hyperplasia. Anal Quant Cytol Histol 1994;16:400-415.
26. Gonzalez RC, Woods RE. Digital image processing. Reading, MA: Addison-Wesley; 1992. p. 229-237.
27. Gregory CW, Hamil KG, Kim D, Hall SH, Mohler JL, French FS. Androgen receptor expression in androgen-independent prostate cancer is associated with increased expression of androgen-regulated genes. Cancer Res 1998, in press.
28. Bonkhoff H, Remberger K. Widespread distribution of nuclear androgen receptors in the basal cell layer of the normal and hyperplastic human prostate. Virch Arch A Pathol Anat Histopathol 1993;422: 35-38.
29. Hobisch A, Culig Z, Radmayr C, Bartsch G, Klocker H, Hittmair A. Distant metastases from prostatic carcinoma express androgen receptor protein. Cancer Res 1995;55:3068-3072.

[CANCER RESEARCH 58, 5718–5724, December 15, 1998]

Androgen Receptor Expression in Androgen-independent Prostate Cancer Is Associated with Increased Expression of Androgen-regulated Genes[1]

Christopher W. Gregory, Katherine G. Hamil, Desok Kim, Susan H. Hall, Thomas G. Pretlow, James L. Mohler, and Frank S. French[2]

Department of Pediatrics [C. W. G., K. G. H., S. H. H., F. S. F.] and Surgery [D. K., J. L. M.], The Laboratories for Reproductive Biology [C. W. G., K. G. H., S. H. H., F. S. F.], and The Lineberger Comprehensive Cancer Center [F. S. F., S. H. H., J. L. M.], The University of North Carolina at Chapel Hill, Chapel Hill, North Carolina 27599, and Institute of Pathology, Case Western Reserve University, Cleveland, Ohio 44106 [T. G. P.]

ABSTRACT

The human prostate cancer (CaP) xenograft, CWR22, mimics human CaP. CWR22 grows in testosterone-stimulated nude mice, regresses after castration, and recurs after 5–6 months in the absence of testicular androgen. Like human CaP that recurs during androgen deprivation therapy, the recurrent CWR22 expresses high levels of androgen receptor (AR). Immunohistochemical, Western, and Northern blot analyses demonstrated that AR expression in the androgen-independent CWR22 is similar to AR expression in the androgen-dependent CWR22 prior to castration. Expression of prostate-specific antigen and human kallikrein-2 mRNAs, two well-characterized androgen-regulated genes in human CaP, was androgen dependent in CWR22. Despite the absence of testicular androgen, prostate-specific antigen and human kallikrein-2 mRNA levels in recurrent CWR22 were higher than the levels in regressing CWR22 tumors from 12-day castrate mice and similar to those in the androgen-stimulated CWR22. Other AR-regulated genes followed a similar pattern of expression. Differential expression screening identified androgen regulation of α-enolase and α-tubulin as well as other unknown mRNAs. Insulin-like growth factor binding protein-5, the homeobox gene *Nkx 3.1*, the AR coactivator ARA-70, and cell cycle genes *Cdk1* and *Cdk2* were androgen regulated in CWR22. In recurrent CWR22, the steady-state levels of all these AR-dependent mRNAs were similar to those in the androgen-stimulated CWR22, despite the absence of testicular androgen. Expression of AR and AR-regulated genes in the androgen-deprived recurrent CWR22 at levels similar to the androgen-stimulated CWR22 suggests that AR is transcriptionally active in recurrent CWR22. Induction of these AR-regulated genes may enhance cellular proliferation in relative androgen absence but through an AR-dependent mechanism. Alternatively, in androgen-independent tumors, induced expression of the AR-regulated gene network might result from a non-AR transcription control mechanism common to these genes.

INTRODUCTION

AR[3] is a member of the subfamily of steroid receptors and the larger family of nuclear receptors that function as transcription factors. AR is activated by androgen, binds specific nucleotide sequences known as androgen response elements, and interacts with other factors to control transcription of androgen-regulated genes, thereby stimulating development and function of the male reproductive tract (1–9). CaP is androgen dependent (10), and its growth is mediated by a network of AR-regulated genes that remains to be fully characterized. CaP regresses after androgen deprivation but eventually recurs in the absence of testicular androgen. AR protein expression in most androgen-independent CaP is similar to that in androgen-dependent CaP (11). This finding has raised the possibility that AR becomes reactivated and has a role in promoting androgen-independent growth of CaP. Recent reports based on cotransfection experiments in cultured cell lines suggested that certain growth factors and other kinase inducers may activate AR in the absence of ligand (12–15).

We are using the human CaP xenograft, CWR22 (16–18), to investigate the role of AR and AR-regulated genes in the androgen-independent growth of CaP. CWR22 is propagated by s.c. transplantation in male nude mice supplemented with testosterone. This xenograft retains the characteristics of human CaP including dependence on androgen for growth. Androgen-dependent cells undergo apoptosis after androgen withdrawal, and the tumors regress in size. However, a subset of androgen-responsive cells survives androgen deprivation. These surviving cells that populate the recurrent tumor express AR and increased levels of Bcl-2, an apoptosis inhibitor.[4] Five to 6 months after the removal of testicular androgen stimulation, tumor cells undergo recurrent growth. AR expression in the recurrent, androgen-independent CWR22 tumor is similar to that in the androgen-stimulated CWR22. The high level of nuclear AR in recurrent CWR22 suggested that AR might be a factor in stimulating androgen-independent growth. As a first step in investigating this possibility, we used CWR22 to identify androgen-regulated mRNAs and measured the levels of these mRNAs in CWR22 after castration and upon recurrence of tumor growth. The results demonstrated that expression of AR-regulated genes is up-regulated in androgen-independent CWR22, consistent with reactivation of AR. They also suggest that androgen-regulated genes have a role in androgen-independent growth of CaP.

MATERIALS AND METHODS

Transplantation of CWR22 Tumors

Nude mice were obtained from Harlan Sprague Dawley, Inc. (Indianapolis, IN). CWR22 tumors were transplanted into nude mice containing s.c. testosterone pellets (12.5 mg for sustained release of ~10 μg/day; Innovative Research of America, Sarasota, FL) as described previously (17). Testosterone pellets eliminated the wide variation in serum testosterone of male nude mice and maintained a serum concentration of ~4.0 ng/ml. Intact mice bearing androgen-stimulated tumors and castrated mice (testes and testosterone pellets were removed) carrying regressed or recurrent CWR22 tumors were exposed to methoxyflurane and sacrificed by cervical dislocation. Tumors were harvested rapidly and frozen in liquid nitrogen or fixed in 10% buffered formalin for paraffin embedding. All procedures used were approved by the Institutional Animal Care and Use Committee of the University of North Carolina at Chapel Hill.

RNA Isolation and Northern Hybridization

Total RNA was isolated from CWR22 tumors as described (19). RNA resuspended in sterile H_2O was glyoxylated and fractionated through 1.0%

Received 6/8/98; accepted 10/14/98.

The costs of publication of this article were defrayed in part by the payment of page charges. This article must therefore be hereby marked *advertisement* in accordance with 18 U.S.C. Section 1734 solely to indicate this fact.

[1] Supported by NIH Grants AG11343 (National Cancer Institute Prostate Cancer Cooperative Network; to J. L. M. and F. S. F.), P30 HD18968 (DNA and Tissue Culture Cores), R37 HD04466 (to F. S. F.), P30 CA16086 (Tumor Model Facility), and The American Foundation for Urologic Disease and Merck US Human Health (to C. W. G.).

[2] To whom requests for reprints should be addressed, at Laboratories for Reproductive Biology, Department of Pediatrics, CB# 7500, 382 MSRB, University of North Carolina, Chapel Hill, NC 27599. Phone: (919) 966-0930; Fax: (919) 966-2203; E-mail: fsfrench@med.unc.edu.

[3] The abbreviations used are: AR, androgen receptor; CaP, prostate cancer; hK-2, human kallikrein-2; IGFBP, insulin-like growth factor binding protein; Cdk, cyclin-dependent kinase; CX, castrate; PSA, prostate-specific antigen; TP, testosterone propionate; ARA-70, AR-associated protein-70.

[4] C. W. Gregory, D. Kim, J. L. Mohler, and F. S. French, unpublished results.

agarose gels and transferred to Biotrans nylon membrane (ICN Biomedicals, Inc., Aurora, OH). cDNA probes were labeled with [^{32}P]dCTP (Amersham Corp., Arlington Heights, IL) using the Prime-a-Gene System (Promega Corp., Madison, WI). Membranes were hybridized in aqueous solution (5× SSC, 5× Denhardt's solution, 1% SDS, and 100 μg/ml salmon sperm DNA) overnight at 68°C. After washing at 50°C for 1 h in 0.1× SSC, 0.1% SDS, the membranes were exposed to X-ray film (Eastman Kodak Co., Rochester, NY) with an intensifying screen at −80°C. hK-2 cDNA was kindly provided by Dr. Charles Y-F. Young (Mayo Clinic, Rochester, MN). IκBα cDNA was from Dr. Albert S. Baldwin (University of North Carolina at Chapel Hill). IGFBP cDNAs were provided by Dr. Shunichi Shimasaki (Scripps Research Institute, La Jolla, CA).

Western Immunoblot Analysis of AR

Lysates were prepared from frozen CWR22 tumors. Tumor tissue (100 mg) was pulverized in liquid nitrogen, allowed to thaw on ice, and mixed with 1.0 ml of RIPA buffer with protease inhibitors (PBS, 1% NP40, 0.5% sodium deoxycholate, 0.1% SDS, 0.5 mM phenylmethylsulfonyl fluoride, 10 μM pepstatin, 4 μM aprotinin, 80 μM leupeptin, and 5 mM benzamidine). Tissue was homogenized on ice for 30 s using a Biohomogenizer (Biospec Products, Inc., Bartlesville, OK). Two μl of 0.2 M phenylmethylsulfonyl fluoride were added and the homogenates incubated 30 min on ice. Homogenates were centrifuged at 10,000 × *g* for 20 min; supernatants were collected and centrifuged again to prepare the final lysates. Supernatant protein (100 μg) from each sample was electrophoresed in 12% SDS-polyacrylamide gels, followed by electroblotting to Immobilon-P membrane (Millipore Corp., Bedford, MA) and immunodetection. Anti-human AR monoclonal antibody F39.4.1 (Biogenex, San Ramon, CA) was used at a 1:10,000 dilution. LNCaP cell lysate was used as a positive control on immunoblots. Secondary antibody (goat-anti-mouse IgG conjugated to horseradish peroxidase, Amersham Corp., Arlington Heights, IL) was used for detection by enhanced chemiluminescence (DuPont, NEN Research Products, Boston, MA).

Immunohistochemical Analysis of AR and Ki-67

Formalin-fixed, paraffin-embedded sections of tumor tissue were processed for AR immunostaining using anti-human AR monoclonal antibody F39.4.1. After deparaffinization and rehydration, tissue sections were heated at 100°C for 30 min in a vegetable steamer in the presence of antigen retrieval solution (CITRA, pH 6.0; Biogenex). F39.4.1 antibody was used at a concentration of 0.13 μg/ml and diaminobenzidine was used to detect immunoperoxidase antigen-antibody reaction products.

Ki-67 immunostaining for cellular proliferation was performed with the MIB-1 monoclonal antibody (Oncogene, Cambridge, MA) at an IgG concentration of 0.5 μg/ml (1:50). All other steps were as described for AR immunostaining. Automated digital image analysis to determine the percentage of tumor cells expressing Ki-67 was performed as described (20).

cDNA Library Construction and Screening

Library Construction. Five μg of poly(A)$^+$ mRNA was used to construct directional cDNA libraries in lambda ZAP II (Stratagene, La Jolla, CA) according to the manufacturer's instructions. The primary library from intact, testosterone-stimulated CWR22 represented 0.95 × 10^6 unique clones (>99% recombinant). The primary library from the recurrent CWR22 represented 1.8 × 10^6 unique clones (91% recombinant). Both libraries were amplified once. The average insert size for the libraries was 1.5 kb.

Library Screening. Lambda phage plaques from the primary unamplified CWR22 library were plated at low density. Two or three individual plaques were placed into each 1.5-ml Eppendorf tube containing 500 μl of suspension media plus chloroform. Ten μl of phage stock were PCR amplified in 50 mM KCl, 10 mM Tris (pH 8.3), 1.5 mM $MgCl_2$, 0.001% gelatin, 50 μM primers (standard M13 forward and reverse primers), 0.1 mM deoxynucleotide triphosphate, 1.5 units of Taq (Perkin-Elmer, Foster City, CA), and 0.25 unit cloned Pfu (Stratagene) in a 60-μl reaction. PCR conditions were 95°C for 3 min, 55°C for 3 min, 68°C for 15 min for 1 cycle, then 95°C for 30 s, 55°C for 1 min, and 72°C for 3 min (36 cycles), followed by a 10-min incubation at 72°C.

PCR products were run on duplicate 1.5% Tris-borate-EDTA agarose gels. After electrophoresis, the gels were photographed and treated for 20 min in 0.4 M NaOH. DNA was transferred to a positively charged nylon membrane (Biotrans, ICN, Costa Mesa, CA) in 0.4 M NaOH by overnight capillary transfer. After transfer, membranes were washed for 10–15 min in 2× SSC followed by 5 min in double-distilled H_2O. Membranes were air-dried and stored at 4°C until hybridization.

Radiolabeled first-strand cDNA was prepared from poly(A)$^+$ mRNA as described previously (21) and used to screen the CWR22 intact library by Southern hybridization. Probes from CWR22 intact and 2-day CX mice were hybridized with duplicate Southern blots (30 lanes, each lane containing a pool of 2–3 pfu). Prehybridization of the duplicate Southerns was done in 5× SSC, 5× Denhardt's, 1% SDS, and 100 μg/ml single-strand DNA at 68°C for 2–3 h. Hybridization was performed overnight at 68°C using either CWR22 intact or CWR22 2-day CX cDNA probes at 10^6 cpm/ml. After hybridization, the blots were washed briefly in 2× SSC-0.1% SDS, followed by 1 h at 50°C in 0.1× SSC-0.1% SDS. Autoradiographs of the duplicate Southern blots hybridized to intact and 2-day CX cDNA probes were analyzed to identify bands with differential hybridization to the two probes. Phage plaques corresponding to bands tentatively identified as being androgen-regulated were plaque purified and reanalyzed by Southern hybridization to confirm androgen regulation. Confirmation of androgen regulation of the mRNA was done using Northern blot analysis. Blots containing total RNA from CWR22 intact, 2-day CX, 6-day CX, 6-day CX + 24 h of TP, and recurrent CWR22 tumors were hybridized to radiolabeled probe prepared from plaque-purified phage.

RNase Protection Assay

The RiboQuant Multiprobe RNase Protection Assay System (PharMingen, San Diego, CA) was used to quantitate mRNA transcripts for Cdk1–4 and p16. Ten μg of total RNA from each of the CWR22 tumors were hybridized with the radiolabeled hCC-1 multiprobe template set (PharMingen) according to the manufacturer's instructions. After RNase treatment, protected probes were resolved on 5% polyacrylamide sequencing gels, followed by exposure of the dried gel to BioMax MR film (Kodak) overnight at −70°C.

RESULTS

AR protein expression in CWR22 human CaP xenografts was determined using immunohistochemical and Western blot analyses. AR staining in nuclei of epithelial cells was abundant in CWR22 tumors from androgen-stimulated intact mice (Fig. 1*A*) and decreased 1–4 days after castration (Fig. 1*B*) during the period of most rapid apoptosis. At 6 days after castration (Fig. 1*C*), AR protein was increased and remained so at 12 days (not shown). In the CWR22 tumor that recurred 5 months after androgen withdrawal (Fig. 1*D*), the intensity of AR staining and strong nuclear localization was similar to that observed in CWR22 tumors from intact androgen-stimulated mice. Western blotting yielded similar results (Fig. 2). AR in the intact androgen-stimulated CWR22 decreased within 1 day after castration, increased 6 and 12 days after castration, but was less than in the recurrent tumor. In the recurrent tumor, AR protein levels were similar to those in CWR22 from androgen-stimulated intact mice. AR mRNA expression was determined by Northern analysis. A normal-sized transcript of 9.6 kb was present, and bands of similar intensity were obtained with CWR22 tumors of androgen-stimulated intact mice and recurrent CWR22 tumors from CX mice (Fig. 3).

Differential expression screening of cDNA libraries constructed from CWR22 tumors was performed to identify androgen-regulated genes in human CaP. A total of 1652 plaques were screened initially by this method (936 from intact CWR22 library and 696 from the recurrent CWR22 library). A second screening to eliminate false positives resulted in 48 regulated clones. Northern blot analysis confirmed androgen regulation of 24 clones. PSA was identified twice, whereas seven clones had no homology to DNA sequences in GenBank (National Center for Biotechnology Information, Bethesda, MD). The remaining 15 clones had sequence homology to transcripts identified previously. Both α-enolase and α-tubulin showed strong

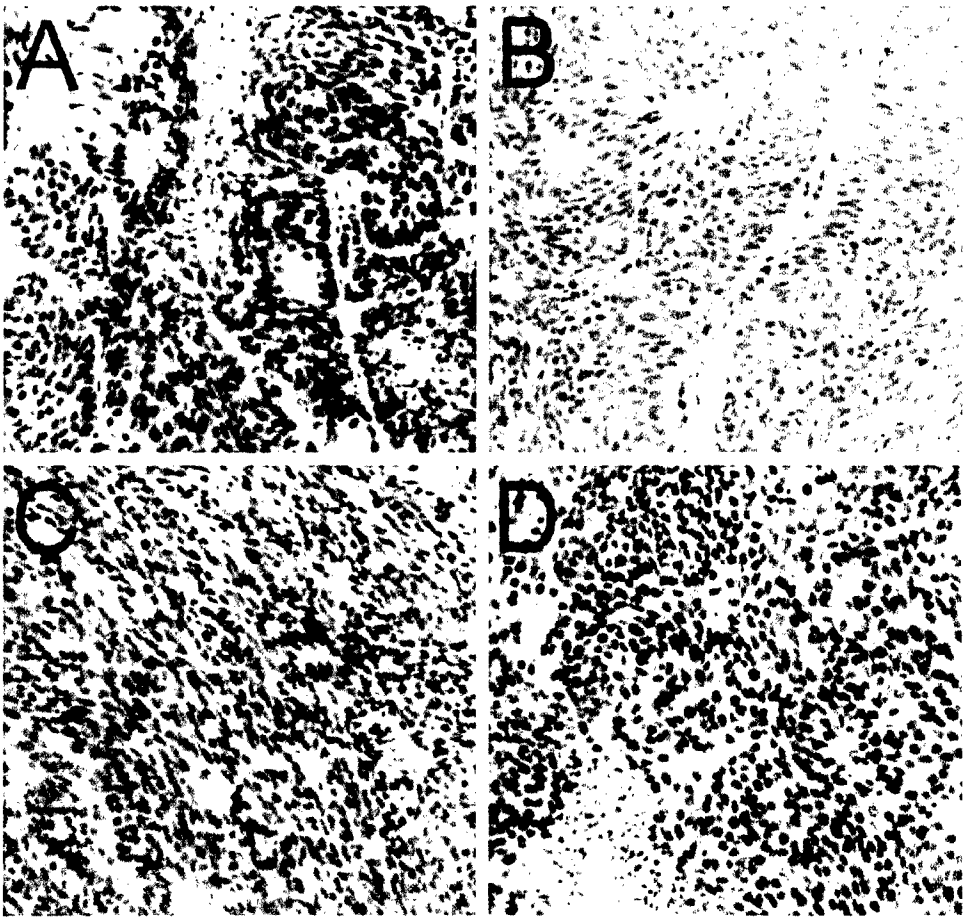

Fig. 1. AR protein localization in CWR22 tumors. Immunostaining for AR was performed on paraffin-embedded sections of CWR22 tumors. Nuclei stained for AR in the majority of cells in CWR22 tumors from intact mice (*A*), whereas AR immunostaining was reduced 1 day after castration (*B*). AR immunostaining increased slightly at 6 days after castration as compared with 1-day castrates (*C*). Recurrent CWR22 tumors growing in the absence of testicular androgen expressed nuclear AR at levels similar to those of androgen-stimulated CWR22 tumors from intact mice (*D*).

up-regulation by androgen, whereas testosterone-repressed prostate message-2 was down-regulated. Vascular endothelial growth factor and mitochondrial hinge protein mRNAs were up-regulated by androgen but <2-fold (data not shown). Several ribosomal protein mRNAs and other unknown transcripts were regulated minimally either in an up or downward direction.

The effects of castration and androgen replacement on mRNAs for a prostate-specific homeobox gene, *Nkx3.1*, and the human kallikrein gene, *hK-2*, both of which are androgen-regulated in human prostate (22–24), were demonstrated using Northern hybridization (Fig. 4). IGFBP-5 was androgen up-regulated, whereas other IGFBP mRNAs (IGFBP-2, IGFBP-3, and IGFBP-6) were unchanged (data not shown). We also found that the AR coactivator ARA-70 was androgen up-regulated. As shown in Fig. 4, the levels of all these mRNAs were decreased 6 and 12 days after castration when compared with the levels in CWR22 tumors from androgen-stimulated intact mice. Treatment of the 6- and 12-day CX mice with TP (0.1 mg/animal) for 24, 48, or 72 h increased the level of each of these mRNA transcripts, implicating AR in the control of their expression. In the CWR22 tumor that recurred in the absence of testicular androgen, levels of all these androgen-regulated mRNAs increased compared with castrates and were similar to those in CWR22 tumors from androgen-stimulated intact mice (Fig. 4).

Androgen regulation of genes controlling cell cycle progression in CWR22 tumors was investigated using RNase protection assays to compare the levels of mRNA transcripts encoding the *Cdks* (*Cdk* 1–4) and the *Cdk* inhibitor *p16* (Fig. 5). Androgen withdrawal from CWR22 tumors for 6 or 12 days resulted in down-regulation of *Cdk1* and *Cdk2* and up-regulation of *p16*. Testosterone treatment of 6- or 12-day CX animals resulted in up-regulation within 24 h of *Cdk1* and *Cdk2* and down-regulation of p16. In recurrent CWR22, *Cdk1* and *Cdk2* were expressed at levels similar to those of the androgen-stimulated CWR22 from intact mice. However, levels of *p16* were variable in 10 different recurrent CWR22 tumors examined. *Cdk4* levels did not change appreciably after castration or with testosterone replacement. Ki-67 immunostaining, which correlates well with bromodeoxyuridine incorporation and thymidine labeling (25), was used to estimate cellular proliferation in CWR22 tumors (Fig. 6). The percentage of Ki-67-positive cells decreased from 79.4 ± 3.6 in tumors from intact mice to 0.8 ± 0.5 at 6 days after castration. Injection of TP (0.1 mg) increased Ki-67 immunostaining to 4.5 ± 0.42 within 24 h and to 31.0 ± 6.7% positive within 48 h. CWR22 tumors that recurred in the absence of testicular androgen demonstrated a high percentage of Ki-67-positive cells (67.1 ± 3.3) similar to that of CWR22 tumors from intact mice.

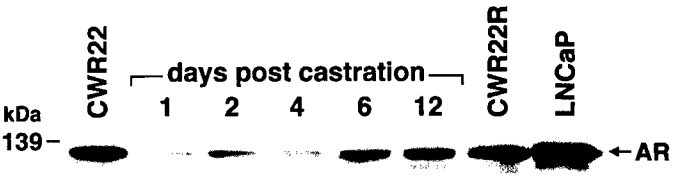

Fig. 2. Western immunoblot analysis of AR protein in CWR22 tumors. Tumor lysates were subjected to Western blot analysis using a monoclonal AR antibody. An AR protein of 110–114 kDa was present in lysates of androgen-stimulated CWR22 tumors from intact mice. AR protein decreased from 1 to 4 days but increased between 6 and 12 days after castration. AR protein in recurrent CWR22 (*CWR22R*) tumors was similar to levels in the intact CWR22. LNCaP cell lysate was used as a positive control for AR. The position of the molecular mass marker (kDa) is indicated. This experiment was performed with two to four different tumors at each time point with similar results.

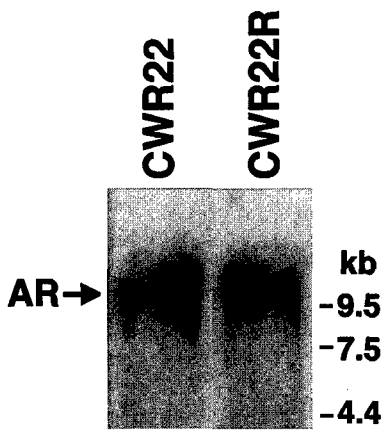

Fig. 3. Northern blot analysis of AR mRNA in CWR22 and recurrent CWR22. Steady-state AR mRNA levels were similar in the androgen-stimulated CWR22 from intact mice and recurrent CWR22 (*CWR22R*) tumors from CX mice. The position of molecular mass markers (kilobases) are indicated.

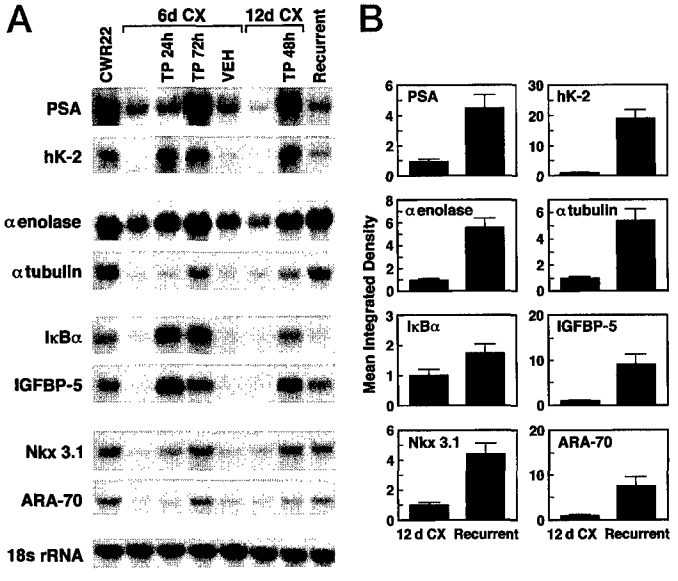

Fig. 4. *A*, Northern blot analysis of androgen-regulated genes in CWR22. Total RNA from CWR22 tumors was analyzed by Northern analysis to examine androgen-regulated changes in expression of several transcripts. All mRNAs examined decreased after castration (6 or 12 days) of mice bearing CWR22 tumors. Treatment of castrated mice with TP for 24, 48, or 72 h restored expression of the mRNAs to levels seen in the intact CWR22. Recurrent CWR22 tumors growing in the absence of testicular androgens expressed the androgen up-regulated mRNAs at levels similar to the mRNA levels in intact CWR22 tumors (non-CX mice containing testosterone pellets). 18S rRNA was used as a control for mRNA loading variability. In *B*, densitometry results compare integrated band densities for all genes examined in CWR22 tumors 12 days after castration with recurrent CWR22 tumors and represent the means of results from three different tumor RNAs at each time point; *bars*, SE. The integrated density of 12-day CX samples was arbitrarily set to 1.0 so that fold induction in the recurrent samples can be appreciated.

DISCUSSION

The levels of AR protein found in CWR22 tumors that recurred 5–6 months after castration were similar to AR levels in most androgen-independent CaPs (11, 26) and allowed this xenograft to be used as a model for determining the role of AR in androgen-independent growth. Because AR is a transcription factor essential to the growth of androgen-dependent CaP, reactivation of AR in the absence of testicular androgen may promote growth in androgen-independent CaP. As a first step in testing this hypothesis, we searched for androgen-regulated mRNAs in androgen-dependent CWR22 and measured levels of expression of these androgen-regulated mRNAs in the recurrent CWR22. Several androgen-regulated mRNAs were identified in CWR22 based on decreased steady-state levels after castration and increased levels after testosterone replacement. In the recurrent tumors, the levels of all androgen-regulated mRNAs were higher than in CWR22 tumors after castration and similar to levels in androgen-stimulated tumors from intact mice. This novel observation is consistent with AR induction of gene transcription in androgen-independent CaP. It suggests also that growth of androgen-independent tumor cells is stimulated by a network of AR-regulated genes.

Several factors are known to control *AR* gene transcription in mammalian cell lines (27–38); however, the specific factors that induce AR expression in CaP remain unknown. Increased AR expression in a significant number of androgen-independent CaPs may result from amplification of the *AR* gene locus. *AR* gene amplification was present in ~30% of CaPs that relapsed after androgen deprivation but in none of the original primary tumors (39). In a series of 54 locally recurrent CaPs from patients who survived for 1 year or more on androgen deprivation therapy, comparative genomic hybridization and interphase fluorescence *in situ* hybridization demonstrated amplification in 15 tumors (40). Amplification was associated with increased expression of AR mRNA and may contribute to the AR expression in recurrent CWR22; however, this remains to be determined.

AR and androgens are essential for development, growth, and function of the prostate. In human and other mammalian species, castration results in apoptosis and loss of androgen-dependent prostate cells. In normal prostate cells that survive androgen deprivation, AR does not become reactivated in the absence of testicular androgen (41). However, in CaP cells, genetic alterations occurring during the months after androgen deprivation might turn on signaling mechanisms and reactivate AR-induced transcription independent of androgen or at a lower concentration of androgen or other steroids (42). AR activation might result from direct effects on AR that alter its structure or phosphorylation state or indirect effects involving protein-protein interactions with AR coactivators or repressors. Modulators of protein kinases A and C might activate AR in the absence of ligand by altering AR phosphorylation (43–46). Other AR-activating pathways might be mediated by transmembrane receptors for growth factors. Studies on CaP cell lines suggested that keratinocyte growth factor, epidermal growth factor, and IGF-I signaling pathways activate AR in

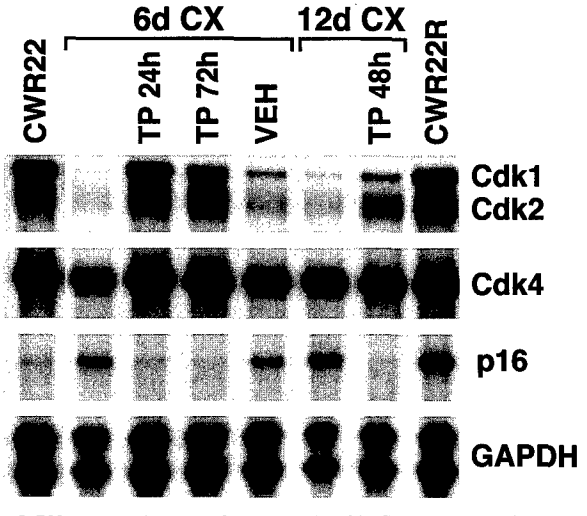

Fig. 5. RNase protection assay for Cdks and p16 in CWR22 tumors. Cdk1 and Cdk2 mRNAs were androgen up-regulated in CWR22 tumors, whereas Cdk4 mRNA levels were unchanged after castration or testosterone treatment. Cdk1 and Cdk2 mRNA levels in recurrent CWR22 (*CWR22R*) tumors were similar or higher than those in intact CWR22 tumors. p16 was negatively regulated by androgens and showed variable expression in recurrent CWR22 tumors. Glyceraldehyde-3-phosphate dehydrogenase (*GAPDH*) is included as a loading control. *6d* and *12d*, 6-day and 12-day, respectively.

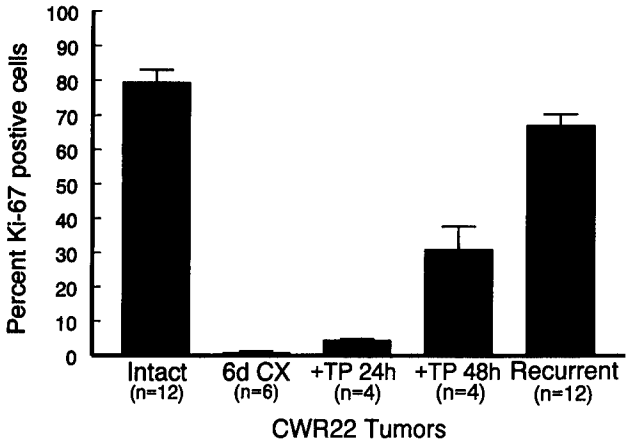

Fig. 6. Quantitative analysis of Ki-67 immunostaining in CWR22 tumors. Cellular proliferation decreased 80-fold 6 days after castration of CWR22-bearing mice. TP (0.1 mg/animal) administration to 6-day CX mice caused a <5-fold increase at 24 h and a >30-fold increase after 48 h. Recurrent CWR22 tumors showed a percentage of Ki-67-positive cells similar to that seen in androgen-stimulated CWR22 tumors from intact mice. *Bars,* SE.

the absence of androgen (47). With respect to IGF-I, our results suggest a mechanism whereby its signaling may be enhanced in the recurrent tumor. Because IGFBP-5 is up-regulated by AR[5] and is a positive modulator of IGF-I in some tissues (48), IGFBP-5 may amplify IGF-I activation of AR in the recurrent tumor thereby creating a self-perpetuating autocrine feedback loop at the level of the IGF-I receptor. Moreover, PSA and hK-2 are AR-regulated members of the human kallikrein family of serine proteases that degrade the IGF-I inhibitor, IGFBP-3 (48). Thus, the increased expression of these proteases in the recurrent tumor could further enhance the activity of IGF-I.

PSA and *hK-2* genes are transcriptionally up-regulated by androgen and contain androgen response elements in their 5′ flanking regions (49–53). Additional upstream *PSA* gene enhancer elements have been identified that amplify androgen responsiveness in a cell type-specific manner, suggesting that other DNA-binding proteins cooperate with AR in amplifying the transcriptional response (49). Studies on several AR-regulated genes indicated that DNA-binding proteins, some of which are androgen-regulated, cooperate with AR in the induction of gene transcription (3–6, 54–57). However, these interacting factors remain to be characterized, and as yet no factor has been shown to induce transcription of these genes in the absence of AR. This leads to the question: What accounts for the increased expression of PSA and hK-2 in CaP that recur after androgen deprivation? The increase in serum PSA associated with tumor recurrence during androgen deprivation treatment has often been explained on the basis of increased tumor volume; however, our studies on CWR22 demonstrate that PSA mRNA is increased per tumor weight. In a recent clinical study of 46 patients undergoing treatment for CaP, de Vere White *et al.* (11) obtained results on AR and PSA similar to our findings in CWR22. In patients who underwent a relatively short period of "combined androgen blockade" for downsizing prior to radical prostatectomy, most residual CaP expressed AR but low to undetectable PSA, whereas CaP that relapsed after a longer period of androgen blockade expressed both AR and PSA, indicating a link between AR and PSA expression in androgen-independent CaP. Factors that modulate PSA expression in androgen-responsive cells may act by enhancing the action of AR. PSA-stimulating activity was identified by Hsieh *et al.* (58) in conditioned medium of an LNCaP cell subline derived from a s.c. xenograft that exhibited relapsed growth after castration of the host male nude mouse. The conditioned medium was active in the absence of testosterone; however, the LNCaP cells expressing PSA were androgen responsive, suggesting the possibility that AR could have mediated the increase in PSA expression. Similarly, vitamin D (1,25-dihydroxyvitamin D_3) increased PSA secretion and inhibited growth of cultured LNCaP cells through what was believed to be an effect on cell differentiation (59). Moreover, Gleave *et al.* (60) demonstrated an increase in LNCaP PSA mRNA expression by treatment with transforming growth factor β that was independent of cellular proliferation.

The finding that several AR-controlled genes are up-regulated in androgen-independent CWR22 strengthens the concept that AR has a role in mediating androgen-independent growth and emphasizes further the importance of identifying AR-regulated, growth-promoting genes. *ARA-70* was first identified in a thyroid carcinoma as a *RET* fusion gene in which 790 5′-nucleotides of the *ARA-70* gene were fused to the tyrosine kinase domain of the *RET* oncogene. The full significance of this rearrangement remains to be established; however, the *RET* gene is mutated frequently in papillary thyroid carcinomas (61). ARA-70 is reported to be an AR coactivator and potentiates the transcriptional activity of AR in DU-145 cells cotransfected with a reporter gene (62). Its up-regulation in recurrent CWR22 could amplify effects of other ligand-independent AR activators.

The *Nkx3.1* gene encodes a 234-amino acid homeodomain protein and is a homologue of the Drosophila *Nk-3* gene (63). Human and mouse proteins are identical within the homeodomain region. In mouse prostate and seminal vesicle, Nkx3.1 mRNA increases in parallel with androgen stimulation of sexual development, and castration reduces mRNA levels in sexually mature mice (64). Nkx3.1 mRNA was demonstrated in prostate and to a lesser extent in testis in adult human males. It is also expressed in LNCaP cells and up-regulated by androgen. Expression was not detected in the PC-3 or DU-145 androgen-independent cell lines that lack AR (23). The *Nkx3.1* gene maps to chromosome 8p2.1, a region commonly mutated in prostate cancer. However, in 50 CaP tissue specimens removed at radical prostatectomy, only one deletion was found, and no sequence-altering mutation was detected in the Nkx3.1 coding region (65). Chromosome 8 alleles are present in both CWR22 and recurrent CWR22 (16), and their *Nkx3.1* mRNAs are of equal size. Homeodomain proteins have the ability to route extracellular signals to specific target genes through protein-protein interactions (66–68). Thus, *Nkx3.1* may integrate a number of growth-promoting signals in both the androgen-dependent and androgen-independent CWR22.

α-Enolase is the glycolytic enzyme that converts 2-phosphoglycerate to phosphoenolpyruvate, the precursor of pyruvate. Glycolysis is believed to have an important role in DNA synthesis (69). Oxidative decarboxylation of pyruvate to form acetyl-CoA links glycolysis with the citric acid cycle. Human and rat prostate secrete large amounts of citric acid formed by the reaction of acetyl-CoA with oxaloacetate and H_2O. Citric acid production is androgen dependent. In the rat, androgens increase the expression of pyruvate dehydrogenase-E1 that catalyzes the conversion of pyruvate to acetyl-CoA and mitochondrial aspartate aminotransferase that converts aspartate to oxaloacetate. The latter was regulated by a combined increase in transcription rate and mRNA stabilization (70–72).

α-Tubulin and β-tubulin subunits, together with their associated proteins, make up the mitotic apparatus, a microtubule machine for separating chromosomes. α-Tubulin has been considered a constitutive housekeeping gene; however, our data indicate its expression is regulated either directly or indirectly by androgen in CWR22. The relatively slow increase in α-tubulin mRNA in response to androgen

[5] C. W. Gregory, D. Kim, P. Ye, A. J. D'Ercole, J. L. Mohler, and F. S. French. Androgen receptor up-regulates insulin-like growth factor binding protein-5 (IGFBP-5) expression in a human prostate cancer xenograft, submitted for publication.

suggests it is a secondary response gene perhaps controlled by multiple gene products, some of which are androgen-regulated. Androgen regulation of α-tubulin may link AR action to cell division in CaP.

Cdks together with cyclins control the normal progression of cells through the cell cycle. Aberrant activation of Cdks may potentiate the growth of certain cancers (73), including CaP. Cdk2 and Cdk4 were positively regulated by androgen in cultured LNCaP cells in association with increased cellular proliferation (74). Cdk1 and Cdk2 mRNAs in androgen-dependent CWR22 decreased after castration and were up-regulated by androgen replacement. In the recurrent CWR22, Cdk1 and Cdk2 mRNAs were expressed at levels similar to those in androgen-dependent CWR22 tumors from intact mice. Cdk4 mRNA remained unchanged after castration or androgen replacement. The up-regulation of Cdk1 and Cdk2 mRNAs after testosterone replacement in 6-day CX mice coincided with an increase in cellular proliferation (as assessed by Ki-67 immunohistochemistry). Whereas protein synthesis and subsequent phosphorylation or dephosphorylation is required for Cdk complex formation with cyclins, our data suggest that AR induction of Cdk1 and Cdk2 mRNA expression is an important step in reactivating the cell cycle. Cdk1, which appeared to be strongly androgen-regulated, complexes with cyclin B and is activated by dephosphorylation just prior to mitosis (75). Negative regulation of the Cdk inhibitor p16 in CWR22 would diminish the inhibitory effect of p16, further enhancing the initiation of cellular proliferation. However, p16 mRNA levels were variable in recurrent CWR22 tumors. Chi *et al.* (76) found similar variability in p16 mRNA expression in 116 human prostate tissue specimens, with 43% of untreated primary CaP showing reduced expression.

Our results indicate that a network of androgen-regulated genes has a role in driving the growth of androgen-independent CaP. Furthermore, they provide a conceptual framework within which to investigate further the role of AR and to identify additional gene products important in the recurrence of CaP after androgen deprivation. The expression of AR and androgen-regulated genes in androgen-independent CaP suggests AR is active in the absence of testicular androgen. Alternatively, a compensatory transcriptional or mRNA-stabilizing mechanism common to androgen-regulated genes might become activated in the absence of androgen stimulation. Pursuit of these possibilities should lead to a better understanding of the transition of CaP from androgen-dependent to androgen-independent growth.

ACKNOWLEDGMENTS

The authors would like to thank Dr. Edward P. Gelmann for sharing his results on *Nkx3.1* prior to publication. We also appreciate the excellent technical assistance of Joseph Giaconia, Natalie Edmund, and Yeqing Chen.

Note Added in Proof

Regulation of androgen receptor gene expression through a TPA (12-*O*-tetradecanoylphorbol-13-acetate)-response element is described in: Kumar, M. V., Jones, E. A., Felts, J. S., Blexrud, M. D., Grossmann, M. E., Blok, L. J., Schmidt, L. J., and Tindall, D. J.: Characterization of a TPA response element in the 5′-flanking region of the androgen receptor gene. J. Androl., *19:* 595–602, 1998.

Another recent paper describes the isolation from and androgen regulation of NKX3.1 in LNCaP cells: Prescott, J. S., Blok, L., and Tindall, D. J.: Isolation and regulation of the human homeobox cDNA, NKX3.1. Prostate, *35:* 71–80, 1998.

REFERENCES

1. Lubahn, D. B., Joseph, D. R., Sullivan, P. M., Willard, H. F., French, F. S., and Wilson, E. M. Cloning of human androgen receptor complementary DNA and localization to the X chromosome. Science (Washington DC), *240:* 327–330, 1988.
2. Lubahn, D. B., Joseph, D. R., Sar, M., Tan, J., Higgs, H., Larson, R. E., French, F. S., and Wilson, E. M. The human androgen receptor: complementary deoxyribonucleic acid cloning, sequence analysis and gene expression in prostate. Mol. Endocrinol., *2:* 1265–1275, 1988.
3. Tan, J-A., Joseph, D. R., Quarmby, V. E., Lubahn, D. B., Sar, M., French, F. S., and Wilson, E. M. The rat androgen receptor: primary structure, autoregulation of its messenger RNA and immunocytochemical localization of the receptor protein. Mol. Endocrinol., *2:* 1276–1285, 1988.
4. Tan, J-A., Marschke, K. B., Ho, K-C., Perry, S. T., Wilson, E. M., and French, F. S. Response elements of the androgen-regulated *C3* gene. J. Biol. Chem., *267:* 4456–4466, 1992.
5. Ho, K-C., Marschke, K. B., Tan, J-A., Power, S. G. A., Wilson, E. M., and French, F. S. A complex response element in intron 1 of the androgen-regulated 20-kDa protein gene displays cell type-dependent androgen receptor specificity. J. Biol. Chem., *268:* 27226–27235, 1993.
6. Avellar, M. C. W., Gregory, C. W., Power, S. G. A., and French, F. S. Androgen-dependent protein interactions within an intron 1 regulatory region of the 20-kDa protein gene. J. Biol. Chem., *272:* 17623–17631, 1997.
7. Zhou, Z., Corden, J. L., and Brown, T. R. Identification and characterization of a novel androgen response element composed of a direct repeat. J. Biol. Chem., *272:* 8227–8235, 1997.
8. Zhou, Z-X., Wong, C-I., Sar, M., and Wilson, E. M. The androgen receptor: an overview. Recent Prog. Horm. Res., *49:* 249–274, 1994.
9. Quigley, C. A., DeBellis, A., Marschke, K. B., el-Awady, M. K., Wilson, E. M., and French, F. S. Androgen receptor defects: historical, clinical, and molecular perspectives. Endocr. Rev., *16:* 271–321, 1995.
10. Huggins, C., and Hodges, C. V. The effect of castration, of estrogen and of androgen injection on serum phosphatases in metastatic carcinoma of the prostate. Cancer Res., *1:* 293–297, 1941.
11. De Vere White, R. W., Meyers, F., Chi, S-G., Chamberlain, S., Siders, D., Lee, F., Stewart, S., Gumerlock, P. H. Human androgen receptor expression in prostate cancer following androgen ablation. Eur. Urol., *31:* 1–6, 1997.
12. Culig, Z., Hobisch, A., Cronauer, M. V., Radmayr, C., Trapman, J., Hittmair, A., Bartsch, G., and Klocker, H. Androgen receptor activation in prostate tumor cell lines by insulin-like growth factor-1, keratinocyte growth factor, and epidermal growth factor. Cancer Res., *54:* 5474–5478, 1994.
13. Ikonen, T., Palvimo, J. J., Kallio, P. J., Reinikainen, P., and Janne, O. A. Stimulation of androgen-regulated transactivation by modulators of protein phosphorylation. Endocrinology, *135:* 1359–1399, 1994.
14. De Ruiter, P. E., Teuwen, R., Trapman, J., Dijkema, R., and Brinkmann, A. O. Synergism between androgens and protein kinase C on androgen-regulated gene expression. Mol. Cell. Endocrinol., *110:* 41–46, 1995.
15. Nazareth, L. V., and Weigel, N. L. Activation of the human androgen receptor through a protein kinase A signaling pathway. J. Biol. Chem., *271:* 19900–19907, 1996.
16. Nagabhushan, M., Miller, C. M., Pretlow, T. P., Giaconia, J. M., Edgehouse, N. L., Schwartz, S., Kung, H-J., de Vere White, R. W., Gumerlock, P. H., Resnick, M. I., Amini, S. B., and Pretlow, T. G. CWR22: the first human prostate cancer xenograft with strongly androgen-dependent and relapsed strains both *in vivo* and in soft agar. Cancer Res., *56:* 3042–3046, 1996.
17. Wainstein, M. A., He, F., Robinson, D., Kung, H-J., Schwartz, S., Giaconia, J. M., Edgehouse, N. L., Pretlow, T. P., Bodner, D. R., Kursh, E. D., Resnick, M. I., Seftel, A., and Pretlow, T. G. CWR22: androgen-dependent xenograft model derived from a primary human prostatic carcinoma. Cancer Res., *54:* 6049–6052, 1994.
18. Tan, J-A., Sharief, Y., Hamil, K. G., Gregory, C. W., Zang, D-Y., Sar, M., Gumerlock, P. H., de Vere White, R. W., Pretlow, T. G., Harris, S. E., Wilson, E. M., Mohler, J. L., and French, F. S. Dehydroepiandrosterone activates mutant androgen receptors expressed in the androgen-dependent human prostate cancer xenograft CWR22 and LNCaP cells. Mol. Endocrinol., *11:* 450–459, 1997.
19. Chirgwin, J. M., Przybyla, A. E., MacDonald, R. J., and Rutter, W. J. Isolation of biologically active RNA from sources enriched in ribonucleases. Biochemistry, *18:* 5294–5299, 1979.
20. Kim, D., Gregory, C. W., Smith, G. J., and Mohler, J. L. Immunohistochemical quantitation of androgen receptor expression using color video image analysis. Cytometry, in press, 1998.
21. Hamil, K. G., and Hall, S. H. Cloning of rat Sertoli cell follicle-stimulating hormone primary response complementary deoxyribonucleic acid: regulation of *TSC-22* gene expression. Endocrinology, *134:* 1205–1212, 1994.
22. Bieberich, C. J., Fujita, K., He, W-W., and Jay, G. Prostate-specific and androgen-dependent expression of a novel homeobox gene. J. Biol. Chem., *271:* 31779–31782, 1996.
23. Prescott, J. L., Blok, L., and Tindall, D. J. Isolation and androgen regulation of the human homeobox cDNA, NKX3.1. Prostate, *35:* 71–80, 1998.
24. Young, C. Y. F., Andrews, P. E., and Tindall, D. J. Expression and androgenic regulation of human prostate-specific kallikreins. J. Androl., *16:* 97–99, 1995.
25. Cher, M. L., Chew, K., Rosenau, W., and Carroll, P. R. Cellular proliferation in prostatic adenocarcinoma as assessed by bromodeoxyuridine uptake and Ki-67 and PCNA expression. Prostate, *26:* 87–93, 1995.
26. Ruizeveld de Winter, J. A., Trapman, J., Vermey, M., Mulder, E., Zegers, N. D., and Van Der Kwast, T. H. Androgen receptor expression in human tissues: an immunohistochemical study. J. Histochem. Cytochem., *39:* 927–936, 1991.
27. Tilley, W. D., Marcelli, M., and McPhaul, M. J. Expression of the human androgen receptor gene utilizes a common promoter in diverse human tissues and cell lines. J. Biol. Chem., *265:* 13776–13781, 1990.
28. Baarends, W. M., Themmen, A. P. N., Blok, L. J., Mackenbach, P., Brinkmann, A. O., Meijer, D., Faber, P. W., Trapman, J., and Grootegoed, J. A. The rat androgen receptor gene promoter. Mol. Cell. Endocrinol., *74:* 75–84, 1990.
29. Faber, P. W., van Rooij, H. J., Schipper, H. J., Brinkmann, A. O., and Trapman, J. Two different, overlapping pathways of transcription initiation are active on the

TATA-less human androgen receptor promoter. J. Biol. Chem., *268:* 9296–9301, 1993.
30. Grossmann, M. E., and Tindall, D. J. The androgen receptor is transcriptionally suppressed by proteins that bind single-stranded DNA. J. Biol. Chem., *270:* 10968–10975, 1995.
31. Song, C. S., Her, S., Slomczynska, M., Choi, S. J., Jung, M. H., Roy, A. K., and Chatterjee, B. A distal activation domain is critical in the regulation of the rat androgen receptor gene promoter. Biochem. J., *294:* 779–784, 1993.
32. Gong, Y., Blok, L. J., Perry, J. E., Lindzey, J. K., and Tindall, D. J. Calcium regulation of androgen receptor expression in the human prostate cancer cell line–LNCaP. Endocrinology, *136:* 2172–2178, 1995.
33. Grossman, M. E., Lindzey, J., Kumar, M. V., and Tindall, D. J. The mouse androgen receptor is suppressed by the 5′-untranslated region of the gene. Mol. Endocrinol., *8:* 448–456, 1994.
34. Mizokami, A., Yeh, S-Y., and Chang, C. Identification of 3′,5′-cyclic adenosine monophosphate response element and other *cis*-acting elements in the human androgen receptor gene promoter. Mol. Endocrinol., *8:* 77–88, 1994.
35. Chatterjee, B., Song, C. S., Jung, M. H., Chen, S., Walter, C. A., Herbert, D. C., Weaker, F. J., Mancini, M. A., and Roy, A. K. Targeted overexpression of androgen receptor with a liver-specific promoter in transgenic mice. Proc. Natl. Acad. Sci. USA, *93:* 728–733, 1996.
36. Supakar, P. C., Song, C. S., Jung, M. H., Slomczynska, M. A., Kim, J-M., Vellanoweth, R. L., Chatterjee, B., and Roy, A. K. A novel regulatory element associated with age-dependent expression of the rat androgen receptor gene. J. Biol. Chem., *268:* 26400–26408, 1993.
37. Chen, S., Supakar, P. C., Vellanoweth, R. L., Song, C. S., Chatterjee, B., and Roy, A. K. Functional role of a conformationally flexible homopurine/homopyrimidine domain of the androgen receptor gene promoter interacting with SP1 and a pyrimidine single strand DNA-binding protein. Mol. Endocrinol., *11:* 3–15, 1997.
38. Dai, J. L., and Burnstein, K. L. Two androgen response elements in the androgen receptor coding region are required for cell-specific up-regulation of receptor messenger RNA. Mol. Endocrinol., *10:* 1582–1594, 1996.
39. Visakorpi, T., Hyytinen, E., Koivisto, P., Tanner, M., Keinanen, R., Palmberg, C., Palotie, A., Tammela, T., Isola, J., and Kallioniemi, O-P. *In vivo* amplification of the androgen receptor gene and progression of human prostate cancer. Nat. Genet., *9:* 401–406, 1995.
40. Koivisto, P., Kononen, J., Palmberg, C., Tammela, T., Hyytinen, E., Isola, J., Trapman, J., Cleutjens, K., Noordzij, A., Visakorpi, T., and Kallioniemi, O-P. Androgen receptor gene amplification: a possible molecular mechanism for androgen deprivation therapy failure in prostate cancer. Cancer Res., *57:* 314–319, 1997.
41. Kyprianou, N., and Isaacs, J. T. Activation of programmed cell death in the rat ventral prostate after castration. Endocrinology, *122:* 552–562, 1988.
42. Labrie, F., Belanger, A., Dupont, A., Luu-The, V., Simard, J., and Labrie, C. Science behind total androgen blockade: from gene to combination therapy. Clin. Invest. Med., *16:* 475–492, 1993.
43. Ikonen, T., Palvimo, J. J., Kallio, P. J., Reinikainen, P., and Janne, O. A. Stimulation of androgen-regulated transactivation by modulators of protein phosphorylation. Endocrinology, *135:* 1359–1399, 1994.
44. De Ruiter, P. E., Teuwen, R., Trapman, J., Dijkema, R., and Brinkmann, A. O. Synergism between androgens and protein kinase C on androgen-regulated gene expression. Mol. Cell. Endocrinol., *110:* 51–56, 1995.
45. Nazareth, L. V., and Weigel, N. L. Activation of the human androgen receptor through a protein kinase A signaling pathway. J. Biol. Chem., *271:* 19900–19907, 1996.
46. Culig, Z., Hobisch, A., Hittmair, A., Cronauer, M. V., Radmayr, C., Zhang, J., Bartsch, G., and Klocker, H. Synergistic activation of androgen receptor by androgen and leutinizing hormone-releasing hormone in prostatic carcinoma cells. Prostate, *32:* 106–114, 1997.
47. Culig, Z., Hobisch, A., Cronauer, M. V., Radmayr, C., Trapman, J., Hittmair, A., Bartsch, G., and Klocker, H. Androgen receptor activation in prostate tumor cell lines by insulin-like growth factor-1, keratinocyte growth factor, and epidermal growth factor. Cancer Res., *54:* 5474–5478, 1994.
48. Rajaram, S., Baylink, D. J., and Mohan, S. Insulin-like growth factor-binding proteins in serum and other biological fluids: regulation and functions. Endocr. Rev., *18:* 801–831, 1997.
49. Cleutjens, K. B. J. M., van Eekelen, C. C. E. M., van der Korput, H. A. G. M., Brinkmann, A. O., and Trapman, J. Two androgen response regions cooperate in steroid hormone regulated activity of the prostate-specific antigen promoter. J. Biol. Chem., *271:* 6379–6388, 1996.
50. Cleutjens, K. B. J. M., van der Korput, H. A. G. M., van Eekelen, C. C. E. M., Sikes, R. A., Fasciana, C., Chung, L. W., and Trapman, J. A 6-kb promoter fragment mimics in transgenic mice the prostate-specific and androgen-regulated expression of the endogenous prostate-specific antigen gene in humans. Mol. Endocrinol., *11:* 1256–1265, 1997.
51. Zhang, S., Murtha, P. E., and Young, C. Y. Defining a functional androgen responsive element in the 5′ far upstream flanking region of the prostate-specific antigen gene. Biochem. Biophys. Res. Commun., *231:* 784–788, 1997.
52. Zhang, J., Zhang, S., Murtha, P. E., Zhu, W., Hou, SS-M., and Young, C. Y. F. Identification of two novel *cis*-elements in the promoter of the prostate-specific antigen gene that are required to enhance androgen receptor-mediated transactivation. Nucleic Acids Res., *25:* 3143–3150, 1997.
53. Murtha, P., Tindall, D. J., and Young, C. Y. Androgen induction of a human prostate-specific kallikrein, hKLK2: characterization of an androgen response element in the 5′ promoter region of the gene. Biochemistry, *32:* 6459–6464, 1993.
54. Rhee, M., Dimaculangan, D., and Berger, F. G. Androgen modulation of DNA-binding factors in the mouse kidney. Mol. Endocrinol., *5:* 564–572, 1991.
55. Lund, S. D., Gallagher, P. M., Wang, B., Porter, S. C., and Ganschow, R. E. Androgen responsiveness of the murine β-glucuronidase gene is associated with nuclease hypersensitivity, protein binding, and haplotype-specific sequence diversity with intron 9. Mol. Cell. Biol., *11:* 5426–5434, 1991.
56. Adler, A. J., Danielson, M., and Robins, D. M. Androgen-specific gene activation via a consensus glucocorticoid response element is determined by interaction with nonreceptor factors. Proc. Natl. Acad. Sci. USA, *89:* 11660–11663, 1992.
57. Rennie, P. S., Bruchovsky, N., Leco, K. J., Sheppard, P. C., McQueen, S. A., Cheng, H., Snoek, R., Hamel, A., Bock, M. E., MacDonald, B. S., Nickel, B. E., Chang, C., Liao, S., Cattini, P. A., and Matusik, R. J. Characterization of two *cis*-acting DNA elements involved in the androgen regulation of the probasin gene. Mol. Endocrinol., *7:* 23–36, 1993.
58. Hsieh, J-T., Wu, H-C., Gleave, M. E., von Eschenbach, A. C., and Chung, L. W. K. Autocrine regulation of prostate-specific antigen gene expression in a human prostatic cancer (LNCaP) subline. Cancer Res., *53:* 2852–2857, 1993.
59. Skowronski, R. J., Peehl, D. M., and Feldman, D. Vitamin D and prostate cancer: 1,25-dihydroxyvitamin D3 receptors and actions in human prostate cancer cell lines. Endocrinology, *132:* 1952–1960, 1993.
60. Gleave, M. E., Hsieh, J-T., Wu, H-C., von Eschenbach, A. C., and Chung, L. W. K. Serum prostate specific antigen levels in mice bearing human prostate LNCaP tumors are determined by tumor volume and endocrine and growth factors. Cancer Res., *52:* 1598–1605, 1992.
61. Santoro, M., Dathan, N. A., Berlingieri, M. T., Bongarzone, I., Paulin, C., Grieco, M., Pierotti, M. A., Vecchio, G., and Fusco, A. Molecular characterization of RET/PTC3: a novel rearranged version of the *RET* proto-oncogene in a human thyroid papillary carcinoma. Oncogene, *9:* 509–516, 1994.
62. Yeh, S., and Chang, C. Cloning and characterization of a specific coactivator, ARA70, for the androgen receptor in human prostate cells. Proc. Natl. Acad. Sci. USA, *93:* 5517–5521, 1996.
63. He, W. W., Sciavolino, P. J., Wing, J., Augustus, M., Hudson, P., Meissner, P. S., Curtis, R. T., Shell, B. K., Bostwick, D. G., Tindall, D. J., Gelmann, E. P., Abate-Shen, C., and Carter, K. C. A novel human prostate-specific, androgen-regulated homeobox gene (*NKX3.1*) that maps to 8p21, a region frequently deleted in prostate cancer. Genomics, *43:* 69–77, 1997.
64. Sciavolino, P. J., Abrams, E. W., Yang, L., Austenberg, L. P., Shen, M. M., and Abate-Shen, C. Tissue-specific expression of murine Nkx3.1 in the male urogenital system. Dev. Dyn., *209:* 127–138, 1997.
65. Voeller, H. J., Augustus, M., Madike, V., Bova, G. S., Carter, K. C., and Gelmann, E. P. Coding region of *NKX3.1,* a prostate-specific homeobox gene on 8p21, is not mutated in human prostate cancers. Cancer Res., *57:* 4455–4459, 1997.
66. Gruenberg, D. A., Simon, K. J., Brennan, K., and Gilman, M. Sequence-specific targeting of nuclear signal transduction pathways by homeodomain proteins. Mol. Cell. Biol., *15:* 3318–3326, 1995.
67. Vershon, A. K. Protein interactions of homeodomain proteins. Curr. Opin. Biotechnol., *7:* 392–396, 1996.
68. Mark, M., Rijli, F. M., and Chambon, P. Homeobox genes in embryogenesis and pathogenesis. Pediatr. Res., *42:* 421–429, 1997.
69. Matrisian, L. M., Rautmann, G., Magun, D. I., and Breathnach, R. Epidermal growth factor or serum stimulation of rat fibroblasts induces an elevation in mRNA levels for lactate dehydrogenase and other glycolytic enzymes. Nucleic Acids Res., *13:* 711–726, 1985.
70. Costello, L. C., and Franklin, R. B. Testosterone regulates pyruvate dehydrogenase activity of prostate mitochondria. Horm. Metab. Res., *25:* 268–270, 1993.
71. Costello, L. C., Franklin, R. B., and Liu, Y. Testosterone regulates pyruvate dehydrogenase E1α in prostate. Endocr. J., *2:* 147–151, 1994.
72. Qian, K., Franklin, R. B., and Costello, L. C. Testosterone regulates mitochondrial aspartate aminotransferase gene expression and mRNA stability in prostate. J. Steroid Biochem. Mol. Biol., *44:* 13–19, 1993.
73. Hunter, T., and Pines, J. Cyclins and cancer II: cyclin D and CDK inhibitors come of age. Cell, *79:* 573–582, 1994.
74. Lu, S., Tsai, S. Y., and Tsai, M-J. Regulation of androgen-dependent prostatic cancer cell growth: androgen regulation of CDK2, CDK4, and CKI *p16* genes. Cancer Res., *57:* 4511–4516, 1997.
75. Pines, J. Cyclins and their associated cyclin-dependent kinases in human cell cycle. Biochem. Soc. Trans., *21:* 921–925, 1993.
76. Chi, S-G., de Vere White, R. W., Muenzer, J. T., and Gumerlock, P. H. Frequent alteration of CDKN2 ($p16^{INK4A}$/MTS1) expression in human primary prostate carcinomas. Clin. Cancer Res., *3:* 1889–1897, 1997.

0013-7227/99/$03.00/0
Endocrinology

Vol. 140, No. 5
Printed in U.S.A.

Androgen Receptor Up-Regulates Insulin-Like Growth Factor Binding Protein-5 (IGFBP-5) Expression in a Human Prostate Cancer Xenograft*

CHRISTOPHER W. GREGORY, DESOK KIM, PING YE, A. JOSEPH D'ERCOLE, THOMAS G. PRETLOW, JAMES L. MOHLER, AND FRANK S. FRENCH

The Laboratories for Reproductive Biology (C.W.G., F.S.F.), The Departments of Surgery (Division of Urology) (D.K., J.L.M.) and Pediatrics (C.W.G., F.S.F., P.Y., A.J.D.) and The Lineberger Comprehensive Cancer Center (A.J.D., J.L.M., F.S.F.), The University of North Carolina at Chapel Hill, Chapel Hill, North Carolina 27599, Department of Pathology, Case Western Reserve University, Cleveland, Ohio (T.G.P.)

ABSTRACT

The insulin-like growth factor (IGF) binding proteins (IGFBPs) are important modulators of IGF action in many tissues including human prostate. IGFBPs and the androgen receptor (AR) are expressed in CWR22, an androgen-dependent epithelial cell human CaP xenograft that retains biological characteristics of human CaPs, including regression following androgen withdrawal and recurrent growth of AR-containing cells in the absence of testicular androgens beginning several months after castration. Northern blot and *in situ* hybridization analyses demonstrated that IGFBP-5 is androgen-regulated in CWR22. IGFBP-5 messenger RNA (mRNA) decreased by 90% following castration of tumor-bearing mice compared with noncastrate androgen-stimulated mice. Testosterone treatment of CWR22 tumor-bearing mice 6 or 12 days after castration increased IGFBP-5 mRNA 10- to 12-fold. Levels of other IGFBP mRNAs did not change following androgen withdrawal and replacement. IGFBP-5 protein in tumor extracts bound ^{125}I-labeled IGF-I in ligand blot assays and the amounts of IGFBP-5 measured by immunoblotting paralleled the levels of IGFBP-5 mRNA. Androgen-induced expression of IGFBP5 was at a maximum level within 24 h after testosterone replacement, whereas the major increase in cell proliferation as measured by Ki-67 immunostaining occurred between 24–48 h. This time course suggested IGFBP-5 may be a mediator of androgen-induced growth of CWR22. In tumors that recurred several months following castration, IGFBP-5 mRNA and protein increased to levels that approached those in androgen-stimulated CWR22 tumors from noncastrate mice. IGFBP-5 immunohistochemical staining of prostate tissue specimens from patients was stronger in androgen-dependent and androgen-independent CaP than in areas of intraepithelial neoplasia (PIN) or benign prostatic hyperplasia (BPH). IGFBP-5 mRNA in these specimens was localized predominantly to stromal cells and IGFBP-5 protein to epithelial cell membranes. (*Endocrinology* **140:** 2372–2381, 1999)

CANCER of the prostate (CaP) is the most commonly diagnosed cancer and the second leading cause of cancer deaths in men in the United States (1). Initially, CaP maintains a dependence on androgens characteristic of the normal human prostate. CaP undergoes apoptosis and regresses following androgen withdrawal but eventually recurs in the absence of testicular androgens.

Insulin-like growth factor (IGF)-I and its cognate receptor have been implicated in CaP cell growth (2–4). IGF-I is not produced at detectable levels by prostate epithelial cells, however prostate cells express the type I IGF receptor. Prostate epithelial cells make IGF-II but lack the type II IGF receptor (4). IGF receptor-mediated signaling appears essential to growth of CaP cells because cell proliferation can be inhibited by antibodies directed against IGF-I receptors (5), peptide analogues of IGF-I that block IGF-I receptor function (6), or a stably transfected antisense RNA expression vector that blocks IGF-I receptor expression (7). IGF-I receptor binding was demonstrated in human benign hyperplastic prostate (8). Recent studies by Chan *et al.* (9) demonstrated a positive correlation of serum IGF-I levels and risk of CaP. Men with high serum IGF-I levels (294–500 ng/ml) were 4.3 times more likely to develop CaP than were men with low serum levels of IGF-I. On the other hand, IGFBP-3 levels correlated inversely with the development of CaP suggesting lower serum IGFBP-3 allows greater bioavailability of IGF-I.

IGF binding proteins (IGFBPs) are secretory proteins that have autocrine and paracrine functions as modulators of IGF action. They have both inhibitory and potentiating effects on IGF actions (10). Moreover, recent studies suggest that some IGFBPs may have their own receptor-mediated functions independent of the IGF receptors (11). IGFBP-5 has been shown to potentiate IGF action (12).

In CaP, the majority of androgen-dependent and androgen-independent cells express AR protein. In clinically localized CaP treated with complete androgen blockade before radical prostatectomy, AR messenger RNA (mRNA) expression correlated directly with pathologic stage and Gleason grade (13). Hobisch *et al.* (14) found that all androgen-independent CaP (n = 22) examined immunohistochemically

Received September 2, 1998.
Address all correspondence and requests for reprints to: Frank S. French, The Laboratories for Reproductive Biology, Department of Pediatrics, CB 7500, 382 MSRB, Chapel Hill, North Carolina 27599. E-mail: fsfrench@med.unc.edu.
* Presented at the 80th Annual Meeting of The Endocrine Society, June 1998. Supported by NIH Grants AG-11343 (NCI Prostate Cancer Cooperative Network) (to J.L.M., F.S.F.), P30 HD-18968 (DNA and Tissue Culture Cores), HD-08299 (to A.J.D.), R37 HD-04466 (to F.S.F.), P30 CA16086 (Tumor Model Facility), and The American Foundation for Urologic Disease and Merck U.S. Human Health (to C.W.G.).

were AR positive. AR expression levels differ little between androgen-dependent and androgen-independent CaP (our unpublished results and 14, 15). In a subset of androgen-independent CaP, AR expression may be enhanced by gene amplification. AR gene amplification was reported in 30% of recurrent tumors (7 of 23), with no amplification detected before androgen deprivation therapy (16).

The human CaP xenograft, CWR22, is propagated sc in nude mice and retains biological characteristics exhibited by most human CaPs, including regression following androgen withdrawal and recurrence after several months in the absence of testicular androgen (17–20). The recurrent tumor expresses a level of AR equal to or higher than that of the androgen withdrawn CWR22 and exhibits nuclear AR immunostaining. CWR22 contains a mutant AR (His874Tyr) with altered ligand specificity. The mutant AR exhibits a wild-type AR response to testosterone and dihydrotestosterone but is more responsive than wild-type AR to activation by estradiol and dehydroepiandrosterone (20). Using this human CaP xenograft, we examined the expression and androgen regulation of the IGFBPs. IGFBP-2, -3, -5, and -6 were expressed in both androgen-dependent and androgen-independent CWR22 but only IGFBP-5 was androgen-regulated. In prostate specimens from patients we found that immunostaining of IGFBP-5 was stronger in CaP than in BPH.

Materials and Methods

Nude mice were obtained from Harlan Sprague Dawley, Inc. (Indianapolis, IN). CWR22 tumors were transplanted as described previously (17). Briefly, tumor cell suspensions from a CWR22 primary human CaP xenograft were injected sc into nude mice at 4–8 weeks of age. A 12.5 mg sustained-release testosterone pellet (Innovative Research of America, Sarasota, FL) was placed sc into each animal 2 days before tumor implantation and at 3-month intervals thereafter. When tumors reached a volume of 1 cm^3, the mice were anesthetized with methoxyflurane, castrated, and the testosterone pellets removed. Before tumor removal, intact mice bearing androgen-stimulated tumors and castrated animals with either regressed androgen-stimulated (testosterone propionate 0.1 mg/animal sc) or recurrent tumors were exposed to methoxyflurane and killed by cervical dislocation. Tumors were removed immediately and frozen in liquid nitrogen or fixed in 10% buffered formalin and paraffin embedded. All procedures were approved by the Institutional Animal Care and Use Committee of the University of North Carolina at Chapel Hill.

Specimens of human benign or malignant prostate tissue obtained by transurethral resection or radical retropubic prostatectomy were fixed in 10% buffered formalin for 24 h, washed in PBS for 24 h, and embedded in paraffin.

RNA isolation and Northern blot analysis

Total RNA was isolated from CWR22 tumors as previously described (21). Frozen tumors (100–200 mg) were pulverized in liquid nitrogen and homogenized in 4 ml 4.0 M guanidine thiocyanate (Fluka Chemical Co., Ronkokoma, NY) for 30–60 sec using a homogenizer from Brinkmann Instruments, Inc. (model PT 10/35, Westbury, NY). Samples were centrifuged 10,000 × *g* for 10 min at 4 C and the supernatants layered onto 1.25 ml cesium chloride cushions and centrifuged 36,000 × *g* for 12 h at 4 C. RNA was dissolved in sterile H_2O and ethanol precipitated overnight at −20 C. RNA samples were resuspended in sterile H_2O, glyoxylated, fractionated by electrophoresis in 1.0% agarose gels and transferred to Biotrans nylon membranes (ICN Biomedicals, Inc., Aurora, OH). complementary DNA (cDNA) probes were labeled with ^{32}P-dCTP (Amersham Corp., Arlington Heights, IL) using the Prime-a-Gene System (Promega Corp., Madison, WI). Membranes were hybridized in aqueous solution (5 × standard sodium citrate (SSC), 5 × Denhardt's solution, 1% SDS, and 100 μg/ml salmon sperm DNA) for 12 h at 68 C. After washing, the membranes were exposed to x-ray film (Eastman Kodak Co., Rochester, NY) at −80 C with an intensifying screen. cDNAs for the IGFBPs 1–6 were provided by Dr. S. Shimasaki (The Scripps Research Institute, La Jolla, CA).

Quantitation of IGFBP-5 mRNA levels was performed by scanning Northern blots with an Ultroscan XL Laser Densitometer (LKB, Uppsala, Sweden). RNA loading differences were normalized by scanning the same blots subsequently hybridized with an 18S ribosomal RNA cDNA probe.

In situ hybridization histochemistry (ISHH)

ISHH was performed as described previously (22). Briefly, dewaxed and rehydrated paraffin sections (6 μm) were treated with 0.2 N HCl, washed extensively with PBS, and hybridized with biotin-labeled IGFBP-5 antisense riboprobe. The IGFBP-5 DNA fragment corresponding to bp 558-1201 of rat IGFBP-5 cDNA (23) was PCR amplified and cloned into pBlueScript (SK) vector (Stratagene, La Jolla, CA). Biotin-labeled IGFBP-5 antisense riboprobe was generated using Genius RNA Labeling kit (Boehringer Mannheim, Indianapolis, IN) and T_3 RNA polymerase. The hybridization buffer contained 75% formamide, 10% dextran sulfate, 3 × SSC, 50 mM sodium phosphate, pH 7.4, and approximately 1 ng/μl of probe. After incubation with probe for 16–18 h at 55 C, slides were washed 4 times with 0.2 × SSC for 1 h at 55 C. IGFBP-5 antisense riboprobe was detected with monoclonal antibiotin antibody conjugated with horseradish peroxidase (Boehringer Mannheim, 1:200) and diaminobenzidine tetrachloride (DAB, Aldrich Chemical Co., Inc., Milwaukee, WI). Rodent liver, a tissue lacking detectable IGFBP-5 mRNA (24 and our unpublished observations), was used as a negative control.

Western immunoblot analysis

Lysates were prepared from frozen CWR22 tumors. One-hundred-milligram tumor was pulverized in liquid nitrogen, allowed to thaw on ice, and mixed with 1.0 ml RIPA buffer with protease inhibitors (PBS, 1% NP40, 0.5% sodium deoxycholate, 0.1% SDS, 0.5 mM phenylmethylsulfonyl fluoride, 10 μM pepstatin, 4 μM aprotinin, 80 μM leupeptin, and 5 mM benzamidine). Tissue was homogenized 30 sec on ice using a Biohomogenizer (BioSpec Products, Inc., Bartlesville, OK) and incubated 30 min on ice. Samples were centrifuged at 10,000 × *g* for 20 min at 4 C, supernatants collected and centrifuged again. Aliquots of 100 μg supernatant protein were electrophoresed on 12% SDS-polyacrylamide gels and electroblotted to Immobilon-P membranes (Millipore Corp., Bedford, MA). Antihuman IGFBP-5 monoclonal antibody (Austral Biologicals, San Ramon, CA) was used at 1:1000 dilution for immunodetection. Human recombinant IGFBP-5 (Austral Biologicals) was used as a positive control on immunoblots and ligand blots. Secondary antibody (goat-antimouse IgG conjugated to horseradish peroxidase (Amersham Corp., Arlington Heights, IL)) was detected by enhanced chemiluminescence (DuPont NEN Research Products, Boston, MA).

^{125}I-IGF-I ligand blot analysis

For ligand blot analysis, 50–100 mg frozen tumor tissue was pulverized, lysed, and sonicated for 30 sec in ice cold lysis buffer (20 mM Tris-HCl, pH 7.4, 2% Triton X-100 and 10 mM EDTA) and centrifuged at 12,000 rpm in a microcentrifuge for 5 min at 4 C. Aliquots of 100 μg supernatant protein were separated by SDS-PAGE in 12% gels and electroblotted to nitrocellulose membranes (Schleicher & Schuell, Inc., Keene, NH). Membranes were incubated with hybridization buffer containing ^{125}I-IGF-I (5 × 10^5 cpm/ml) as described previously (25) for ligand blot analysis. Blots were exposed to Biomax MS film (Eastman Kodak Co., Rochester, NY) with an intensifying screen at −80 C for 2–4 days.

Immunohistochemical analysis

Formalin-fixed, paraffin-embedded sections of CWR22 tumors were antigen retrieved by heating at 100 C for 30 min in a vegetable steamer in the presence of antigen retrieval solution (CITRA, pH 6.0, BioGenex

Laboratories, Inc., San Ramon, CA) and cooled for 10 min. Slides were preincubated with 2% normal horse serum for 5 min at 37 C and washed with automation buffer (Fisher Scientific International, Inc., Pittsburgh, PA). AR monoclonal antibody F39.4.1 (BioGenex Laboratories, Inc.) was diluted 1:300 (0.13 μg/ml in PBS containing 0.1% BSA, pH 7.4) and reacted for 120 min at 37 C. Slides were incubated in biotinylated antimouse IgG (Vector Laboratories, Inc., Burlingame, CA) for 15 min at 37 C (1:200 in PBS, pH 7.4) and in horseradish peroxidase-conjugated avidin-biotin complex (Vector Laboratories, Inc.) for 15 min at 37 C (1:100 in PBS, pH 7.4). The immunoperoxidase complexes were visualized using DAB for 8 min at 37 C (0.75 mg/ml in Tris buffer containing 0.003% hydrogen peroxide, pH 7.6). Slides were counterstained with hematoxylin (Gill's formula, 1:6 dilution, Fisher Scientific International, Inc.) for 12 sec.

Monoclonal antibody MIB-1 (Oncogene Science, Inc., Cambridge, MA) reacts with the cell-cycle-associated antigen Ki-67 that is highly expressed during the proliferative phases (G_1, S, G_2, and M) but is absent in the resting phase (G_0) of the cell cycle. Ki-67 staining was performed at an IgG concentration of 0.5 μg/ml (1:50). All other steps were as described for AR immunostaining.

Formalin-fixed, paraffin-embedded sections (6 μm) of human prostate tissue were prepared for IGFBP-5 immunostaining with antihuman IGFBP-5 IgG monoclonal antibody (Austral Biologicals) using a 1:50 dilution (2 μg/ml in PBS). The antigen retrieval method was as described above for AR and Ki-67. Twenty tissue blocks each from benign prostatic hyperplasia (BPH) and androgen-dependent CaP and fifteen blocks from androgen-independent CaP were obtained for study. Tissue specimens of BPH and androgen-dependent CaP usually contained areas of prostatic intraepithelial neoplasia (PIN).

A second immunostaining procedure to identify basal epithelial cells was performed to distinguish between CaP and prostatic intraepithelial neoplasia (PIN) and BPH. Basal epithelial cells in all BPH and the majority of PIN specimens stain positive for the high molecular weight cytokeratins whereas CaP does not contain cytokeratin-positive basal cells (26). Following elution with glycine buffer (pH 2.3) to remove unreacted antibody, all slides were incubated with 1.7 μg/ml 34-β-E12 anti-cytokeratin IgG monoclonal antibody (Enzo Diagnostics, Inc., Farmingdale, NY) for 15 min at 42 C. Antibody reaction was visualized using 3-amino-9-ethylcarbazole (AEC, BioGenex Laboratories, Inc.).

Quantitative analysis of IGFBP-5 immunostaining

Image acquisition. Imaging hardware consisted of a Zeiss Axioskop microscope (Carl Zeiss, Inc., Thornwood, NY), a 3-chip CCD camera (C5810, Hamamatsu Photonics Inc., Hamamatsu, Japan) and camera control board (Hamamatsu Photonics Inc.) and a Pentium-based personal computer. Optical settings were calibrated using procedures described previously (27). Images were sampled throughout histologic sections but areas that contained necrosis, preparation artifacts or the edges of sections were avoided. Three representative fields of view were digitized for each histologic tissue type (as identified by a pathologist): androgen-dependent CaP (n = 20), androgen-independent CaP (n = 15), PIN (n = 20) or BPH (n = 20) for a total of 75 prostatectomy specimens. Each field of view for IGFBP-5-stained slides was digitized at total magnification 600× using a 20× dry objective (numerical aperture [NA] =0.6). A digitized image consisted of 512 by 480 pixels in 16.7 million color modes (but equivalent to 256 grayscale levels).

Digital image analysis. Immunopositive cells were recognized by intense cytoplasmic staining for IGFBP-5 in malignant glands and weak homogeneous staining with focal intense staining in PIN. An automatic image analysis algorithm was developed based on these immunostaining features. Segmentation of glandular areas was done using a convolution of Gaussian function with SD of 10 pixels and an adaptive local thresholding (28). Once the glandular area was segmented, a classification operation was performed to detect image pixels representing intense IGFBP-5 staining. Percent (% positivity) of the immunopositive area within the segmented glandular area was measured.

Statistical analysis. IGFBP-5 positive areas in BPH, PIN, and cancer specimens are expressed as the mean ± SE. Results were compared statistically by ANOVA. Significant differences among the means were determined using Fisher's test with $P < 0.05$.

Results

AR protein in nuclei of tumor epithelial cells, as measured by immunohistochemistry, was similar in the androgen-dependent CWR22 and CWR22 tumors that recurred several months after castration (Fig. 1).

IGFBP expression in CWR22 was examined by Northern hybridization of total RNA (Fig. 2A). IGFBP-2, -3, -5, and -6 mRNAs were detected as single bands of 1.8, 2.6, 6.0, and 1.4 kb, respectively. IGFBP-1 mRNA was not detected, and IGFBP-4 mRNA gave a weak hybridization signal. Of the IGFBP mRNAs expressed in CWR22, only IGFBP-5 was androgen regulated. IGFBP-5 mRNA was decreased by 90% at 6 and 12 days after castration of CWR22-bearing mice and treatment with testosterone increased IGFBP-5 mRNA 10–12 fold within 24 h (Fig. 2, A and B). Proliferation of tumor cells, measured by Ki-67 immunohistochemistry, was reduced in the 6-day castrate to 1% of the intact, was increased 4-fold at 24 h and 40-fold after 48 h of testosterone replacement (Table 1). Cyclohexamide treatment (2.3 mg/mouse injected ip 3 h before tumor removal) of 6 day castrated CWR22-bearing mice did not change the level of IGFBP-5 mRNA, suggesting that message stability was not altered by androgen with-

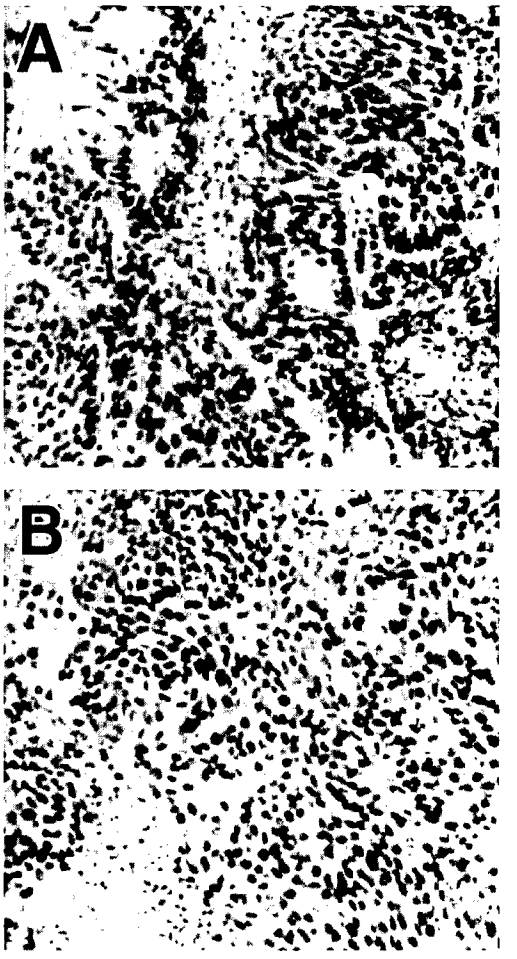

FIG. 1. AR protein levels are similar in CWR22 and recurrent CWR22 tumors. Immunohistochemical staining for AR was performed on paraffin-embedded sections of CWR22 tumors. A, CWR22 tumor from intact, androgen-stimulated male mouse; B, recurrent CWR22 tumor from mouse 150 days post castration.

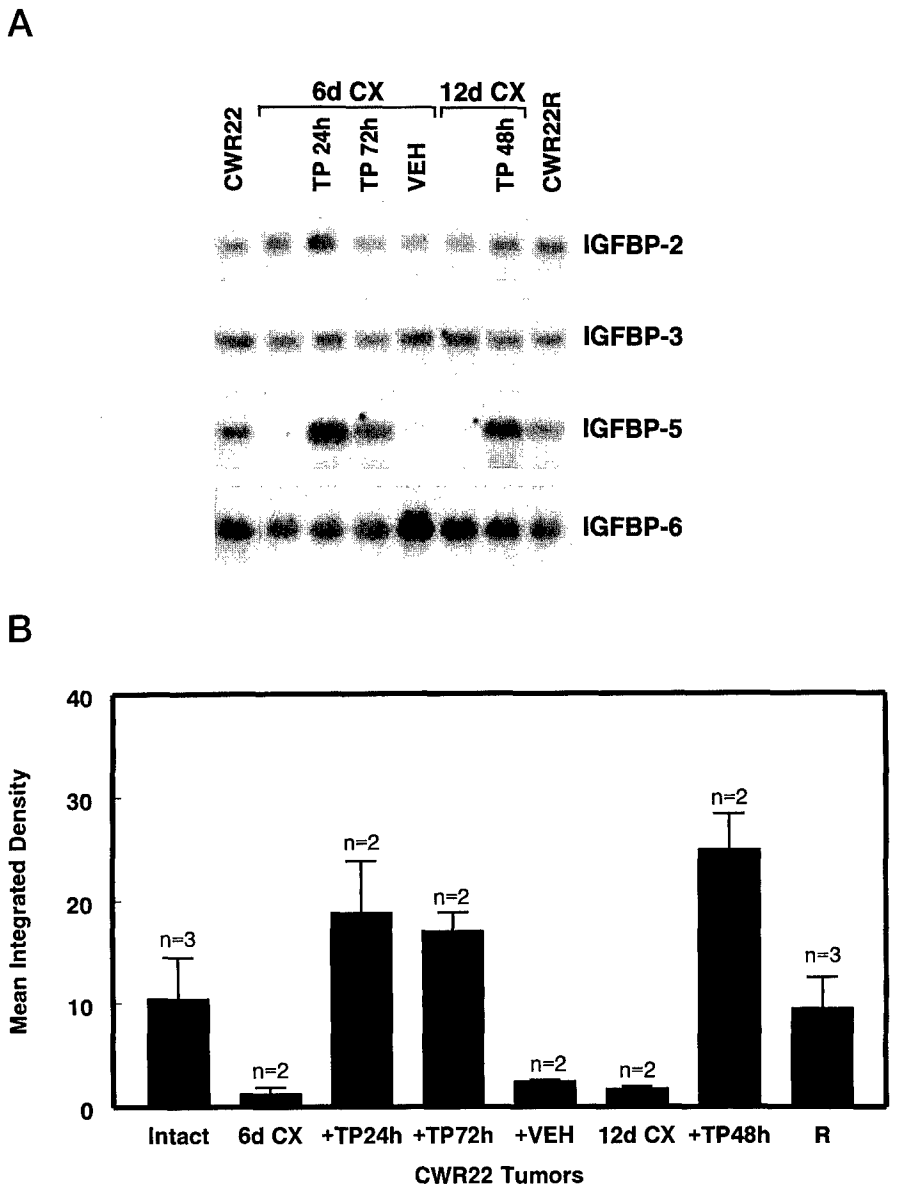

FIG. 2. IGFBP-5 mRNA is androgen-regulated in CWR22 tumors. A, Northern blot analysis was performed using total RNA (10 μg/lane) prepared from CWR22 tumors from intact, androgen-stimulated mice (CWR22), animals castrated 6 days earlier (6d CX), 6d CX animals supplemented with testosterone propionate (TP) (0.1 mg/animal sc) for 24 or 72 h, a 6d CX treated with sesame oil vehicle (VEH), animals castrated 12 days earlier (12d CX), 12 d CX animals treated with TP for 48 h, and recurrent CWR22 tumors (CWR22R). Blots were hybridized with ^{32}P-labeled cDNAs for IGFBPs 1–6. B, Quantitation of IGFBP-5 mRNA from Northern blots.

TABLE 1. Cellular proliferation in CWR22 tumors

Tumors	Labeling index (% Ki-67 positive cells)
Intact CWR22 (n = 12)	79.4 ± 3.6
6 day CX (n = 6)	0.8 ± 0.5
6 day CX + TP 24 h (n = 4)	4.5 ± 0.42
6 day CX + TP 48 h (n = 4)	31.0 ± 6.7
6 day CX + TP 72 h (n = 2)	34.3 ± 5.8
Recurrent CWR22 (n = 12)	67.1 ± 3.3

Values are the mean ± SEM derived from manual counts of 300 cells/tumor section. CX, Castrate.

drawal (data not shown). In CWR22 tumors that recurred 4–6 months after castration, IGFBP-5 mRNA was increased severalfold higher than in CWR22 tumors from 6- and 12-day castrate mice and similar to levels in CWR22 tumors from intact, androgen-stimulated mice.

IGFBP-5 mRNA expression in CWR22 CaP tumors was analyzed further by ISHH to determine the effects of androgen withdrawal and replacement on expression in individual tumor cells. IGFBP-5 mRNA was uniformly expressed in the CWR22 tumor from an intact, androgen-stimulated mouse with hybridization of the antisense riboprobe in 75–80% of epithelial cells (Fig. 3A). In tumors removed 6 days after castration, relatively few epithelial cells were positive, and immunostaining of the riboprobe was weaker (Fig. 3B). Treatment of 6 day castrate animals with testosterone propionate restored IGFBP-5 mRNA in 90–95% of the epithelial cells within 24 h (Fig. 3C). In a tumor that recurred several months following castration, IGFBP-5 mRNA was detected in approximately 50% of the epithelial cells (Fig. 3D) despite the absense of testicular androgen. Compared with tumor tissue from the 6-day castrate mouse, both the number of cells expressing IGFBP-5 mRNA and the intensity of the signal increased markedly. In contrast to the epithelial cell expression of IGFBP-5 in CWR22, in prostate specimens from patients

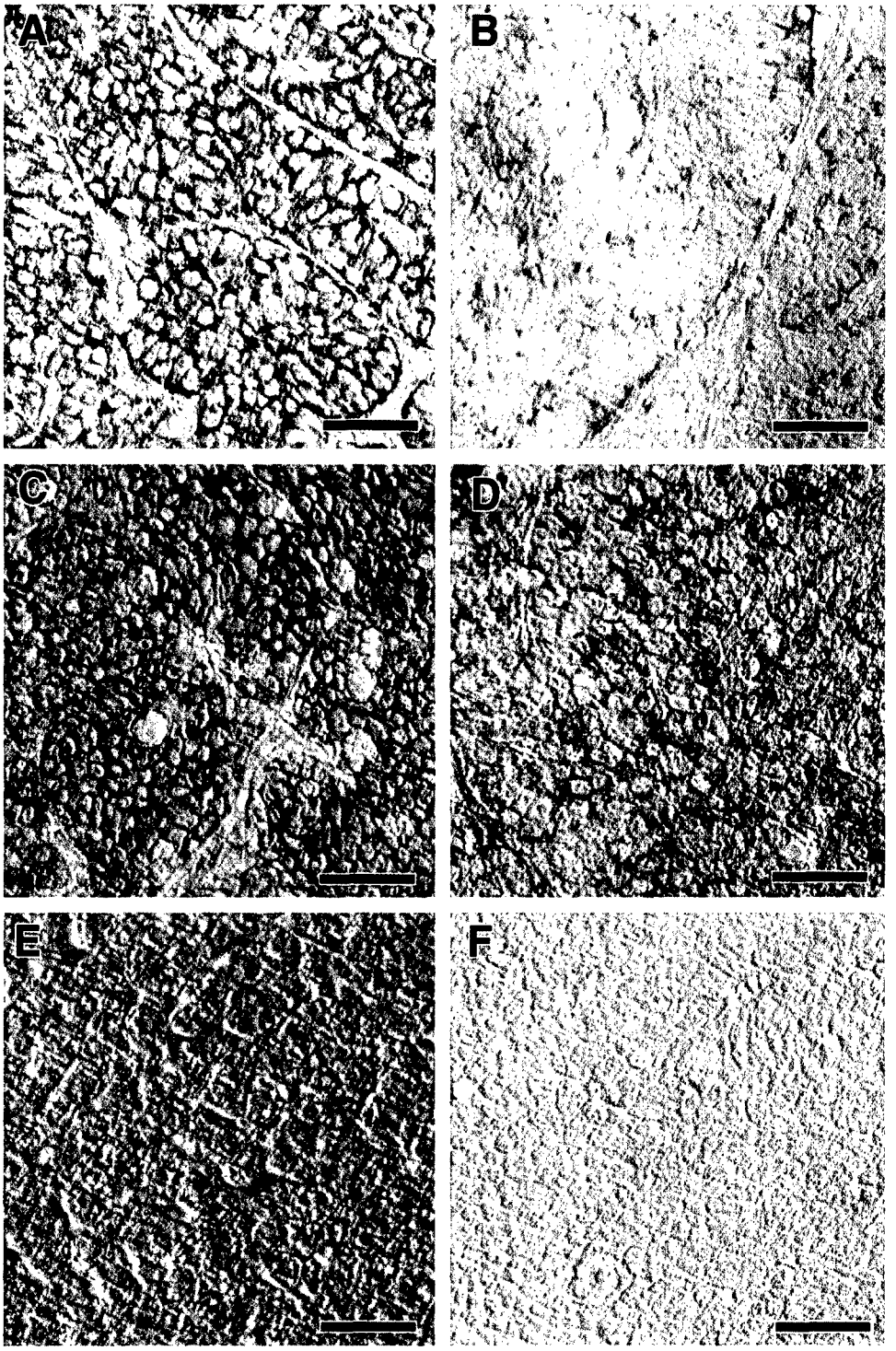

FIG. 3. *In situ* hybridization of IGFBP-5 in CWR22 demonstrates a pattern of IGFBP-5 regulation similar to that observed by Northern analysis. Paraffin sections of CWR22 tumors were hybridized with a biotin-labeled IGFBP-5 antisense riboprobe. Seventy-five to 80% of epithelial cells in CWR22 tumors express IGFBP-5 mRNA (A), with a decrease in IGFBP-5 mRNA at 6 days CX (B). Testosterone propionate (0.1 mg/animal sc) replacement for 24h increases IGFBP-5 mRNA in 6 day CX animals (C) and 50–75% of epithelial cells in recurrent CWR22 tumors are positive for IGFBP-5 mRNA (D). Mouse liver served as a negative control, with IGFBP-5 riboprobe (E) and without IGFBP-5 riboprobe (F). *Scale bar*, (50 μm).

with CaP, IGFBP-5 mRNA localized to the stromal component in areas containing BPH and CaP (Fig. 4).

To determine the influence of androgen on expression of IGFBP-5 protein, immunoblot and ligand blot analyses were made of protein extracts from androgen-dependent CWR22 tumors before and after castration and from the recurrent CWR22. Western immunoblotting for IGFBP-5 revealed a doublet of 33–35 kDa, the upper band being the glycosylated form (10) (Fig. 5). IGFBP-5 protein decreased following castration and increased in response to androgen replacement at 6 and 12 days post castration. These changes paralleled the androgen-regulated changes in mRNA expression described above. Moreover, IGFBP-5 protein levels in the recurrent tumor were 3- to 4-fold higher than in CWR22 tumors from 12-day castrate mice and similar to levels in protein extracts of CWR22 tumors from the intact, testosterone-stimulated mice. IGFBP-5 protein from CWR22 and recurrent CWR22 bound ^{125}I-IGF-I in Western ligand blot analyses (Fig. 6) demonstrating the protein is functional with respect to IGF-I binding. In the recurrent tumors, compared with the andro-

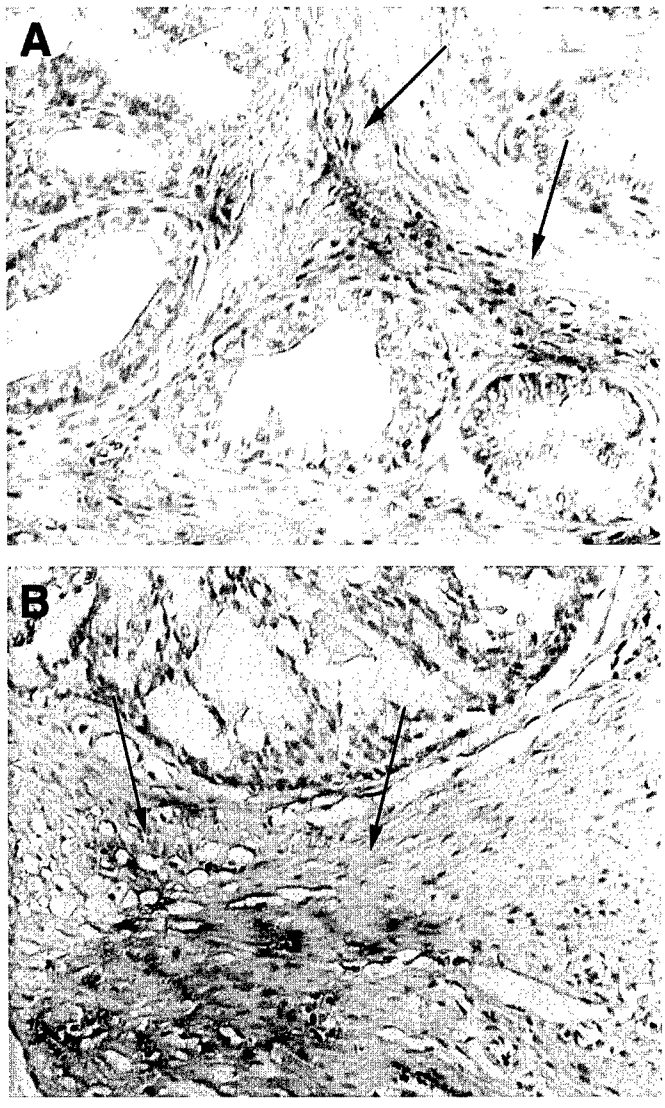

FIG. 4. IGFBP-5 mRNA is localized to stromal cells in human BPH and CaP. *In situ* hybridization histochemistry for IGFBP-5 was performed on paraffin-embedded sections of BPH (A) and androgen-independent CaP (B). IGFBP-5 mRNA (*arrow* designates IGFBP-5 positivity) is localized to stroma associated with benign and malignant glands.

gen-stimulated tumors from intact mice, the ratio of immunoreactive to ligand-bound IGFBP-5 appeared higher than in CWR22 suggesting ligand-binding activity may be reduced in the recurrent tumor.

Androgen-regulated IGFBP-5 expression in the human CaP xenograft led us to determine if there are changes in IGFBP-5 associated with neoplastic transformation from BPH to androgen-dependent CaP to androgen-independent CaP. BPH usually contained regions of prostatic intraepithelial neoplasia (PIN). Immunohistochemical staining of IGFBP-5 protein was increased in epithelial cells of androgen-dependent and androgen-independent CaP (Fig. 7, C–F) compared with BPH and PIN (Fig. 7, A and B), (Fig. 8).

Discussion

Our results demonstrate AR regulation of IGFBP-5 mRNA and protein expression in CWR22, a xenograft that exhibits

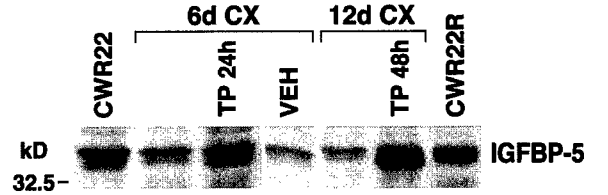

FIG. 5. IGFBP-5 protein expression correlates with IGFBP-5 RNA expression. CWR22 tumor lysates were prepared and 100 μg aliquots were subjected to gel electrophoresis and electroblotting to Immobilon. Membranes were incubated with IGFBP-5 monoclonal antibody and detected by enhanced chemiluminescence. IGFBP-5 protein was detected as a doublet of 33–35 kDa. Similar results were obtained with two to three different tumors at each treatment point.

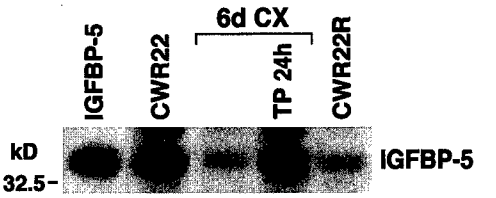

FIG. 6. Immunoreactive IGFBP-5 binds IGF-I. Western blots of lysates from CWR22 tumors were analyzed by Western ligand blotting using ^{125}I-IGF-I as a probe. Changes in IGF-I binding following castration of CWR22-bearing mice were similar in repeated experiments with two or three different tumors at each treatment point.

the androgen-dependent human CaP phenotype. Androgen withdrawal from CWR22 tumors caused a marked decrease in IGFBP-5 mRNA and androgen replacement in castrated CWR22-bearing animals increased IGFBP-5 mRNA 10- to 12-fold within 24 h. The increase in IGFBP-5 following androgen stimulation occurred before the major increase in cell proliferation, as measured by Ki-67 immunohistochemistry. Expression of IGFBP-5 mRNA and protein increased in the recurrent CWR22 tumors despite the absence of testicular androgen.

In situ hybridization analysis confirmed the results obtained by Northern blotting and demonstrated uniform expression of IGFBP-5 mRNA in CWR22 epithelial cells. IGFBP-5 protein was expressed in parallel with mRNA and was active in binding ^{125}I-IGF-I in ligand blot assays. However, the ratio of ^{125}I-IGF-I bound relative to the amount of immunoreactive IGFBP-5 appeared lower in the recurrent tumor than in CWR22 from intact, androgen-stimulated mice. Immunohistochemical analysis of IGFBP-5 protein in human CaP tissue specimens demonstrated stronger immunostaining in CaP compared with BPH. The epithelial cell expression of IGFBP-5 mRNA and protein in CWR22 differed from expression in clinical CaP tissue samples where IGFBP-5 mRNA was predominantly in stromal cells. CaPs in general contain variable amounts of stroma, whereas CWR22 tumors are composed of xenografted epithelium and contain only small amounts of murine stroma. Nonetheless, in CaP tissue samples from patients as in CWR22, IGFBP-5 protein was associated with epithelial cells.

Our findings in CaP tissue samples from patients agree with results of an earlier study of radical prostatectomy specimens in which IGFBP-5 mRNA was higher in CaP than in BPH. IGFBP-5 mRNA localized to stromal cells surround-

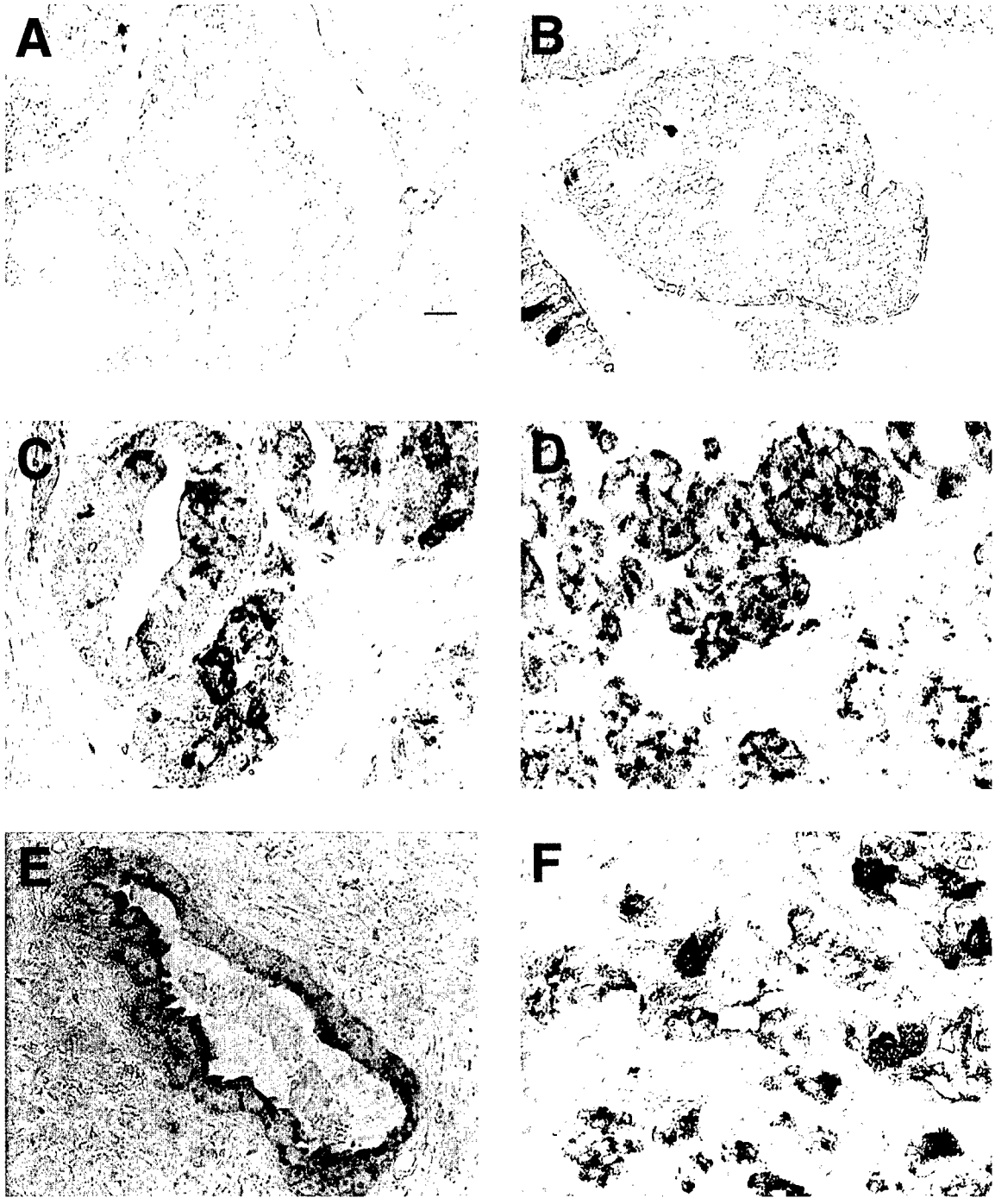

FIG. 7. IGFBP-5 protein expression increases in CaP. Paraffin-embedded sections of human prostate tissue containing BPH and PIN and tumor specimens of androgen-dependent (ADCaP) and androgen-independent CaP (AICaP) were double-stained with IGFBP-5 and anticytokeratin antisera. There were 20 prostate specimens with BPH, 20 with PIN, 20 with androgen-dependent CaP, and 15 with androgen-independent CaP. BPH was cytokeratin positive and only weakly positive for IGFBP-5 (A) while PIN specimens had decreased cytokeratin and slightly increased IGFBP-5 staining (B). Epithelial cells in androgen-dependent CaP (AD-CaP, Gleason scores of 4–7) (C and D) and androgen-independent CaP (AI-CaP, Gleason scores 8–10) (E and F) showed stronger IGFBP-5 immunostaining compared with BPH and PIN.

ing acinar structures, whereas the protein was associated with cell membranes of epithelium and stroma (29). The increased epithelial cell expression of IGFBP-5 mRNA and protein in CWR22 suggests these cells have compensated for loss of human stroma by increasing expression of IGFBP-5 that could function to stimulate epithelial cells in an autocrine rather than a paracrine mode. The elevated IGFBP-5 expression in CaP glands compared with BPH implicates IGFBP-5 in the growth and progression of CaP. Figueroa *et al.* (30) found that mRNAs for IGFBP-5 and -2 were higher in CaP with higher Gleason scores while IGFBP-3 was lower, suggesting differential expression of these IGFBPs.

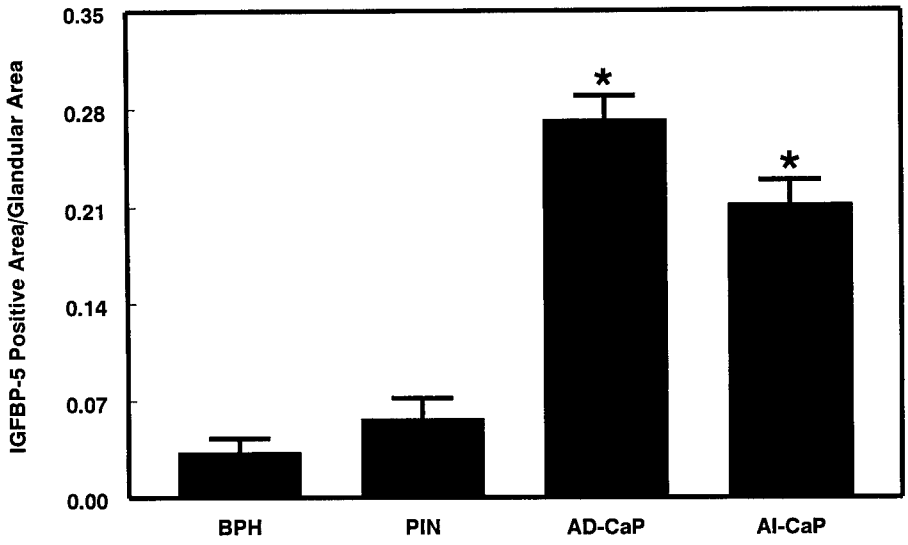

FIG. 8. Quantitation of immunohistochemical staining of IGFBP-5. IGFBP-5 immunostaining was quantitated using video image analysis. Plotted values represent the mean ± SE, * increased IGFBP-5 staining in comparison with BPH ($P < 0.0005$).

IGFBPs regulate target cell availability of IGFs for interaction with IGF receptors. Six IGFBPs have been described (IGFBP-1–6) (10, 12). IGFBP-1, -3, -4, and -6 inhibit IGF action in most systems studied, whereas IGFBP-2 and -5 can potentiate IGF-I functions. A carboxy-truncated form of IGFBP-5 stimulated mitogenesis of cultured osteoblasts (11). Thus, AR-stimulated expression of IGFBP-5 in CaP might enhance IGF-I action and tumor growth. IGFBP-5 binds specifically to plasminogen activator inhibitor-1 and to other components of the extracellular matrix in several cell and tissue types (31). Plasminogen activator-inhibitor-1 binding partially protects IGFBP-5 from proteolysis *in vitro* and may thereby regulate IGFBP-5 activity. The serine protease thrombin cleaves IGFBP-5 at physiological concentrations, thereby releasing IGF-I and increasing its bioavailability (32).

Previous studies on the regulation of IGFBP-5 have been largely confined to cell lines. Both IGF-I and IGF-II increase IGFBP-5 production (33–35). In some cell-types, IGF increases secretion of IGFBP-5 without detectable changes in mRNA (34–37), whereas in other cell types (33, 37), mRNA levels and secretion of IGFBP-5 are increased. More recently, androgen was found to enhance the stimulatory effect of IGF-I on IGFBP-5 mRNA and protein in cultured human genital skin fibroblasts (38). Androgen induction was at the transcriptional level as shown by nuclear run-on assays and analysis of IGFBP-5 promoter activity (39). Because the AR is also expressed in stromal fibroblasts of human CaP, this observation suggests that androgen is likely also to enhance the stromal cell production of IGFBP-5. Other factors, however, have been reported to contribute to IGFBP-5 regulation, including cAMP (40), 1,25-dihydroxyvitamin D_3, PTH (35), interleukin-1α (36), transforming growth factor-β (41), and retinoic acid (40, 41). The human IGFBP-5 gene is on chromosome 2q 33–34 and consists of 4 exons. Promoter activity resides in the 461 bp 5′ flanking region (42, 43). In cotransfection assays, Duan and Clemmons (43) observed cell-type specific induction of promoter activity with forskolin and found that AP-2 contributed to the cAMP responsiveness of this gene.

In the recurrent CWR22 tumors, IGFBP-5 expression is increased through a mechanism that remains to be determined. We have identified several mRNAs that are up-regulated by androgen in the androgen-dependent CWR22, and these are also up-regulated in the recurrent tumor, whereas the levels of most mRNAs that are not androgen-regulated remain unchanged in the recurrent CWR22 (44). This observation suggests that androgen-regulated genes are up-regulated in the recurrent tumor by a common mechanism. Because AR expression is abundant in the recurrent tumor, one possibility is that AR becomes reactivated in the recurrent tumor despite the absence of testicular androgen. Androgen-independent activation of AR has been reported in CaP cell lines. Using PC-3 cells transiently cotransfected with AR and a reporter gene, Nazareth and Weigel (45) found that AR was transcriptionally activated by forskolin, an activator or protein kinase A. In similar assays using DU-145 cells, Culig *et al.* (46) reported that IGF-I alone stimulated AR-mediated gene transcription to the same extent as did the synthetic androgen methyltrienolone. In their study, IGF-I was a more effective activator of AR than either keratinocyte growth factor or epidermal growth factor. However, in CV-1 cells, Reinikainen *et al.* (47), using a different reporter vector and transfection method, found IGF-I and EGF increased AR transactivation only in the presence of androgen. Similarly, LNCaP cells required dihydrotestosterone in addition to IGF-I for growth stimulation.

IGF-I is known to stimulate CaP cell growth (4) and might be potentiated by IGFBP-5. Thus, androgen-stimulated IGFBP-5 could increase the growth effects of IGF-I in androgen-dependent CWR22. A similar effect could result from increased expression of IGFBP-5 in recurrent CWR22. Type I IGF receptor mRNA is expressed in both the androgen-dependent CWR22 and recurrent CWR22 tumors. The growth-promoting effect of IGF-I is modulated by IGFBP-3, which binds IGF-I and reduces its effect on epithelial cells. However, proteolysis of IGFBP-3 lowers its affinity for IGF-I (12). The IGFBP-3 proteases, prostate-specific antigen (PSA) and human kallikrien-2 (hK2) are AR-induced genes (48) that degrade IGFBP-3 (12, 49) and could thereby increase IGF-I

stimulation of cell proliferation. PSA and hK2 are up-regulated by androgen in the androgen-dependent CWR22. Their expression is also increased in the recurrent CWR22 (44). Thus AR-induced increases in IGFBP-5, PSA, and hK2 might act in concert to potentiate IGF-I stimulation of cell growth both in androgen-dependent and androgen-independent CaP.

Acknowledgments

The excellent technical assistance of Yeqing Chen, Natalie Edmund, Katherine Hamil, and Joseph Giaconia is greatly appreciated.

References

1. **Wingo PA, Landis S, Ries LAG** 1997 An adjustment to the 1997 estimate for new prostate cancer cases. Cancer 80:1810–1813
2. **Cohen P, Peehl DM, Lamson G, Rosenfeld RG** 1991 Insulin-like growth factors (IGFs), IGF receptors, and IGF-binding proteins in primary cultures of prostate epithelial cells. J Clin Endocrinol Metab 73:401–407
3. **Cohen P, Peehl DM, Baker B, Liu F, Hintz RL, Rosenfeld RG** 1994 Insulin-like growth factor axis abnormalities in prostatic stromal cells from patients with benign prostatic hyperplasia. J Clin Endocrinol Metab 79:1410–1415
4. **Cohen P, Peehl DM, Rosenfeld RG** 1994 The IGF axis in the prostate. Horm Metab Res 26:81–84
5. **Kimura G, Kasuya J, Giannini S, Honda Y, Mohan S, Kawachi MH, Akimoto M, Fujita-Yamaguchi Y** 1996 Insulin-like growth factor system components in human prostate cancer cell lines: LNCaP, DU145, PC-3. Int J Urol 3:39–46
6. **Piertzkowski Z, Mulholland G, Gomella L, Jameson BA, Wernicke D, Baserga R** 1993 Inhibition of growth of prostatic cancer cell lines by peptide analogues of insulin-like growth factor 1. Cancer Res 53:1102–1106
7. **Burfeind P, Chernicky CL, Rininsland F, Ilan J, Ilan J** 1996 Antisense RNA to the type I insulin-like growth factor receptor suppresses tumor growth and prevents invasion by rat prostate cancer cells *in vivo*. Proc Natl Acad Sci USA 93:7263–7268
8. **Fiorelli G, DeBellis A, Longo A, Giannini S, Natlai A, Costantini A, Vannelli GB, Serio M** 1991 Insulin-like growth factor-I receptors in human hyperplastic prostate tissue: characterization, tissue localization, and their modulation by chronic treatment with a gonadotropin-releasing hormone analog. J Clin Endocrinol Metab 72:740–746
9. **Chan JM, Stampfer MJ, Giovannucci E, Gann PH, Ma J, Wilkinson P, Hennekens CH, Pollack M** 1998 Plasma insulin-like growth factor-I and prostate cancer risk: a prospective study. Science 279:563–566
10. **Clemmons DR** 1997 Insulin-like growth factor binding proteins and their role in controlling IGF actions. Cytokine Growth Factor Rev 8:45–62
11. **Andress DL, Birnbaum RS** 1992 Human osteoblast-derived insulin-like growth factor (IGF) binding protein-5 stimulates osteoblast mitogenesis and potentiates IGF action. J Biol Chem 267:22467–22472
12. **Rajaram S, Baylink DJ, Mohan S** 1997 Insulin-like growth factor-binding proteins in serum and other biological fluids: regulation and functions. Endocr Rev 18:801–831
13. **DeVere White R, Meyers FJ, Chi SG, Chamberlain S, Siders D, Lee F, Stewart S, Gumerlock PH** 1997 Human androgen receptor expression in prostate cancer following androgen ablation. Eur Urol 31:1–6
14. **Hobisch A, Culig Z, Radmayr C, Bartsch G, Klocker H, Hittmair A** 1996 Androgen receptor status of lymph node metastases from prostate cancer. Prostate 28:129–135
15. **Ruizeveld de Winter JA, Janssen PJ, Sleddens HM, Verleun-Mooijman MC, Trapman J, Brinkmann AO, Santerse AB, Schroder FH, van der Kwast TH** 1994 Androgen receptor status in localized and locally progressive hormone refractory human prostate cancer. Am J Pathol 144:735–746
16. **Visakorpi T, Hyytinen E, Koivisto P, Tanner M, Keinanen R, Palmberg C, Palotie A, Tammela T, Isola J, Kallioniemi O-P** 1995 *In vivo* amplification of the androgen receptor gene and progression of human prostate cancer. Nat Genet 9:401–406
17. **Wainstein MA, He F, Robinson D, Kung H-J, Schwartz S, Giaconia JM, Edgehouse NL, Pretlow TP, Bodner DR, Kursh ED, Resnick MI, Seftel A, Pretlow TG** 1994 CWR22: androgen-dependent xenograft model de-rived from a primary human prostatic carcinoma. Cancer Res 54: 6049–6052
18. **Gregory CW, Sharief Y, Hamil KG, Hall SH, Pretlow TG, Mohler JL, French FS** 1995 Apoptosis in an androgen-dependent xenograft model derived from a primary human prostatic carcinoma. Mol Biol Cell 6:240a (Abstract)
19. **Nagabhushan M, Miller CM, Pretlow TP, Giaconia JM, Edgehouse NL, Schwartz S, Kung H-J, deVere White RW, Gumerlock PH, Resnick MI, Amini SB, Pretlow TG** 1996 CWR22: the first human prostate cancer xenograft with strongly androgen-dependent and relapsed strains both *in vivo* and in soft agar. Cancer Res 56:3042–3046
20. **Tan J-A, Sharief Y, Hamil KG, Gregory CW, Zang D-Y, Sar M, Gumerlock PH, deVere White RW, Pretlow TG, Harris SE, Wilson EM, Mohler JL, French FS** 1997 Dehydroepiandrosterone activates mutant androgen receptors expressed in the androgen-dependent human prostate cancer xenograft CWR22 and LNCaP cells. Mol Endocrinol 11:450–459
21. **Chirgwin JM, Przybyla AE, MacDonald RJ, Rutter WJ** 1979 Isolation of biologically active RNA from sources enriched in ribonucleases. Biochemistry 18:5294–5299
22. **Ye P, Carson J, D'Ercole AJ** 1995 *In vivo* actions of insulin-like growth factor-I (IGF-I) on brain myelination: studies of IGF-I and IGF binding protein-1 (IGFBP-1) transgenic mice. J Neurosci 15:7344–7356
23. **Shimasaki S, Shimonaka M, Zhang H-P, Ling N** 1991 Identification of five different insulin-like growth factor binding proteins (IGFBPs) from adult rat serum and molecular cloning of a novel IGFBP-5 in rat and human. J Biol Chem 266:10646–10653
24. **Kou K, Jenkins NA, Gilbert DJ, Copeland NG, Rotwein P** 1994 Organization, expression, and chromosomal location of the mouse insulin-like growth factor binding protein 5 gene. Genomics 20:412–418
25. **Price WA, Stiles AD, Moats-Staats BM, D'Ercole AJ** 1992 Gene expression of insulin-like growth factors (IGFs), the type 1 IGF receptor, and IGF-binding proteins in dexamethasone-induced fetal growth retardation. Endocrinology 130:1424–1432
26. **Sherwood ER, Theyer G, Steiner G, Berg LA, Kozlowski JM, Lee C** 1991 Differential expression of specific cytokeratin polypeptides in the basal and luminal epithelia of the human prostate. Prostate 18:303–314
27. **Mize RR, Holdefer RN, Nabors LB** 1988 Quantitative immunohistochemistry using an image analyzer I. Hardware evaluation, image processing, and data analysis. J Neurosci Methods 26:1–24
28. **Otsu N** 1979 A threshold selection method from gray-level histograms. IEEE Trans Syst Man Cybern 9:62–66
29. **Tennant MK, Thrasher JB, Twomey PA, Birnbaum RS, Plymate SR** 1996 Insulin-like growth factor binding proteins (IGFBP)-4, -5 and -6 in the benign and malignant human prostate: IGFBP-5 messenger ribonucleic acid localization differs from IGFBP-5 protein localization. J Clin Endocrinol Metab 81:3783–3792
30. **Figuero JA, De Raad S, Tadlock L, Speights VO, Rinehart JJ** 1998 Differential expression of insulin-like growth factor binding proteins in high versus low Gleason score prostate cancer. J Urol 159:1379–1383
31. **Nam TJ, Busby W, Clemmons DR** 1997 Insulin-like growth factor binding protein-5 binds to plasminogen activator inhibitor-1. Endocrinology 138:2972–2978
32. **Zheng B, Clarke JB, Busby WH, Duan C, Clemmons DR** 1998 Insulin-like growth factor-binding protein-5 is cleaved by physiological concentrations of thrombin. Endocrinology 139:1708–1714
33. **Backeljauw PF, Dai Z, Clemmons DR, D'Ercole AJ** 1993 Synthesis and regulation of insulin-like growth factor binding protein-5 in FRTL-5 cells. Endocrinology 132:1677–1681
34. **Sheikh MS, Shao ZM, Hussain A, Clemmons DR, Chen JC, Roberts CT, LeRoith D, Fontana JA** 1993 Regulation of insulin-like growth factor-binding-protein-1, 2, 3, 4, 5, and 6: synthesis, secretion, and gene expression in estrogen receptor-negative human breast carcinoma cells. J Cell Physiol 155:556–567
35. **Camacho-Hubner C, Busby WH, McCusker RH, Wright G, Clemmons DR** 1992 Identification of the forms of insulin-like growth factor-binding proteins produced by human fibroblasts and the mechanisms that regulate their secretion. J Biol Chem 267:11949–11956
36. **Sunic D, McNeil JD, Rayner TE, Andress DL, Belford DA** 1998 Regulation of insulin-like growth factor-binding protein-5 by insulin-like growth factor I and interleukin-1α in ovine articular chondrocytes. Endocrinology 139:2356–2362
37. **Schmid C, Schlapfer I, Gosteli-Peter MA, Froesch ER, Zapf J** 1995 Expression, effects, and fate of IGFBP-5 are different in normal and malignant osteoblast cells. Prog Growth Factor Res 6:167–173
38. **Yoshizawa A, Busby W, Clarke J, Clemmons DR,** Androgen-IGF-I interaction in controlling IGFBP production in androgen responsive foreskin fibroblasts. Program of the 79th Annual Meeting of The Endocrine Society, Minneapolis, MN, 1997 P2–263 (Abstract)
39. **Yoshizawa A, Clemmons DR** 1998 IGF binding protein-5 synthesis is regulated by testosterone through gene transcriptional mechanisms in androgen responsive human fibroblasts. Program of the 80th Annual Meeting of The Endocrine Society, New Orleans, LA, 1998, P2–299 (Abstract)
40. **Schmid C, Schlapfer I, Gosteli-Peter MA, Hauri C, Froesch ER, Zapf J** 1996 1α, 25-dihydroxyvitamin D3 increases IGF binding protein-5 expression in cultured osteoblasts. FEBS Lett 392:21–24
41. **Hwa V, Oh Y, Rosenfeld RG** 1997 Insulin-like growth factor binding protein-3 and -5 are regulated by transforming growth factor-β and retinoic acid in the human prostate adenocarcinoma cell line PC-3. Endocrine 6:235–242
42. **Allander SV, Larsson C, Ehrenborg E, Suwanichkul A, Weber G, Morris SL, Bajalica S, Kiefer MC, Luthman H, Powell DR** 1994 Characterization of the chromosomal gene and promoter for human insulin-like growth factor binding protein-5. J Biol Chem 269:10891–10898

43. **Duan C, Clemmons DR** 1995 Transcription factor AP-2 regulates human insulin-like growth factor binding protein-5 gene expression. J Biol Chem 270:24844–24851
44. **Gregory CW, Hamil KG, Kim D, Hall SH, Pretlow TG, Mohler JL, French FS** 1998 Androgen receptor expression in androgen-independent prostate cancer is associated with increased expression of androgen-regulated genes. Cancer Res 58:5718–5724
45. **Nazareth LV, Weigel NL** 1996 Activation of the human androgen receptor through a protein kinase A signaling pathway. J Biol Chem 271: 19900–19907
46. **Culig Z, Hobisch A, Cronauer MV, Radmayr C, Trapman J, Hittmair A, Bartsch G, Klocker H** 1994 Androgen receptor activation in prostatic tumor cell lines by insulin-like growth factor-I, keratinocyte growth factor, and epidermal growth factor. Cancer Res 54:5474–547
47. **Reinikainen P, Palvimo JJ, Janne OA** 1996 Effects of mitogens on androgen receptor-mediated transactivation. Endocrinology 137:4351–4357
48. **Young CYF, Andrews PE, Tindall DJ** 1995 Expression and androgenic regulation of human prostate-specific kallikreins. J Androl 16:97–99
49. **Gibson TLB, Tremblay RR, Dub JY, Cohen P,** Human kallikrein-2 is a potent insulin-like growth factor binding protein protease. Program of the 79th Annual Meeting of The Endocrine Society 79th, Minneapolis, MN, 1997 (Abstract P1–334)

IN PRESS, J. ANDROLOGY
ANTICIPATED PUBLICATION JULY 2001

ANDROGEN RECEPTOR REGULATION OF G1 CYCLIN AND CYCLIN-DEPENDENT KINASE FUNCTION IN THE CWR22 HUMAN PROSTATE CANCER XENOGRAFT[1]

Christopher W. Gregory[2], Raymond T. Johnson, Jr., Sharon C. Presnell, James L. Mohler, Frank S. French

Departments of Pediatrics, The Laboratories for Reproductive Biology [CWG, RTJ, FSF], Pathology and Laboratory Medicine [SCP, JLM] and Surgery, Division of Urology [JLM], and The Lineberger Comprehensive Cancer Center [JLM, FSF], The University of North Carolina at Chapel Hill, Chapel Hill NC 27599

Running title: **Cell cycle regulation in prostate cancer**

[1]Supported by The American Foundation for Urologic Disease and Merck US Human Health (C.W.G.), NIH Grant CA77739 (J.L.M.;F.S.F.), United States Army Medical Research and Materiel Command 98-1-8538 (J.L.M.), R37-HD04466 (F.S.F.), and through cooperative agreement U54-HD-35041 as part of the Specialized Cooperative Centers Program in Reproduction Research (DNA and Tissue Culture Cores), and P30-CA16086 (Animal Experimentation Core).

[2]To whom requests for reprints should be addressed, at Laboratories for Reproductive Biology, Department of Pediatrics, CB# 7500, 382 MSRB, University of North Carolina, Chapel Hill, NC 27599. Phone: (919) 966-0928; Fax: (919) 966-2203; E-mail: cgregory@med.unc.edu

ABSTRACT

Human prostate cancer is initially dependent on androgens for growth and androgen-dependent cells undergo apoptosis after castration. However, a subset of androgen-responsive cells survives and eventually proliferates in the absence of testicular androgen. The high levels of androgen receptor in both androgen-dependent and recurrent tumors led us to investigate androgen regulation of cell cycle proteins in human prostate cancer using the CWR22 xenograft. Cellular proliferation decreased dramatically in CWR22 tumors after castration. Testosterone propionate (TP) treatment of castrate mice restored cellular proliferation after 24-48 h. Growth of CWR22 tumors in the absence of testicular androgen recurred several months after castration. CDK1 and 2 and cyclin A and B1 mRNAs were decreased 6 days after castration, increased 6-12 h after TP treatment and were expressed at high levels in recurrent CWR22 tumors. Co-immunoprecipitated cyclin B1/CDK1 and cyclin D1/CDK4 protein complexes decreased after castration and increased after TP treatment of castrate mice. In addition, CDK1 and 2 kinase activities were up regulated by androgen in parallel with hyperphosphorylation of Rb protein. Despite the absence of testicular androgen in recurrent CWR22, the levels of these androgen regulated cyclin/CDK protein complexes and hyperphosphorylation of Rb were equal to or greater than in tumors from intact mice. The results indicate that androgen receptor regulates cellular proliferation by control of CDK and cyclins at the transcriptional level and by posttranslational modifications influencing cell cycle protein activity.

Key words: prostate cancer, androgen receptor, cyclin, cyclin-dependent kinase, xenograft

INTRODUCTION

Prostate cancer is the second leading cause of cancer death in men (Landis et al, 1998). During the initial stages of prostate cancer, growth of malignant epithelial cells is androgen-dependent (Roy et al, 1999), mediated by a network of androgen receptor (AR) regulated genes. Androgen deprivation causes apoptosis of prostate cancer epithelial cells, resulting in tumor regression, however prostate cancer eventually recurs in the absence of testicular androgen (Isaacs, 1994). AR protein expression levels are similar in androgen-dependent and recurrent CaP (DeVere White et al, 1997; Gregory et al, 1998) and several AR-regulated genes are expressed in recurrent prostate cancer (Gregory et al, 1998), suggesting AR has a role in mediating recurrent growth of prostate cancer in the absence of testicular androgen.

AR is activated by androgen, binds to specific DNA response elements and interacts with coactivators to control gene transcription, thereby regulating development, function and growth of the prostate (Roy et al, 1999; Quigley et al, 1995). In the adult prostate, androgen maintains a balance between cell proliferation and cell death. AR mutations in prostate cancer can alter the specificity of ligand induced transcriptional activation (Veldscholte et al, 1990; Culig et al, 1993; Tan et al, 1997).

Cyclins, cyclin-dependent kinases (CDKs) and CDK inhibitors regulate cellular proliferation and progression through the cell cycle (Nurse, 1994; Hunter and Pines, 1994). Two checkpoints in the cell cycle have been characterized: the G_1-S transition that controls initiation and completion of DNA replication in S phase, and the G_2-M transition that controls mitosis and cell division (Hartwell and Weinert, 1989). Progression through the cell cycle requires activation or inactivation of cyclin/CDK complexes at or before these checkpoints. We and others have described androgen regulation of CDK1, CDK2, CDK4, and CDKI p16 mRNAs *in vivo* and *in vitro*, using the CWR22 human prostate cancer xenograft (Gregory et al, 1998) and the LNCaP cell line (Lu et al, 1997).

CWR22 xenograft tumors represent the major phenotype of human prostate cancer (Wainstein et al, 1994; Nagabhushan et al, 1996; Tan et al, 1997). Tumors depend upon androgens for growth and after castration androgen-dependent cells undergo apoptosis. However, a subset of androgen-responsive (but not androgen-dependent) cells survives and, after several months, undergoes proliferation that results in recurrent tumors in the absence of testicular androgen. These findings led us to investigate androgen regulation of cell cycle proteins in human prostate cancer using the CWR22 xenograft. The data suggest that AR-regulated expression of cell cycle genes is responsible, in part, for tumor cell proliferation not only in androgen-dependent tumors but also in tumors that undergo recurrent growth in the absence of testicular androgen.

MATERIALS AND METHODS

Transplantation of CWR22 Tumors

Nude mice were obtained from Harlan Sprague Dawley, Inc. (Indianapolis, IN). CWR22 tumors were transplanted into nude mice containing subcutaneous testosterone pellets (12.5 mg sustained release) (Innovative Research of America, Sarasota, FL) to standardize serum testosterone levels (~4.0 ng/ml) as previously described (Wainstein et al, 1994). Intact mice bearing androgen-stimulated tumors and castrated mice (testosterone pellets and testes removed) carrying regressed or recurrent CWR22 tumors were exposed to methoxyflurane and sacrificed by cervical dislocation. Testosterone replacement of castrates was performed by injecting subcutaneously 1.0 mg testosterone propionate (TP) (Schein Pharmaceuticals, Inc., Port Washington, NY) per mouse. Tumors were harvested rapidly and frozen in liquid nitrogen or fixed in 10% buffered formalin for paraffin embedding. All procedures used were approved by the Institutional Animal Care and Use Committee of the University of North Carolina at Chapel Hill.

DNA Fragmentation Analysis

Genomic DNA for fragmentation analysis was prepared as described previously (Strauss, 1998) with slight modifications. 100 mg of tumor tissue was pulverized under liquid nitrogen with mortar and pestle and resuspended in 1.5 ml digestion buffer (100 mM NaCl, 10 mM Tris-HCl, 25 mM EDTA, pH 8.0, 0.5% sodium dodecyl sulfate, 0.1 mg/ml proteinase K). Samples were agitated at 37°C overnight. Samples were treated with 0.75 mg RNase A and incubated for 4 h at 37°C. DNA was extracted twice with phenol:chloroform:isoamyl alcohol (25:24:1) and once with chloroform, followed by precipitation with ethanol at -80°C overnight. DNA was collected by centrifugation at 13,000xg for 10 min. The pellet was recovered in TE (10 mM Tris-HCl, 0.1 mM EDTA, pH 8.0) and incubated at 65°C for 30 min to dissolve the DNA. DNA (500 ng) was 3′ end-labeled with [^{32}P]-ddATP and terminal deoxynucleotide transferase (Roche Biomedical, Indianapolis, IN) as previously described (Tilley and Hsueh, 1993). 10 µl of

the labeled samples were resolved on 2% agarose gels by electrophoresis for 2.5 h at 4 V/cm in 1X TBE solution (89 mM Tris base, 89 mM boric acid, 2 mM EDTA). Gels were dried and exposed as autoradiographs for 15-30 min.

In Situ Apoptosis Detection

CWR22 xenograft tumors from intact and castrated mice were stained for apoptosis using the TdT-mediated dUTP-X nick end labeling (TUNEL) technique and the ApopTag Plus In Situ Apoptosis Detection Kit-Fluorescein (Oncor Inc., Gaithersburg, MD), and for total DNA content with propidium iodide (PI) counterstain. Briefly, 10 μm cryosections were mounted on Superfrost®/Plus microscope slides (FisherScientific, Pittsburgh, PA), fixed in 10% neutral buffered formalin for 10 min at room temperature, and post-fixed in ethanol:acetic acid (2:1) for 5 min at -20°C. Sections were equilibrated and incubated with terminal deoxynucleotidyl transferase (TdT) enzyme at 37°C for 1h. Digoxigenin-nucleotide-labeled DNA was detected by incubation with anti-digoxigenin-fluorescein at room temperature for 30 min. Positive control slides were 5 μm thick sections of mouse mammary glands obtained at the fourth day after weaning. Negative controls were tumor sections that were not incubated with the TdT enzyme. Control sections showed no fluorescein-stained cells. Reactive cells were viewed by epi-fluorescence at 494 nm using both 20X and 40X objectives and a Nikon Microphot FXA microscope.

Ribonuclease (RNase) Protection Assay

Total RNA was isolated from CWR22 tumors as described (Chirgwin et al, 1979). The RiboQuant™ Multiprobe RNase Protection Assay System (PharMingen, San Diego, CA) was used to quantitate mRNA transcripts for CDK1, 2 and 4 and cyclins A, B1, D1, E, and F. 10 μg of total RNA from each of the CWR22 tumors was hybridized with the radiolabeled hCC-1, h-CYC-1, and hCYC-2 multi-probe template sets (PharMingen) according to the manufacturer's instructions. Following RNase treatment, protected probes were resolved on 5% polyacrylamide sequencing gels followed by exposure of the

dried gel to BioMax™ MR film (Kodak) overnight at -80°C. Quantitation of mRNA levels for the CDK, cyclin and CDKI genes was performed by scanning autoradiographs with an Ultroscan XL Laser Densitometer (LKB, Uppsala, Sweden). RNA loading differences were normalized by scanning the GAPDH bands and standardizing band intensities for all autoradiographs.

Immunohistochemical Analysis of Ki-67

Formalin-fixed, paraffin-embedded sections of tumor tissue were subjected to antigen retrieval for all antibodies described. Briefly, after deparaffinization and rehydration, tissue sections were heated at 100°C for 30 min in a vegetable steamer in the presence of antigen retrieval solution (CITRA, pH 6.0; Biogenex, San Ramon, CA). Sections were immunostained with the MIB-1 monoclonal antibody (Oncogene, Cambridge, MA) to detect the Ki-67 cellular proliferation antigen at an IgG concentration of 0.5 μg/ml (1:50). Diaminobenzidine was used to detect immunoperoxidase antigen-antibody reaction products. Ki-67 positivity in CWR22 tumors was quantitated by manually counting 300 nuclei per stained section to determine the percent of cells stained.

Western Immunoblot Analysis, Immunoprecipitation and Kinase Assays

Whole cell lysates were prepared from frozen CWR22 tumors. Tumor tissue (100 mg) was pulverized in liquid nitrogen, allowed to thaw on ice, and mixed with 1 ml RIPA buffer with protease inhibitors (PBS, 1% NP40, 0.5% sodium deoxycholate, 0.1% SDS, 0.5 mM phenylmethylsulfonyl fluoride (PMSF), 10 μM pepstatin, 4 μM aprotinin, 80 μM leupeptin, and 5 mM benzamidine). Tissue was homogenized on ice for 30 sec using a Biohomogenizer (Biospec Products, Inc., Bartlesville, OK). Two μl of 0.2 M PMSF were added and the homogenates incubated 30 min on ice. Homogenates were centrifuged at 10,000xg for 20 min and supernatants were collected and centrifuged again to prepare the final lysates. Supernatant protein (25-50 μg) from each sample was electrophoresed in 12% polyacrylamide gels containing SDS, followed by electroblotting

to Immobilon-P membrane (Millipore Corp., Bedford, MA) and immunodetection. CDK1 (17), CDK2 (M2)-G, CDK4 (C-22), cyclin A (H-432), cyclin B1 (GNS1), cyclin D1 (A-12), and Rb (IF8) antibodies (Santa Cruz Biotechnology, Inc.) were used at 1:2500 or 1:5000 dilutions. Secondary antibodies (horseradish-peroxidase conjugated anti-mouse, anti-rabbit or anti-goat) (Promega Corporation, Madison, WI) were used at 1:10,000 dilutions. Antigen-antibody complexes were detected using enhanced chemiluminescence (DuPont, NEN Research Products, Boston, MA).

To examine cyclin/CDK complex formation, anti-CDK4 or anti-cyclin B1 antibodies conjugated to protein A-agarose (Santa Cruz Biotechnology, Inc.) were used to immunoprecipitate CWR22 protein lysates made in co-immunoprecipitation buffer (50 mM Tris-HCl, pH 7.6, 150 mM NaCl, 1 mM EDTA, 0.1% NP-40, 1 mM DTT and protease inhibitors as described above). Prior to immunoprecipitation with specific antibody-agarose conjugates, samples were incubated with mouse IgG-agarose conjugate to remove IgG from the lysates. Following immunoprecipitation overnight at 4°C with constant rotation and washing in co-immunoprecipitation buffer, immunoprecipitates were analyzed by Western blotting with the appropriate antiserum.

CDK1, CDK2 and CDK4 kinase assays (Serrano et al, 1997) were performed with anti-CDK1/CDK2/CDK4 immunoprecipitates from CWR22 tumor lysates. Immunoprecipitates were washed twice in kinase buffer (20 mM Tris-HCl [pH 8.0], 10 mM $MgCl_2$, 1mM EDTA, 1mM DTT) and the agarose beads were resuspended in 25 µl kinase buffer containing 10 µCi [γ-^{32}P] ATP (3000 Ci/mmol), 1 µM unlabeled ATP, and either 2.5 µg histone H1 or 1.5 µg GST-Rb fusion protein (epitope corresponding to amino acids 769-921 of mouse origin, Santa Cruz Biotechnology). After 20 min at room temperature, reaction products were resolved on 10% polyacrylamide gels containing SDS, which were dried and analyzed by autoradiography. Relative kinase activities were quantitated using a LKB densitometer as described for RNase protection assays.

RESULTS

Androgen regulation of cell death and proliferation in CWR22 tumors Mice bearing CWR22 androgen-dependent tumor xenografts were castrated and tumors were harvested at various intervals after castration. Apoptosis in CWR22 tumors was monitored by TUNEL staining and the DNA laddering assay (Figure 1). 24 hours after androgen withdrawal, apoptotic cells were detectable and the number of dying cells and quantity of fragmented DNA increased up to day 4 after castration. On day 6 after castration, apoptosis decreased and remained low throughout the 5-month interval to tumor recurrence. Recurrent tumors had relatively low levels of apoptosis. Cellular proliferation was assessed in these same tumors by Ki-67 immunostaining (Figure 2). Androgen-dependent CWR22 tumors were highly proliferative (Figure 2A) and cell division decreased to a low level within 6 days after castration (Figure 2B). Testosterone propionate (TP, 1 mg/mouse) replacement of 6 day castrated mice restored cellular proliferation after 24-48 hours (Figure 2C-F). CWR22 tumors recurred several months after castration, beginning as individual foci of proliferating cells at 120 days after castration (Figure 2G). Recurrent growth of CWR22 tumors (Figure 2H) resulted from an increase in the cellular proliferation:apoptosis ratio.

Fig. 1

Fig. 2

CDK and cyclin mRNA expression in CWR22 tumors CWR22 tumor-bearing mice were castrated and after 6 days were treated with 1 mg TP for 6, 12, 18, 24, or 48 hours. Tumors were harvested and RNA was prepared for ribonuclease (RNase) protection analysis. CDK1 and CDK2 mRNAs were decreased 10- and 5-fold, respectively, on day 6 after castration and remained low on days 12 and 120 after castration (Figure 3). Both were increased within 6-12 hours of TP treatment; CDK1 reached maximum expression after 48 hour TP and CDK2 after 24 hour TP treatment. CDK1 and 2 mRNAs were expressed at high levels in CWR22 tumors undergoing recurrent growth in the absence of testicular androgen (Figure 3). CDK4 mRNA did not change with castration and in the recurrent CWR22 was expressed at a level similar to that in tumors from intact mice.

Fig. 3

Cyclin A and B1 mRNAs showed androgen-regulated changes (Figure 4) similar to CDK1 and 2. Cyclin A and cyclin B1 mRNAs decreased 10-fold after castration and in tumors from day 6 castrates with TP treatment for 6 hours, cyclin A and B1 mRNAs were increased above the level of the day 6 castrates and increased 30-40-fold after 24-48 hours of TP treatment. Cyclin D1 mRNA decreased only 50% in the day 6 castrates and was restored rapidly by TP (Figure 4). All three cyclin mRNAs were expressed highly in tumors that recurred in the absence of testicular androgen with cyclin D1 showing highest levels (Figure 4). mRNA expression of cyclins E and F also decreased after castration (data not shown). 24 hour TP treatment of day 6 castrates caused a slight increase whereas 48 hour TP treatment resulted in restoration of cyclin E and F mRNA to levels seen in CWR22 from intact animals. Both cyclin mRNAs were expressed in recurrent tumors at levels similar to those from androgen-dependent CWR22 tumors.

Fig. 4

CDK and cyclin protein expression Androgen regulation of CDK and cyclin proteins was examined using Western blot analysis of CWR22 tumor protein lysates. CDK1 (cdc2 p34, 34 kDa) protein was reduced in CWR22 tumors on days 2 and 6 after castration and did not increase within 48 hours after TP replacement. However, in recurrent CWR22, CDK1 protein increased to levels similar to those in CWR22 tumors from intact mice (Figure 5). CDK2 (34 kDa) was expressed in CWR22 and recurrent CWR22 tumors at similar levels and showed no change in response to castration or testosterone treatment. CDK4 (34 kDa) was unchanged by castration or TP replacement. Cyclins A (60 kDa), B1 (62 kDa), and D1 proteins were reduced by castration and TP replacement for 48 h restored cyclin D1 protein to levels similar to those seen in CWR22 tumors from intact mice. Cyclins A, B1 and D1 proteins were expressed at similar or higher levels in recurrent CWR22 as compared to CWR22 from intact mice (Figure 5).

Fig. 5

Coimmunoprecipitation of cyclin/CDK complexes in CWR22 tumors CDKs must interact with and be activated by their cyclin partners as cells progress through the cell cycle. Activated CDKs phosphorylate downstream effectors, including Rb, which in its hyperphosphorylated form induces cells to progress from G_1 to S (Sidle et al, 1996). To determine the relationship between cyclin/CDK complexes and cell proliferation induced

by androgen, co-immunoprecipitation studies utilized tumors from intact, castrate, and TP treated castrate mice. A comparison was made with CWR22 tumors that recurred 5 months following castration. Tumor lysates were immunoprecipitated with cyclin B1 antibody and immunoblotted with CDK1 antibody (Figure 6A). Cyclin B1/CDK1 complexes decreased after castration and were 3-fold lower on day 6 after castration. TP treatment of 6 day castrates increased cyclin B1/CDK1 complexes within 12 hours to levels somewhat higher than in CWR22 tumors from intact animals. Cyclin B1/CDK1 was abundant in recurrent CWR22 tumors, similar to levels in tumors from TP-treated castrated mice.

Fig. 6

CDK1 kinase activity was determined by immune complex kinase assay using histone H1 substrate (Figure 6B). CDK1 kinase activity was decreased by 70% in tumors from mice 6 days after castration, compared to tumors from intact mice. 48 hour TP treatment of 6 day castrate mice restored CDK1 activity and activity was increased further in recurrent CWR22 tumors.

Tumor whole cell lysates were immunoprecipitated with CDK4 antibody and immunoblotted with cyclin D1 antibody (Figure 6C). Cyclin D1/CDK4 complexes decreased following castration and were not detected 6 days after castration, increased slightly within 12 hours of TP treatment of 6 day castrate mice and were higher at 48 hours than in tumors from intact mice. In recurrent CWR22 tumors, cyclin D1/CDK4 complexes were about10-fold higher than in CWR22 tumors from intact mice.

Rb phosphorylation in CWR22 tumors Immunoprecipitated CDK2 was assayed for kinase activity using Rb protein as substrate (Figure 7A). On day 6 after castration, CDK2 phosphorylation of Rb was reduced 40% compared to CDK2 activity in CWR22 tumors from intact mice. 48 hour TP treatment of 6 day castrates restored CDK2 activity to the levels in CWR22 tumors from intact mice. In recurrent CWR22 tumors, CDK2 kinase activity with Rb was increased 2.5-fold above levels in tumors from intact mice. Immunoprecipitated CDK4 also phosphorylated Rb substrate but showed no androgen-dependent change (data not shown).

Fig. 7

Phosphorylation of Rb by a cyclin D1/CDK complex is required for entrance of cells into S phase (Chew et al, 1998). Western immunoblot analysis was also used to determine the phosphorylation state of Rb in CWR22 tumors (Figure 7B). Androgen-stimulated CWR22 tumors from intact mice expressed the 110 kDa hypo- and 116 kDa hyperphosphorylated forms of Rb and the hyperphosphorylated (upper band) form was predominant. Both forms of Rb were reduced 3-fold on day 6 after castration and the hyperphosphorylated band was increased nearly 2-fold 48 hours after TP treatment but did not return to the level of the intact. In recurrent CWR22 tumors growing in the absence of testicular androgen, hyperphosphorylated Rb was higher than in tumors from intact mice and increased 5-fold over the levels in tumors from 6 day castrates, possibly reflecting the higher activity of cyclin D1/CDK2/CDK4 in recurrent CWR22 tumors.

DISCUSSION

Immediately after castration of CWR22-bearing mice, tumor cells underwent a brief period (1-4 days) of apoptosis, as measured by DNA laddering and TUNEL assay. On day 6 after castration, apoptosis was decreased to low levels similar to the levels in androgen-dependent CWR22 and recurrent CWR22 tumors. Cellular proliferation was also decreased after castration and reached a low steady-state level at 6 days that was maintained during tumor regression until about 120 days after castration when small foci of proliferating cells appeared. TP replacement in 6-day castrate mice was followed by increased cellular proliferation of CWR22 beginning after 24 to 48 hours. By 150 days after castration, tumor growth recurred in most xenografts despite the absence of testicular androgen. Recurrent tumor growth resulted from the combination of a low rate of cell death and increased cell proliferation. Clonal recurrent growth of CaP cells following androgen deprivation of another androgen-dependent prostate cancer, the LAPC-9 xenograft, was described recently (Craft et al, 1999), consistent with the results in the CWR22 model.

Thus, CWR22 tumors exhibit the major phenotype of human prostate cancer and are well suited for studies on androgen-dependent growth and the transition to recurrent growth after androgen deprivation. We have used the CWR22 human prostate cancer xenograft model to identify androgen-regulated cell cycle proteins that control recurrent growth of human prostate cancer in the absence of testicular androgen. Our results in the androgen-dependent CWR22 after castration demonstrated that androgen activation of AR increased the levels of mRNAs for cyclins and CDKs well before there was a major increase in cellular proliferation, and that cyclin B1:CDK1 complex formation and cyclin D1 protein expression were regulated acutely by androgen. Active cyclin/CDK complexes (cyclin B1:CDK1 and cyclin D1:CDK4) were present in proliferating CWR22 tumor cells from intact, androgen-stimulated mice and castrate mice replaced with TP. Increased levels of cyclin:CDK complexes (B1:CDK1, D1:CDK4) and

Fig. 8

hyperphosphorylated Rb were associated with recurrent tumor growth in the absence of testicular androgen.

The time course of increases in CDK1, CDK2, cyclin A, and cyclin B1 mRNAs following TP replacement in tumors from 6 day castrate mice suggested that they are primary delayed response genes (Dean and Sanders, 1996) regulated by other factors in addition to AR or secondary androgen response genes that are not regulated directly by AR but by other androgen controlled factors. CDK1 and CDK2 mRNA increased in 6-12 hours after androgen replacement but required 48 hour TP stimulation to restore it to levels of CWR22 from intact mice. Cyclin A and B1 mRNAs were also fully restored only after 48 hour TP replacement. The decrease in CDK and cyclin mRNAs after castration paralleled the decrease in cell proliferation. Increased cell division occurred 24 to 48 hours after androgen replacement in association with further increases in CDK1, CDK2, cyclin A, and B1 mRNAs. On the other hand, the smaller decrease in cyclin D1 mRNA after castration was reversed within 6 hours after androgen replacement. Increased expression of these cell cycle mRNAs appears to be an important event in androgen-regulation of cellular proliferation in prostate cancer (Figure 8, pathway 1).

CDK1, cyclin A and cyclin B1 proteins appeared to be androgen-regulated in that they decreased following castration, however, in contrast to their mRNAs that increased in response to 48 hour testosterone treatment of the 6 day castrate, protein levels remained low. The amounts of CDK2 and CDK4 proteins were not affected by androgen withdrawal or TP treatment. Contrary to results in CWR22, cyclin A protein levels were responsive to androgen in LNCaP cells (Lu et al, 1997). CDK2 protein was reported to be unaffected by androgen in LNCaP cells. The cyclin A:CDK2 complex is active during S phase of the cell cycle and CDK2 activity, as measured by Rb phosphorylation, was regulated by androgen in androgen-dependent CWR22 while its activity was elevated in recurrent CWR22 in the absence of testicular androgen.

Cyclins and CDKs can be regulated by a variety of mechanisms including synthesis/degradation, phosphorylation/dephosphorylation and cyclin:CDK complex

formation. Levels of the cyclin B1:CDK1 complex were regulated by androgen in CWR22 tumors from intact and castrate mice. In recurrent CWR22 tumors, the complex was abundant in the absence of testicular androgen. CDK1 is activated by dephosphorylation of Thr^{14} and Tyr^{15} (Chew et al, 1998). Following dephosphorylation of CDK1, active cyclin B1:CDK1 complexes form and remain active during the G_2 to M transition and early M (Figure 8, pathway 2).

Although CDK4 mRNA and protein levels showed little dependence on androgen, cyclin D1:CDK4 complexes formation appeared androgen-dependent. However, the striking further increase in cyclin D1:CDK4 complexes in the recurrent CWR22 suggested that factors other than androgen influence either the formation or stability of these active complexes. Cyclin D1/CDK4/CDK2 complexes are active during the G_1 phase of the cell cycle. D-type cyclins bind and activate CDK4/CDK6 and the active cyclin D1:CDK4 complex phosphorylates Rb (Resnitzky et al, 1994). Blocking cyclin D1 protein by antisense RNA or immunoneutralizing antibodies inhibited neuronal differentiation and progression of myocytes through G_1 (Xiong et al, 1997a; Xiong et al, 1997b), suggesting that cyclin D1 protein levels can be rate-limiting for cell cycle progression. Chen et al (Chen et al, 1998) showed that over expression of cyclin D1 in LNCaP cells increased the number of cells in S-phase, allowed the cells to proliferate in the absence of androgen, and resulted in higher levels of Rb phosphorylation. Tumors formed from these cells grew more rapidly and were refractory to androgen deprivation. Cyclin D1was shown previously to bind directly the estrogen receptor and to enhance its activation in the absence of estrogen (Zijsen et al, 1997). Conversely, cyclin D1 also was reported to complex with AR, but this interaction inhibited androgen-induced transcriptional activation of a prostate-specific antigen (PSA) reporter construct (Knudsen et al, 1999). Likewise, cyclin D1 inhibited androgen-induced transcriptional activation of mouse mammary tumor virus promoter (Gregory and French, unpublished results).

The retinoblastoma tumor suppressor protein Rb is a principal target for cyclin-associated kinase activity. The function of Rb during cell cycle progression is regulated

by phosphorylation. During G_1, Rb exists as an unphosphorylated or underphosphorylated form, but it is highly phosphorylated from late G_1 to the end of M. Underphosphorylated Rb has a growth inhibitory effect (Ludlow et al, 1993). Rb associates with several proteins including p107 and p130 and sequesters the E2F family of transcription factors required for protein synthesis, thereby inhibiting S phase progression (Sidle et al, 1996). Upon Rb phosphorylation, E2F and other proteins are released and become functional as transcription factors. The cyclin D1:CDK4 complex phosphorylates Rb and cyclin (A or E):CDK2 and cyclin B1:CDK1 complexes maintain Rb phosphorylation allowing cells to enter S phase (Scherr, 1996; Wang et al, 1994). An increase in Rb phosphorylation was observed in ventral prostates of castrated rats treated with TP (Furuya et al, 1995; Chen et al, 1996). Recently, Knudsen et al demonstrated Rb phosphorylation is required for LNCaP cells to traverse the G_1-S transition. Down-regulation of cyclin D1:CDK4 activity and dephosphorylation of Rb contributed to G_1 arrest following androgen withdrawal (Knudsen et al, 1998). Cyclin D1-transfected LNCaP cells had higher CDK4 kinase activity and higher levels of Rb phosphorylation than mock-transfected LNCaP cells (Chen et al, 1998).

In CWR22 tumors, the amount of hyperphosphorylated Rb was reduced on day 6 after castration, concomitant with loss of tumor cell proliferation. Within 48 hours after TP replacement to 6-day castrates, Rb protein was increased in association with increased cell proliferation and in the rapidly dividing recurrent CWR22 tumor cells hyperphosphorylated Rb was further increased. Likewise, cyclin D1:CDK4 complexes were abundant in recurrent CWR22 tumors and CDK4 was active in phosphorylating Rb *in vitro* (data not shown). Increased expression of cyclin D1 in recurrent CWR22 tumors, as detected by immunohistochemical staining, was reported recently (Agus et al, 1999). Additionally, cyclin B1:CDK1 complexes were elevated in recurrent tumors and likely maintained Rb phosphorylation. Continuous phosphorylation of Rb in recurrent tumors would lead to a progressive loss of Rb function as cells proceed through G_1 and S phase (Harbour and Dean, 2000).

In cotransfection assays, Rb was reported to interact directly with AR and increase its transcriptional activity (Yeh et al, 1998). Loss of Rb inhibited AR but not glucocorticoid receptor activity (Lu and Danielsen, 1998). Although these *in vitro* experiments led to the suggestion that loss of Rb activity during the transition from androgen-dependent to androgen-independent growth of prostate cancer might result in decreased androgen responsiveness, our *in vivo* data suggest AR is active in recurrent CWR22 CaP tumors (Gregory et al, 1998) and enhances cellular proliferation through activation of the receptor in the absence of testicular androgen (Figure 8, pathway 3).

In conclusion, recurrent growth of CWR22 tumors was associated with elevated expression of AR and androgen-regulated genes suggesting that AR has a role in stimulating tumor cell growth in the absence of testicular androgen (Gregory et al, 1998). In the CWR22 model, mRNAs for CDK1, CDK2 and cyclins A, B1 and D1 were androgen regulated and their expression increased in recurrent tumors. Expression levels of CDK1, cyclin A, B1 and D1 proteins in castrated mice were influenced by androgen status. Cyclin B1:CDK1 and cyclin D1:CDK4 complexes decreased after castration and were restored by androgen replacement therapy. Moreover, these complexes were expressed at high levels in recurrent tumors. In the androgen-dependent CWR22 these effects of androgen coincided with hyperphosphorylation of Rb and upon tumor recurrence hyperphosphorylated Rb was increased together with cyclin:CDK complexes. The results suggest that androgen activation of AR stimulates cell proliferation through effects on multiple checkpoints in the cell cycle (Figure 8). We recently reported that recurrent CWR22 tumors and recurrent prostate cancer cell lines express AR with increased stability associated with hypersensitivity to low androgen levels. In recurrent CWR22, AR may become reactivated in the presence of castrate levels of androgen and act in concert with other growth stimulatory factors to promote cell proliferation.

ACKNOWLEDGEMENTS

We greatly appreciate the technical assistance of Natalie Edmund and Yeqing Chen. We thank Young Whang and Elizabeth M. Wilson for critical review of the manuscript.

FIGURE LEGENDS

Figure 1. DNA fragmentation and TUNEL analyses for apoptosis in CWR22 xenograft tumors. (A) Genomic DNA was prepared from frozen CWR22 tumors and 3′ end-labeled with ^{32}P-ddATP and terminal deoxynucleotide transferase. Labeled DNAs were resolved on 2% agarose gels by electrophoresis. The positions of DNA molecular mass markers (bp-base pairs) are indicated. (B) Frozen sections of CWR22 tumors were stained for apoptosis using the TdT-mediated dUTP-X nick end-labeling (TUNEL) technique. Cells labeled with fluoroscein (green) are apoptotic. 0, CWR22 tumor from intact mouse; 1-6, CWR22 tumors from mice castrated for 1-6 days; R, recurrent CWR22.

Figure 2. Ki-67 immunostaining of CWR22 tumors. Immunostaining for the cell proliferation marker Ki-67 was performed on paraffin-embedded sections of CWR22 tumors. CWR22 tumors from intact mice (A), day 6 after castration (B), testosterone propionate (TP) replacement of 6 day castrates (1.0 mg/mouse) for 6 hours (C), 12 hours (D), 24 hours (E), 48 hours (F), day 120 after castration (G), and recurrent CWR22 tumors (H). Numbers indicate the percent of Ki-67 positive cells ± SE.

Figure 3. RNase protection assay for CDK1, CDK2 and CDK4 mRNA expression in CWR22 tumors. RNase protection was performed with 10 μg RNA from CWR22 tumors from intact mice, castrates, castrates + TP, and 150 day castrates bearing recurrent tumors using the hCC-1 human multi-probe template set (Pharmingen). Glyceraldehyde-3-phosphate dehydrogenase (GAPDH) was included as a loading control. CX, castrate; TP, testosterone propionate. Densitometry of protected bands was performed and plotted for CDK1 and CDK2. Results are representative of three independent experiments. Bar, SE.

Figure 4. RNase protection assay for cyclin A, B1 and D1 mRNA expression in CWR22 tumors. RNase protection was performed with 10 μg RNA from CWR22

tumors from intact mice, castrates, castrates + TP, and 150 day castrates (recurrent) using the hCyc-1 human multi-probe template set (Pharmingen). GAPDH was included as a loading control. CX, castrate; TP, testosterone propionate. Densitometry of protected bands was performed and plotted for CDK1 and CDK2. Results are representative of three independent experiments. Bar, SE.

Figure 5. Western immunoblot analysis of CDK and cyclin proteins in CWR22 tumors. Tumor lysates were subjected to Western blot analysis. CDK 1, cyclin A, cyclin B1 and cyclin D1 protein decreased on days 2 and 6 after castration (CX). CDK2, CDK4 proteins were not changed by castration. All proteins were expressed at similar or higher levels in recurrent CWR22 tumors as compared to CWR22 from intact mice.

Figure 6 Co-immunoprecipitation of CDK1/cyclin B1 and CDK4/cyclin D1 complexes and immune complex kinase assay of CDK1. CWR22 tumor lysates were subjected to immunoprecipitation with agarose-conjugated cyclin B1, CDK1 and CDK4 antibodies. (A) Lysates immunoprecipitated with cyclin B1 antibody and immunoblotted with CDK1 antibody. (B) Lysates immunoprecipitated with agarose-conjugated CDK1 antibody followed by kinase assay with histone H1 substrate. (C) Lysates immunoprecipitated with CDK4 and immunoblotted with cyclin D1 antibody. The positions of molecular mass markers (kDa) are indicated. CX, castrate; TP, testosterone propionate.

Figure 7 Rb phosphorylation in CWR22 tumors. (A) CDK2 immunoprecipitates were used for kinase assay with a 46 kDa Rb fusion protein substrate. Band intensities were measured by densitometry of autoradiographs and the level in CWR22 tumors from intact mice was designated as 1.0. (B) Tumor lysates were subjected to Western blot analysis with a monoclonal Rb antibody. Hypo- (lower band) and hyperphosphorylated Rb protein (upper band) of 110-112 kDa was present in lysates of androgen-stimulated CWR22 tumors from intact mice. Rb phosphorylation and expression was decreased on day 6 after castration. TP replacement for 48 h increased the level of hyperphosphorylated Rb. Hyperphosphorylated Rb protein in recurrent CWR22 tumors

was higher than levels in intact CWR22. The position of the molecular mass marker (kDa) is indicated.

Figure 8 Pathways by which androgen receptor (AR) may induce cellular proliferation in the presence and absence of testicular androgen. AR is activated by DHT in androgen-dependent prostate cancer and may be activated by an alternate signaling pathway in recurrent prostate cancer. AR may induce cellular proliferation by: 1) direct or secondary regulation of mRNAs for CDKs and cyclins; 2) posttranslational modifications of CDKs and cyclins resulting in activation (phosphorylation or dephosphorylation); or 3) direct interaction with cyclin D1 and Rb proteins.

REFERENCES

Agus DB, Cordon-Cardo C, Fox W, Drobnjak M, Koff A, Golde DW, Scher HI. Prostate cancer cell cycle regulators: Response to androgen withdrawal and development of androgen independence. *J Natl Cancer Inst.* 1999;91:1869-1876.

Chen Y, Robles AI, Martinez LA, Liu F, Gimenez-Conti IB, Conti CJ. Expression of G1 cyclins, cyclin-dependent kinases, and cyclin-dependent kinase inhibitors in androgen-induced prostate proliferation in castrated rats. *Cell Growth & Diff.* 1996;7:1571-1577.

Chen Y, Martinez LA, LaCava M, Coghlan L, Conti CJ. Increased cell growth and tumorigenicity in human prostate LNCaP cells by overexpression to cyclin D1. *Oncogene* 1998;16:1913-1920.

Chew YP, Ellis M, Wilkie S, Mittnacht S. pRB phosphorylation mutants reveal role of pRB in regulating S phase completion by a mechanism independent of E2F. *Oncogene* 1998;17:2177-2186.

Chirgwin JJ, Przbyla AE, MacDonald RJ, Rutter WJ. Isolation of biologically active ribonucleic acid from sources enriched in ribonuclease. *Biochem.* 1979;18:5294-5299.

Craft N, Chhor C, Tran C, Belldegrun A, DeKernion J, Witte ON, Said J, Reiter RE, Sawyers CL. Evidence for clonal outgrowth of androgen-independent prostate cancer cells from androgen-dependent tumors through a two-step process. *Cancer Res.* 1999;59:5030-5036.

Culig Z, Hobisch A, Cronauer MV, Cato AC, Hittmair A, Radmayr C, Eberle J, Bartsch G, Klocker H. Mutant androgen receptor detected in an advanced-stage prostatic carcinoma is activated by adrenal androgens and progesterone. *Mol Endocrinol.* 1993;7:1541-1550.

Dean DM, Sanders MM. Ten years after: reclassification of steroid-responsive genes. *Mol Endocrinol.* 1996;10:1489-95.

De Vere White RW, Meyers F, Chi S-G, Chamberlain S, Siders D, Lee F, Stewart S, Gumerlock PH. Human androgen receptor expression in prostate cancer following androgen ablation. *Eur Urol.* 1997;31:1-6.

Furuya Y, Lin XS, Walsh JC, Nelson WG, Isaacs JT. Androgen ablation-induced programmed death of prostatic glandular cells does not involve recruitment into a defective cell cycle or p53 induction. *Endocrinol.* 1995;136:1898-1906.

Gregory CW, Hamil KG, Kim D, Hall SH, Pretlow TG, Mohler JL, French FS. Androgen receptor expression in androgen-independent prostate cancer is associated with increased expression of androgen-regulated genes. *Cancer Res.* 1998;58:5718-5724.

Harbour JW, Dean DC. Rb function in cell-cycle regulation and apoptosis. *Nature Cell Biol.* 2000;2:65-67.

Hartwell LH, Weinert TA. Checkpoints: controls that ensure the order of cell cycle events. *Science* 1989;246:629-634.

Hunter T, Pines J. Cyclins and cancer II: cyclin D and CDK inhibitors come of age. *Cell* 1994;79:573-582.

Isaacs JT. Role of androgens in prostate cancer. *Vitam Horm.* 1994;49:433-502.

Knudsen KE, Arden KC, Cavenee WK. Multiple G1 regulatory elements control the androgen-dependent proliferation of prostatic carcinoma cells. *J Biol Chem.* 1998;273:20213-20222.

Knudsen KE, Cavenee WK, Arden KC. D-type cyclins complex with the androgen receptor and inhibit its transcriptional transactivation ability. *Cancer Res.* 1999;59:2297-2301.

Landis SH, Murray T, Bolden S, Wingo PA. Cancer statistics, 1998. *Ca. a Cancer J for Clinicians.* 1998;48:6-29.

Lu S, Tsai SY, Tsai M-J. Regulation of androgen-dependent prostatic cancer cell growth: androgen regulation of *CDK2, CDK4*, and CKI *p16* genes. *Cancer Res.* 1997;57:4511-4516.

Lu J, Danielsen M. Differential regulation of androgen and glucocorticoid receptors by retinoblastoma protein. *J Biol Chem.* 1998;273:31528-31533.

Ludlow JW, Glendening CL, Livingston DM, DeCaprio J. Specific enzymatic dephosphorylation of the retinoblastoma protein. *Mol Cell Biol.* 1993;13:367-372.

Nagabhushan M, Miller CM, Pretlow TP, Giaconia JM, Edgehouse NL, Schwartz S, Kung H-J, de Vere White RW, Gumerlock PH, Resnick MI, Amini SB, Pretlow TG. CWR22: the first human prostate cancer xenograft with strongly androgen-dependent and relapsed strains both *in vivo* and in soft agar. *Cancer Res.* 1996;56:3042-3046.

Nurse P. Ordering S phase and M phase in the cell cycle. *Cell* 1994;79:547-550.

Quigley CA, DeBellis A, Marschke KB, el-Awady MK, Wilson EM, French FS. Androgen receptor defects: historical, clinical, and molecular perspectives. *Endocr Rev.* 1995;16:271-321.

Resnitzky D, Gossen M, Bujard H, Reed SI. Acceleration of the G1/S phase transition by expressions of cyclins D1 and E with an inducible system. *Mol Cell Biol.* 1994;14:1669-1679.

Roy AK, Lavrovsky Y, Song CS, Chen S, Jung MH, Velu NK, Bi BY, Chatterjee B. Regulation of androgen action. *Vitam Horm.* 1999;55:309-352.

Serrano M, Lin AW, McCurrach ME, Beach D, Lowe SW. Oncogenic ras provokes premature cell senescence associated with accumulation of p53 and $p16^{INK4a}$. *Cell* 1997;88:593-602.

Scherr CJ. Cancer cell cycles. *Science* 1996;274:1672-1677.

Sidle A, Palaty C, Dirks P, Wiggan O, Kiess M, Gill RM, Wong AK, Hamel PA. Activity of the retinoblastoma family proteins, pRB, p107, and p130, during cellular proliferation and differentiation. *Crit Rev Biochem Molec Biol.* 1996;31:237-271.

Strauss WM. Preparation of genomic DNA from mammalian tissue. (Ausubel FM., Brent R, Kingston RE, Moore DD, Seidman JG, Smith JA, Struhl K, eds.), 2.2.1-2.2.3, Greene Publishing and Wiley-Interscience, New York.

Tan J-A, Sharief Y, Hamil KG, Gregory CW, Zang D-Y, Sar M, Gumerlock PH, de Vere White RW, Pretlow TG, Harris SE, Wilson EM, Mohler,JL, French FS. Dehydroepiandrosterone activates mutant androgen receptors expressed in the androgen-dependent human prostate cancer xenograft CWR22 and LNCaP cells. *Mol Endocrinol.* 1997;11:450-459.

Tilley JL, Hsueh AJW. Microscale autoradiographic method for the qualitative and quantitative analysis of apoptotic DNA fragmentation. *J Cell Phys.* 1993;154:519-526.

Veldscholte J, Ris-Stalpers C, Kuiper GG, Jenster G, Berrevoets C, Claassen E, van Rooij HC, Trapman J, Brinkmann AO, Mulder EA. A mutation in the ligand binding domain of the androgen receptor of human LNCaP cells affects steroid binding characteristics and response to anti-androgens. *Biochem Biophys Res Comm.* 1990;173:534-540.

Wainstein MA, He F, Robinson D, Kung H-J, Schwartz S, Giaconia JM, Edgehouse NL, Pretlow TP, Bodner DR, Kursh ED, Resnick MI, Seftel A, Pretlow TG. CWR22: androgen-dependent xenograft model derived from a primary human prostatic carcinoma. *Cancer Res.* 1994;54:6049-6052.

Wang JY, Knudsen ES, Welch PJ. The retinoblastoma tumor suppressor protein. *Adv Cancer Res.* 1994;64:25-85.

Xiong W, Pestell RG, Rosner, MR. Role of cyclins in neuronal differentiation of immortalized hippocampal cells. *Mol Cell Biol.* 1997a;17:6585-6597.

Xiong W, Pestell RG, Watanabe MR, Rosner MR, Hershenson MB. Cyclin D1 is required for S-phase traversal in bovine tracheal myocytes. *Am J Phys.* 1997b;272:L1205-L1210.

Yeh S, Miyamoto H, Nishimura K, Kang H, Ludlow J, Hsiao P, Wang C, Su C, Chang C. Retinoblastoma, a tumor suppressor, is a coactivator for the androgen receptor in human prostate cancer DU145 cells. *Biochem Biophys Res Comm.* 1998;248:361-367.

Zijsen RML, Wientjens E, Klompmaker R, van der Sman J, Bernards R, Michalides RJAM. CDK-independent activation of estrogen receptor by cyclin D1. *Cell* 1997;88:4050415.

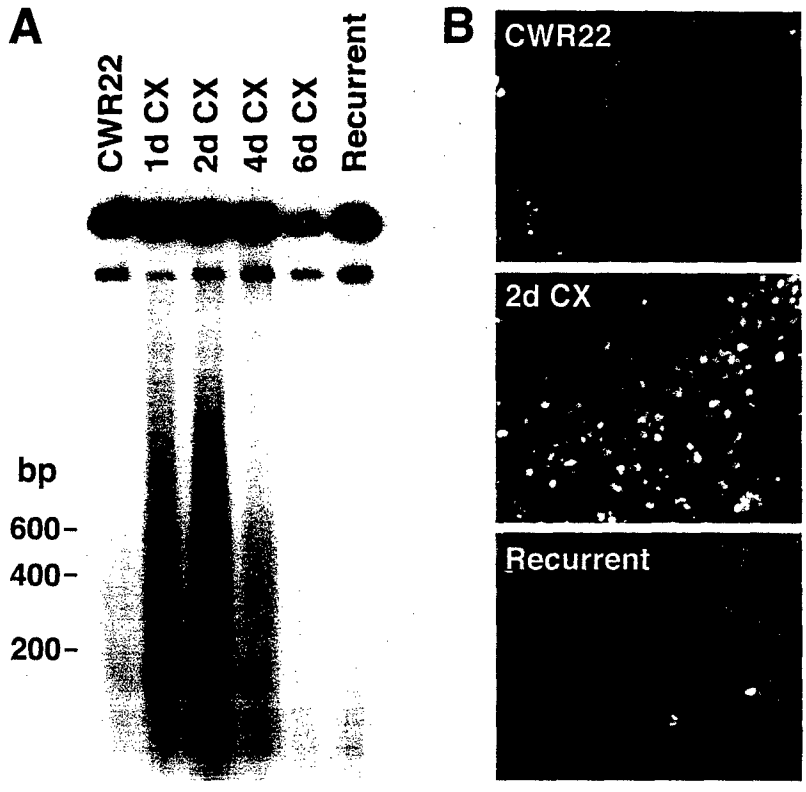
A
CWR22
1d CX
2d CX
4d CX
6d CX
Recurrent
bp
600-
400-
200-
B
CWR22
2d CX
Recurrent

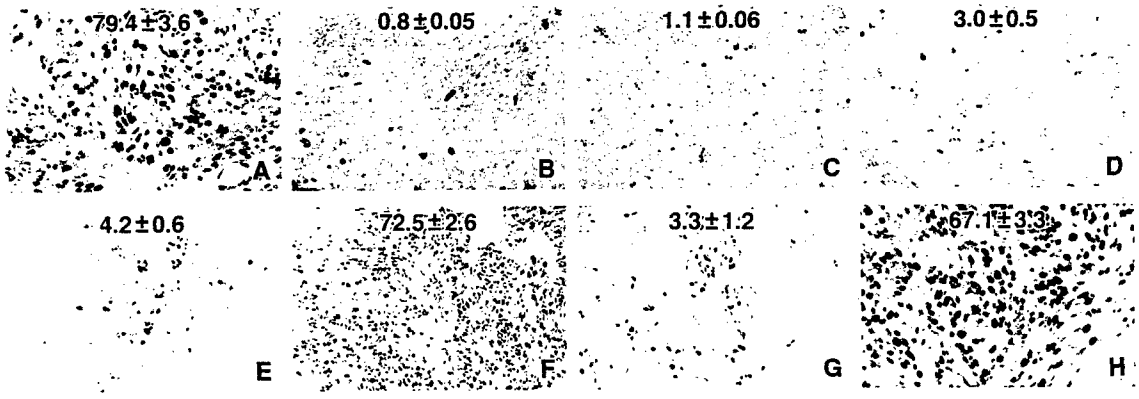
79.4±3.6
A
0.8±0.05
B
1.1±0.06
C
3.0±0.5
D
4.2±0.6
E
72.5±2.6
F
3.3±1.2
G
67.1±3.3
H

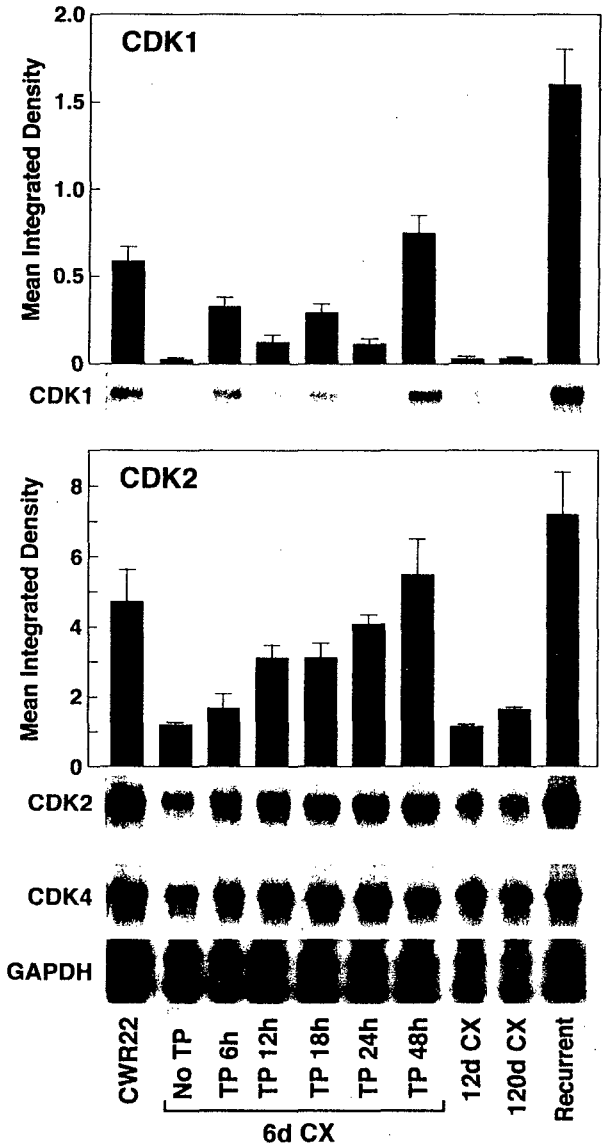
CDK1
Mean Integrated Density
2.0
1.5
1.0
0.5
0
CDK1
CDK2
Mean Integrated Density
8
6
4
2
0
CDK2
CDK4
GAPDH
CWR22
No TP
TP 6h
TP 12h
TP 18h
TP 24h
TP 48h
6d CX
12d CX
120d CX
Recurrent

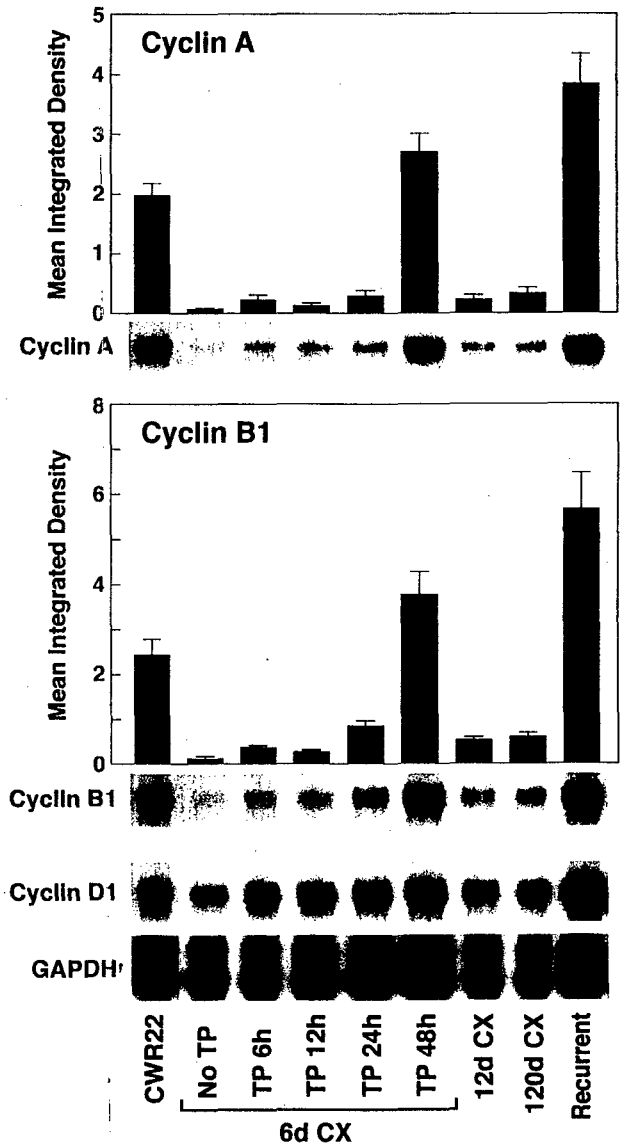
Cyclin A
Mean Integrated Density
5
4
3
2
1
0
Cyclin A
Cyclin B1
Mean Integrated Density
8
6
4
2
0
Cyclin B1
Cyclin D1
GAPDH
CWR22
No TP
TP 6h
TP 12h
TP 24h
TP 48h
6d CX
12d CX
120d CX
Recurrent

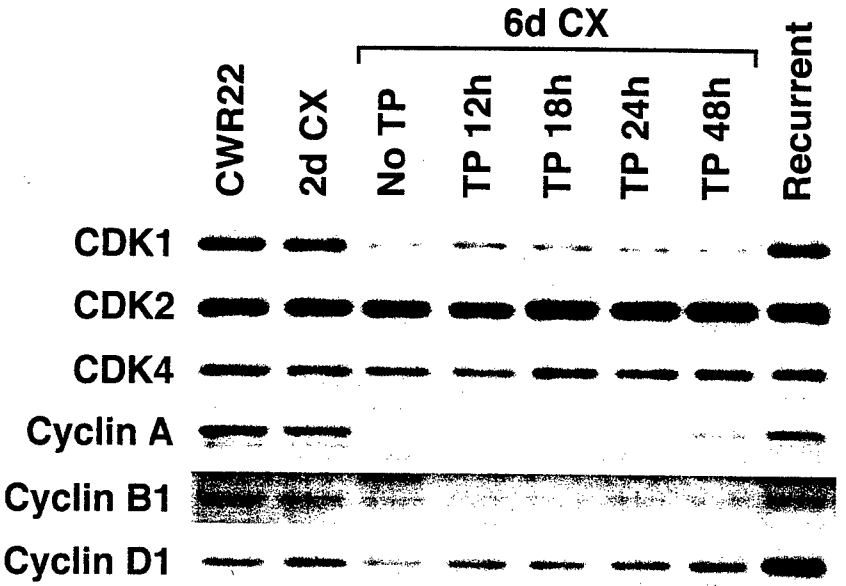
6d CX
CWR22
2d CX
No TP
TP 12h
TP 18h
TP 24h
TP 48h
Recurrent
CDK1
CDK2
CDK4
Cyclin A
Cyclin B1
Cyclin D1

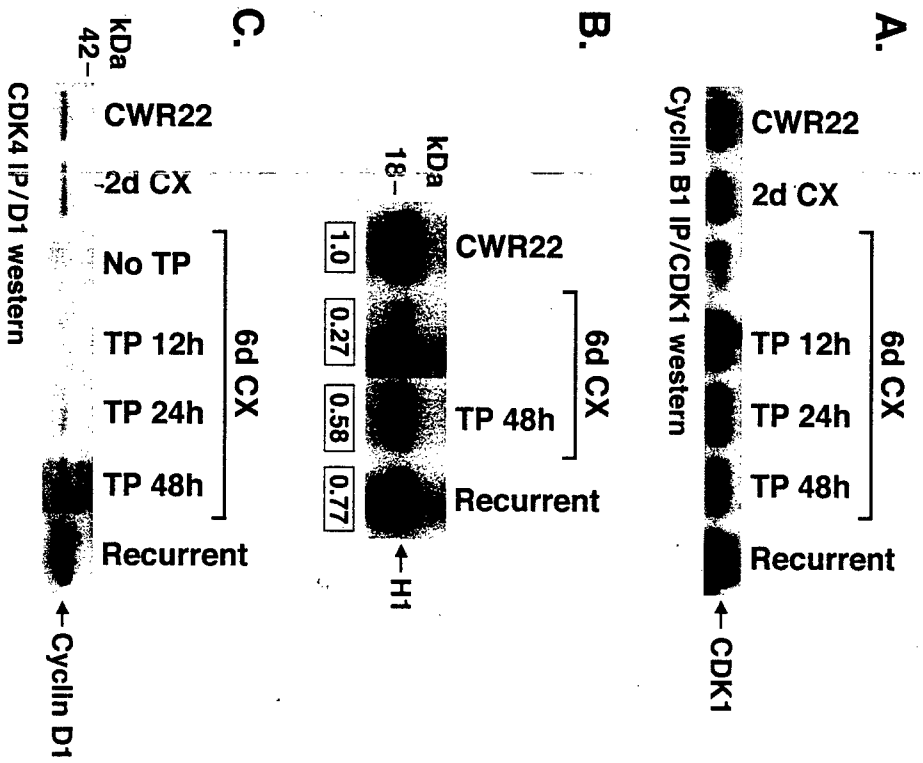
A.
Cyclin B1 IP/CDK1 western
CWR22
2d CX
TP 12h
TP 24h
TP 48h
6d CX
Recurrent
CDK1
B.
kDa
18–
CWR22
1.0
0.27
0.58
0.77
TP 48h
6d CX
Recurrent
H1
C.
kDa
42–
CDK4 IP/D1 western
CWR22
2d CX
No TP
TP 12h
TP 24h
TP 48h
6d CX
Recurrent
Cyclin D1

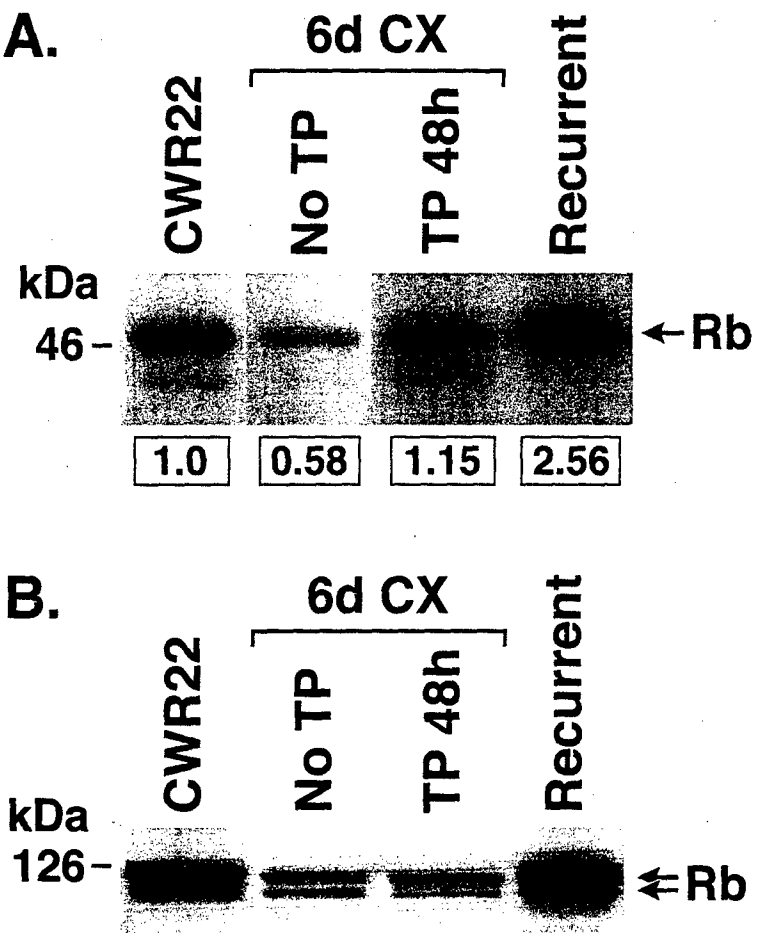
A.
6d CX
CWR22
No TP
TP 48h
Recurrent
kDa
46 –
Rb
1.0
0.58
1.15
2.56
B.
6d CX
CWR22
No TP
TP 48h
Recurrent
kDa
126 –
Rb